2021

Predicting Anthropogenic Underwater Pile Driving Noise Using Pile Driving Analyzer (PDA) DATA

Brandon Alfredo Rivera
University of North Florida, n01457669@unf.edu

Predicting Anthropogenic Underwater Pile Driving Noise Using Pile Driving Analyzer (PDA) Data

By

BRANDON A. RIVERA

A THESIS PRESENTED TO THE GRADUATE SCHOOL
OF THE UNIVERSITY OF NORTH FLORIDA IN PARTIAL FULFILLMENT
OF THE REQUIREMENTS FOR THE DEGREE OF
MASTER OF SCIENCE IN COASTAL AND PORT ENGINEERING

UNIVERSITY OF NORTH FLORIDA

2021

“To my wife Shayna for all her love and encouragement.”

ACKNOWLEDGMENTS

I would like to thank my advisor, Dr. Raphael Crowley, for the knowledge and guidance that he has provided me over the course of my graduate degree and in preparing this thesis. He has selflessly supported the U.S. Navy Ocean Facilities Program and enabled our service members to become a part of the UNF Osprey community. None of this could have been possible without his commitment and support.

TABLE OF CONTENTS

page

LIST OF TABLES

LIST OF FIGURES

Figure page

ABSTRACT

PREDICTING ANTHROPOGENIC UNDERWATER PILE DRIVING NOISE USING PILE DRIVING ANALYZER (PDA) DATA By

Brandon A. Rivera

December 2021

Chair: Raphael Crowley
Major: Coastal & Port Engineering

In the past several years, there has been increasing concern about anthropogenic noise generated during marine pile driving. This concern is expected to increase concomitantly with increases in waterfront construction efforts associated with aging infrastructure and sea level rise. Several guidelines are available to help predict underwater noise transmission due to pile driving, but the issue with all these methods is that they require one to measure sound pressure levels at one locus or more from the driven pile. In the context of marine construction, adding specifications for underwater noise collection may be expensive or difficult because contractors typically have little experience making such measurements. A better solution would be to utilize data that are already regularly collected during pile driving noise to predict underwater sound levels. This thesis focused on investigating whether such a method could be developed using Pile Driving Analyzer (PDA) data since PDA data are always collected prior to production scale driving during roadway construction in the state of Florida. PDA data are often also collected throughout pile driving activities on all drives during roadway construction. Sound data were collected using a hydrophone-equipped buoy system at various sites across the state of Florida. Once sound data were collected, correlations were developed between the sound data and data from the PDAs. Results appeared to indicate that a correlation appears to exist between sound-level data and PDA results. This would

appear to indicate that development of a noise-prediction method using PDA data may be possible in the future.

CHAPTER 1
INTRODUCTION

1.1 Background Information

Underwater pile driving is a fundamental activity in construction and repairs for bridges, wharfs, piers, and dock systems used throughout the United States. These activities are expected to increase both internationally and locally in Florida as sea level rise increases and infrastructure continues to age. As these construction activities increase, there has been increasing concern about the effects of anthropogenic noise during these construction efforts – particularly effects associated with underwater pile driving.

Beginning in 2009, under the Federal Joint Subcommittee on Ocean Science and Technology, an interagency task force was formed to address anthropogenic noise and the effects on the marine environment. The priorities of the task force were to:

> (1) develop and validate mitigation measures to minimize demonstrated adverse effects from anthropogenic noise;
>
> (2) test/validate mitigating technologies to minimize sound output and/or explore alternatives to sound sources with adverse effects;
>
> (3) explore the need for and effectiveness of time/area closures versus operational mitigation measures (Berube, 2019).

In November 2016, the Ocean Noise Policy developed by the National Marine Fisheries Service (NMFS), agreed to address the impacts of anthropogenic noise to marine wildlife over the next decade. The National Environmental Policy Act (NEPA) established regulations that ensured environmental review for construction projects. In December 2016, these responsibilities were assigned to the Florida Department of Transportation (FDOT) and would be regulated on all federal highway projects across the state of Florida.

More recently, the NMFS and U.S. Fish and Wildlife Service (USFWS) expressed particular concern for marine wildlife affected by anthropogenic noise generated from pile driving. With the anticipated increases in construction efforts and involvement from regulatory agencies, a better understanding of the sound levels produced from marine pile driving is needed to address these concerns.

1.1 Recent Transmission Loss Work

As sound emanates from any source, its energy tends to spread as a function of distance. Thus, due to conservation of energy, at a given distance from the sound source, the sound waves at any point from the source will have a reduced amplitude when compared to sound waves at the source. This phenomenon is known as transmission loss (TL), shown in Figure 1-1 for the case of cylindrical spreading.

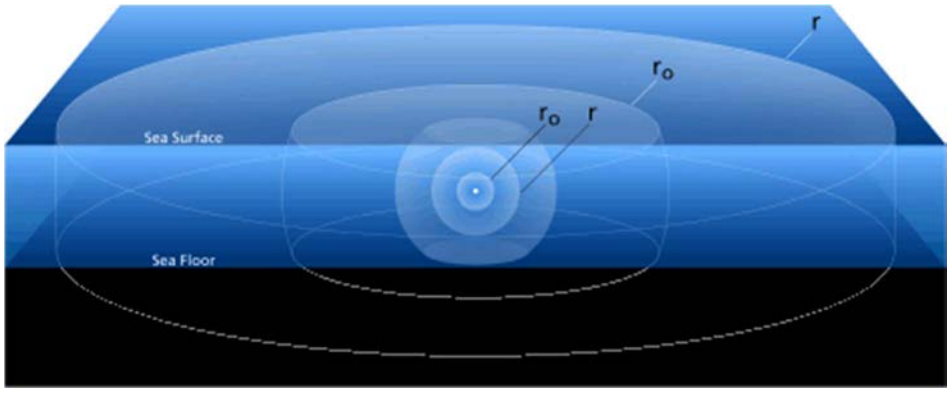

Figure 1-1. Example of Transmission Loss for Cylindrical Spreading (University of Rhode Island and Inner Space Center, n.d.)

Over the past ten years, most research efforts associated with underwater pile driving noise have been associated with TL associated with these drives. Examples of these efforts include work by Berube, 2019; Martin & Barclay, 2019; Lippert, Ainslie, & Estorff, 2018; Dahl & Dall'Ostro, 2017; Lippert, Galindo-Romero, Gavrilov, & Estorff,

2015; Dahl, Dall'Osto, & Farrell, 2015; Galindo-Romero, Lippert, & Gavrilov, 2015; Lippert & Estorff, 2014; Dahl & Reinhall, 2013; Zampoli, et al., 2013; Reinhall & Dahl, 2011.

Generally, the commonality associated with most TL loss studies is that their goal is to determine where certain sound thresholds are exceeded. While several guidelines for fish injury are available (Guan, Brookens, & Vignola, 2021; Hawkins, Johnson, & Popper, 2020; Martin, Lucke, & Barclay, 2020; Popper & Hawkins, 2019; Buehler, Oestman, Reyff, Pommerench, & Mitchell, 2015), generally, the guidelines below in Table 1 are the current design standard.

Table 1-1: NMFS Guidelines for underwater sound produced by pile driving (NMFS 2015)

Effect	Metric	Fish Mass	Threshold
Onset of Physical Injury	Peak Pressure (L_{Peak})	N/A	206 dB
	Accumulated Sound Exposure Level ($SEL_{cumulative}$)	≥ 2 g	187 dB
		< 2g	183 dB
Adverse Behavioral Effects	Root Mean Square Pressure (RMS)	N/A	150 dB

In Table 1, sound exposure level (SEL) is defined as:

$$SEL = 10\log_{10} \int_0^T P^2(t)dt \tag{1-1}$$

SEL is the integral of sound over time While the root mean squared (RMS) sound pressure is defined as:

$$RMS = \sqrt{\frac{\sum_1^n (a_1^2 + a_2^2 + \cdots a_n^2)}{n}} \tag{1-2}$$

in which the pressure amplitude $(a_1, a_2 \ldots a_n)$ is squared and averaged. Peak sound pressure is simply the highest sound pressure associated with a pile drive. Current guidelines for determining TL are relatively simple and easy to implement. The most commonly used expression for sound propagation is.

$$L(R) = L(R_o) - F \log_{10}(R) \tag{1-3}$$

In this expression, the sound level, *L* at range, *R* from the point source, R_0 can be computed using a simple base-10 logarithmic decay function that is dependent upon a the TL coefficient, *F*. Solving for TL in Eq. 1-3 leads to:

$$TL = F \log_{10}(R) \tag{1-4}$$

Current guidelines (NOAA 2021) indicate that *F=15* may be assumed. This assumption (Eq. 1-5, below) is known as the "practical spreading loss model" and assumes that sound is a monopole point-source whose TL is dominated by mode stripping.

$$TL = 15 \log_{10}(R) \tag{1-5}$$

Several authors have pointed out that this model has its issues – particularly because pile driving is not a monopole point source but rather is a transient line source – see Crowley, et al., 2022; Bosco, 2021; Lippert, Ainslie, & Estorff, 2018; Reinhall & Dahl, 2011.

1.2 The Need for a Source Sound Prediction Method

All the aforementioned TL relationships presume that $L(R_0)$ is known. In practice, measuring $L(R_0)$ in the field may be arduous or expensive. It would be better to find an alternative method for predicting $L(R_0)$ using information that is normally readily available either during or prior to pile driving. One such parameter that is typically tested during pile driving in Florida are Pile Driving Analyzer (PDA) data.

The Pile Driving Analyzer ® is a dynamic loading and pile driving monitoring system commonly used for marine pile driving. The PDA system is able to determine static soil resistance, pile structural integrity, dynamic pile stresses, and hammer energy transferred to the pile during driving events. Of particular interest is energy transferred from the hammer to the pile, which is known as EMX in the PDA system. EMX can be expressed as:

$$EMX = Maximum\left\{\int Force_{Hammer} velocity_{Hammer} dt\right\} \quad (1\text{-}6)$$

In a more practical sense, the EMX is the maximum energy emitted by the pile hammer during a driving event for a given interval. It was hypothesized that a correlation should exist between EMX and sound levels in the field. It was further hypothesized that other PDA data beyond EMX may be even better correlated to sound. For example, as resistance to pile penetration increases, then hammer energy transferred to the pile may be converted to some other form of energy – i.e., heat due to friction and sound. This resistance to loading would mean increased compressive stresses along the pile during pile driving, and these data are also recorded in the PDA system.

1.3 Goals and Objectives

The goal of this study was to preliminarily assess whether or not PDA data during pile driving could be an accurate predictor of underwater pile driving noise. More specifically, the goal was to determine if EMX could be correlated to $L(R)$. Then, additional correlations to $L(R)$ were evaluated such as Maximum Pile Compression Stress (CSX), Pile Compression Stress at Bottom (CSB), and Maximum Pile Tension Stress (TSX). Using best-fit regression data fitting, sound level data were collected at several sites in

Florida and correlations were developed between these PDA outputs and measured sound-levels.

CHAPTER 2
MATERIALS AND METHODS

This chapter provides an overview of the data collection system used to acquire pile driving sound data, the post-processing of the collected data, and the methodology to achieve the goals of this study.

2.1 Materials

2.1.1 Data Collection System

The data collection system used in the study is the legacy platform developed and utilized by Berube during his work on anthropogenic pile driving noise (Berube, 2019). The data collection system consists of five data collection buoys, shown in Figure 2-1. Each buoy is comprised of an aluminum frame, flotation pontoons, electronics housing, hydrophone and associated electronics, Wi-Fi mast, and anchoring system.

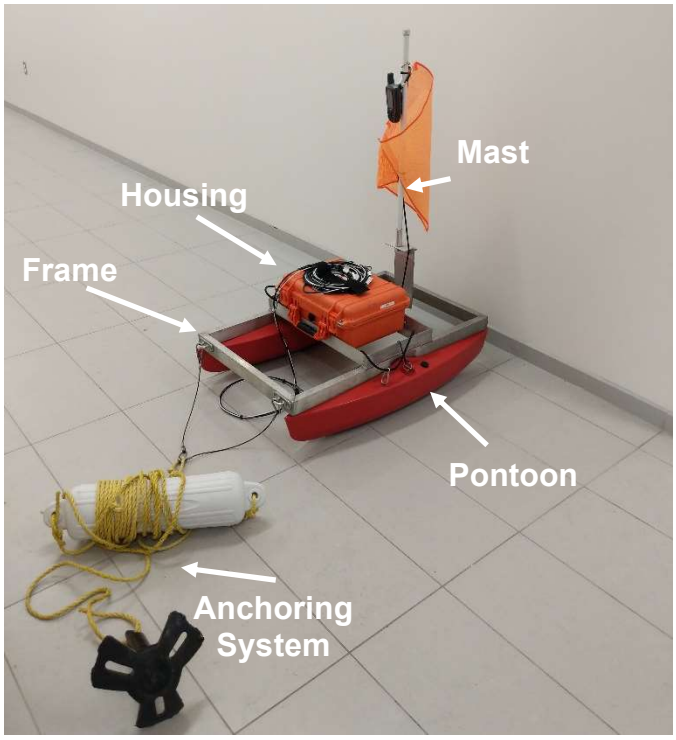

Figure 2-1. Buoy Data Collection System

The fully welded aluminum frame consists of 2-inch x 1-inch rectangular aluminum tubing; 2-inch square aluminum angles; and 4-inch by 6-inch aluminum plate bracket to secure the Wi-Fi antennae and safety flag. Each frame is pinned to two pontoons and internally welded to ensure watertightness. The frame has a two-point anchor connection opposite of the mast bracket to prevent capsizing.

The electronic housing is a Pelican 1450 case which mounts and secures onto the frame system. The external hydrophone cable, was routed through Scanstruct cable clam/deck deals to the internal electronics. Similarly, using a MENCOM MDE45-8FR-RJ45-BM connection, ethernet cable from the mounted Wi-Fi mast was routed to the associated internal electronics. The data collection system is also equipped with a thermocouple cable; however, this was not used during this study. These connections are shown in Figure 2-2.

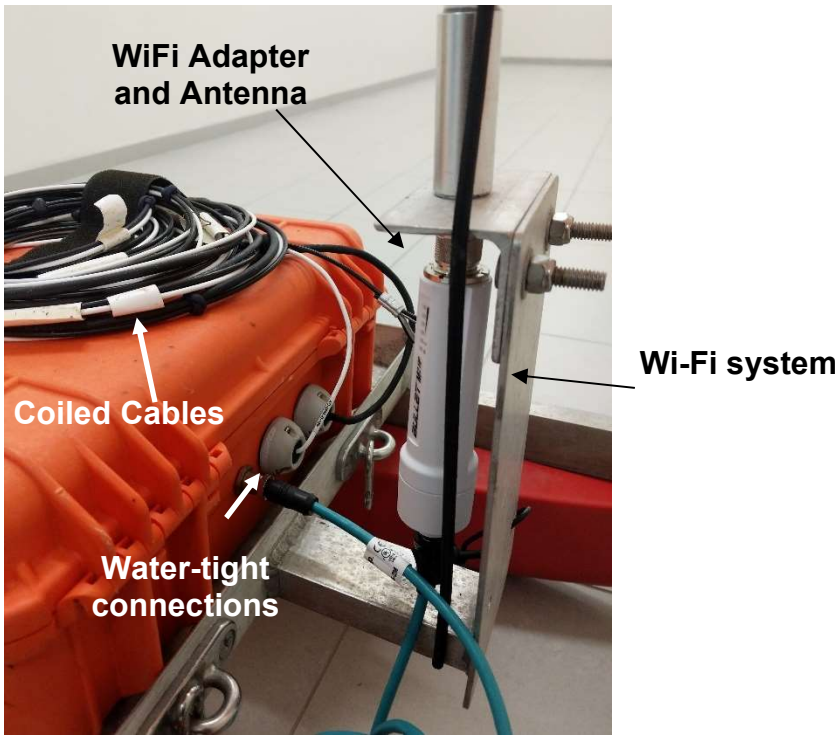

Figure 2-2. External Connections

Contained in the electronic housing are a Bruel and Kjaer 2250 handheld analyzer; Bruel and Kjaer 2647 charge converter; L-com BT-CAT5-P1 power-over-Ethernet converter; two 12-volt [serial] motorcycle batteries; and Pace Scientific XR-440M pocket logger. The Pace Scientific XR-440M pocket loggers are used in conjunction with the external Pace Scientific PT960 temperature probe; however, this was not used during this study. These devices are shown in Figure 2-3.

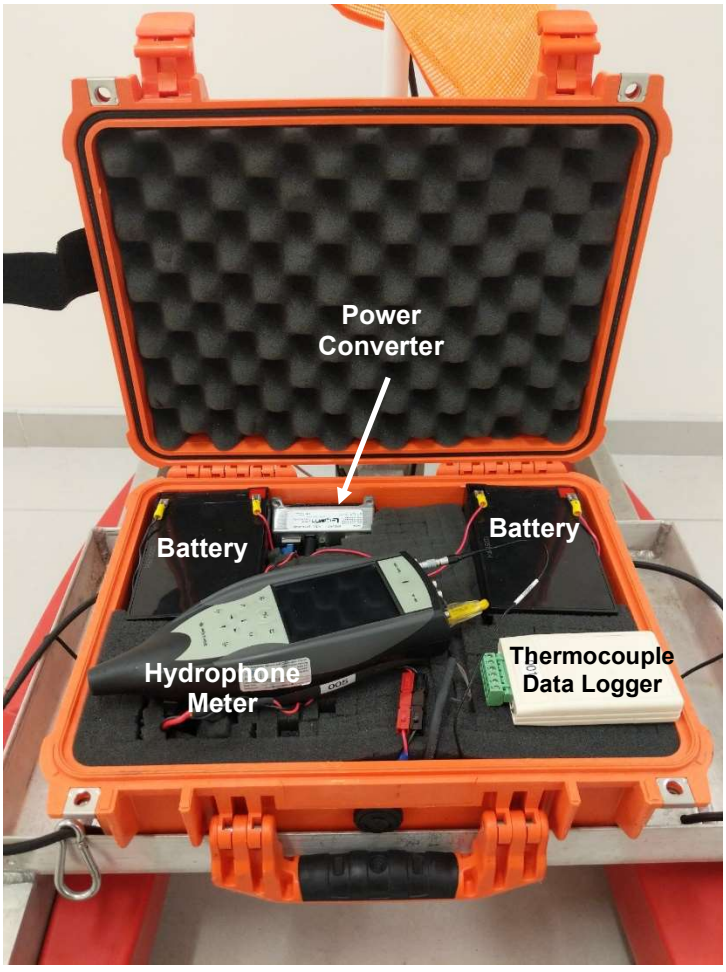

Figure 2-3. Internal Devices

External to the electronic housing are the Bruel and Kjaer 8103 hydrophone; Pace Scientific PT960 temperature probe (not used); Garmin GPSMAP 64s; and the Wi-Fi mast which consists of an Ubiquiti Bullet M2 wireless access point and an L-COM HG2409UP antennae. These devices are shown in Figure 2-4. A safety flag was secured to each Wi-Fi mast as a marine safety measure for possible boat traffic during testing.

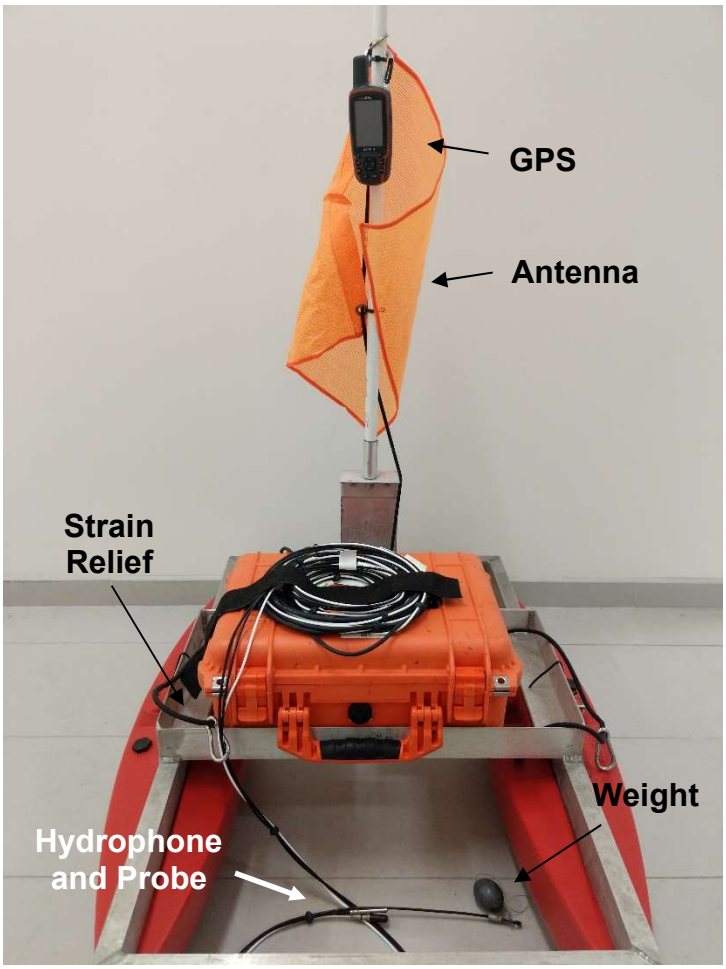

Figure 2-4. External System

The external hydrophone and thermocouple cables were looped together with a steel cable for strain relief when deployed. The looped cables were marked every 18 inches (0.5 meters) with a clinch knot for quickly adjusting depth during deployment. Bulkhead connectors were affixed to the aluminum frame using marine grade weld epoxy. Carabiner clips secured a steel cable that was coupled with the hydrophone cable to the bulkhead connectors. The thermocouple cable was also aligned with the steel cable and hydrophone cable but was not used during this study.

During data collection, the cables were secured to a strain relief system at the center of the data collection buoy. When deployed, this strain relief system was affixed at the appropriate clinch knot to maintain accurate depth. A loop was crimped at the end of the steel cable to secure a 12 oz fishing weight. This weight, when deployed kept the cables approximately vertical in the water column. A figure of the cables and strain relief system are also shown in Figure 2-4.

The anchoring system consisted of an anchor bridle using steel cable and carabiners. A 20 lb. river anchor was secured to this connection using a bowline knot. Half-inch hollow braid polypropylene was used at a length of approximately 1.5 to 2 times the depth for each buoy location to mitigate against capsizing and drift. 24-inch buoys were secured in series between the anchor bridle and polypropene rope for efficient and safe retrieval of the buoys.

2.1.2 Data Collection Procedures

Prior to any buoy deployment, the internal devices were fully charged, the GPS units were installed with new batteries, and memory card data storage was verified to mitigate against data loss. Hydrophones were calibrated and tested in a setting with minimal ambient noise suing a Bruel and Kjaer 4229 calibrator. During buoy deployment,

the internal electronics were powered on and sound/GPS recording were initiated. Buoys were launched one at a time at distances of approximately 25 meters (Buoy 1), 50 meters (Buoy 2), 100 meters (Buoy 3), 200 meters (Buoy 4), and 400 meters (Buoy 5) from the pile bent where driving was occurring.

Once initially deployed and sea conditions allowed, buoys were manually adjusted incrementally to ensure proper line of sight to the source pile driving. If construction site conditions allowed, Buoy 1 was placed as close to the source pile driving as safely possible. It was observed that the Wi-Fi system, though functional, rapidly depleted the power source. A likely contributor to this depletion was the high temperatures observed in the summer months in Florida. To mitigate against possible data loss, the Wi-Fi system was not used during most of these pile drives, but recording was maintained locally onboard the buoys using secure digital (SD) cards.

2.2 Methodology

Data collection was coordinated among the Florida Department of Transportation (FDOT) and contractors around the state of Florida where pile driving was scheduled. The sites used in this study were of similar intercoastal characteristics. Specific water and geotechnical data were not included in this study. Site locations shown in Figure 2-6 and are summarized in Table 2-1. Pile information is summarized in Table 2-2.

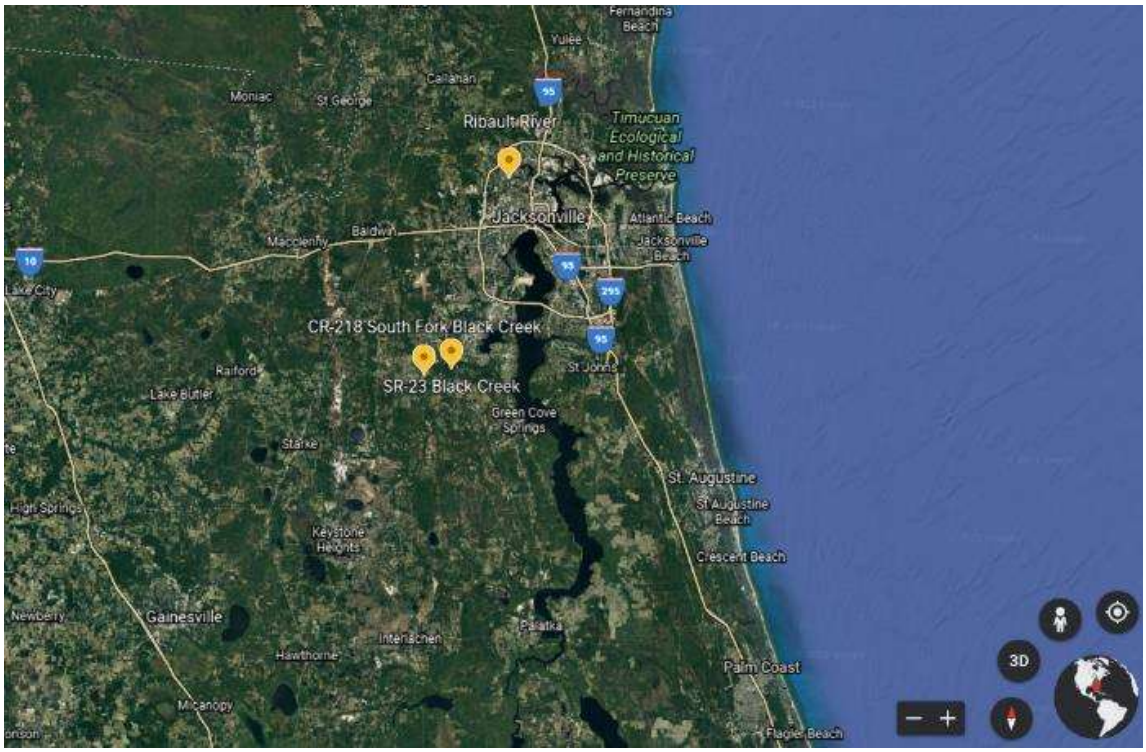

Figure 2-5. Pile Driving Site Locations

Table 2-1: Bridge Site Location Summary

Site Name	Latitude	Longitude	Date(s) of Visit
Ribault River Bridge	30°23'43.99"N	81°42'52.21"W	5/7/19
CR-218 over South Fork Black Creek	30°03'37.61"N	81°52'17.53"W	12/04/2020 & 01/15/2021
SR-23 over Black Creek	30°04'19.23"N	81°49'7.53"W	01/08/2021 & 01/21/2021

Table 2-2: Pile-Type and Hammer Information

Site Name	Number of Piles	Pile-Type	Hammer Information
Ribault River Bridge	1	24” square PCP	APE D50
CR-218 over South Fork Black Creek	2	24” square PCP	APE 62-55 & APE 66-55
SR-23 over Black Creek	11	24” square PCP	APE D62/70

For all sites, data were collected from Buoys 1 through 5 using the procedure outlined in Section 2.1.2. While data were collected from all five buoys at all these sites,

usually only the buoy closest to the pile (i.e., Buoy 1) was used for data analysis in this study. However, during one of SR-23 data collection days (January 8, 2021 specifically), it was noticed that ambient sound levels were abnormally high near Buoy 1; this was likely caused by unusually loud construction noise. As a result of this ambient background noise, it was difficult to observe the increases in sound level associated with the pile drives. Therefore, the next closest buoy, which was approximately 50 m from the pile drive, was used for analysis.

Due to time synchronization issues, there were differences in recorded timestamps associated with sound data, PDA data, and GPS data. For consistency, the Buoy GPS system was used as the official times throughout this work. For days in which there were multiple drives, the order of drives from the driving logs were compared to the order of sound data collected to ensure correct pile number assignments. Differences between PDA system blow counts and recorded blows from the sound signals were also observed. There are two explanations for this. Either (1) the PDA system may have recorded false strikes, dry fires, high rebounds etc.; or (2) during post-processing, it is possible the computer algorithms used in this study “missed” some of the hammer strikes. During data analysis, investigators tried to ensure that the number of recorded blows matched the number of blows recorded in the pile driving logs. When this was not possible, the PDA blow count data were normalized relative to the sound level blow count data.

2.2.1 Raw Sound Data

During data collection the raw sound data were collected for the duration of the pile driving events across all sites at a sampling rate of 48 kHz. Consequently, these data included the sound from the pile driving but also included ambient noise likely due to

marine wildlife, current, vehicle traffic, construction, etc. To isolate the pile driving sound, a MATLAB (Mathworks, 2021) script was utilized to identify the local peaks or maxima during the time of the pile driving using the built-in “findpks” command. These local maxima sound levels are the sound propagations from the marine pile driving and thus, the number of peaks represents the number of blows issued by the pile hammer.

2.2.2 PDA Data Interpolation

Separately gathered from field testing were the PDA data for each pile drive. These data included the EMX delivered by the pile hammer. Since the EMX is over an interval of hammer blows, there is not a value of EMX for each hammer blow. A MATLAB script was used to interpolate values of EMX for each hammer blow based upon the individual hammer blows derived from the raw sound data unique to each site using the built-in “interp1” command.

2.2.3 EMX Correlation

Post-processing described in Section 2.2.1 leads to sound data as a function of blow number. Post-processing described in Section 2.2.2 leads to EMX data as a function of blow number. Thus, sound data per blow could also be plotted as a function of EMX per blow. This analysis was completed next, and correlations were developed between EMX and sound data using a Pearson’s correlation.

2.2.4 Normalizing EMX

Note from Eq. 1-6, EMX is a maximum value over a given interval. This time interval is not necessarily constant from drive to drive nor is it even necessarily constant during the same drive (i.e., EMX may output after 30 blows, then again after 100 blows). Thus, EMX output data were normalized by the blow count interval over which it was measured. This new term was dubbed *Effective Hammer Energy (EMX*)* measured in

kips-blows. Since these data are functions of blow-number, they allow the data to be comparable between different drives and different sites.

Furthermore, the EMX is not a value which can be controlled by operator and is dependent on the equipment – i.e., the hammer, pile cushion, hammer cusion, etc. However, the PDA also records the hammer stroke height, which is the height at which the hammer was raised during a given blow. EMX was separately normalized by the hammer stroke height to derive another *Effective Hammer Energy (EMX**)* measured in kips for possible correlation to sound level.

2.2.5 Pile Stress Correlations

As mentioned in Chapter 1, pile stresses during driving events are also measured in the PDA system. These values are CSX, CSB, and TSX. It was hypothesized that these data could relate to the resistance which the pile is experiencing in response to the hammer. Using the same data interpolation method outlined in Section 2.2.2, sound was expressed as a function of these values as well. Finally, EMX data was also normalized by each of these stress outputs to identify a possible *resistance factor* based on energy and stress, to correlate to sound level.

CHAPTER 3
RESULTS

This chapter provides the complete data analysis for each site location tested: Ribault River, FL; SR-23 Black Creek, FL; and CR-218 South Fork Black Creek, FL. Pile characteristics are also noted in this chapter. All piles analyzed in this study were Prestressed Concrete (PSC) piles.

3.1 Howell Dr. over Ribault River, FL

3.1.1 Howell Dr. over Ribault River, FL – Pile 1

- Date: 05/07/2019
- Pile: Intermediate Bent 3 Pile 1
- Dimensions: 24” x 110’ PSC Test Pile

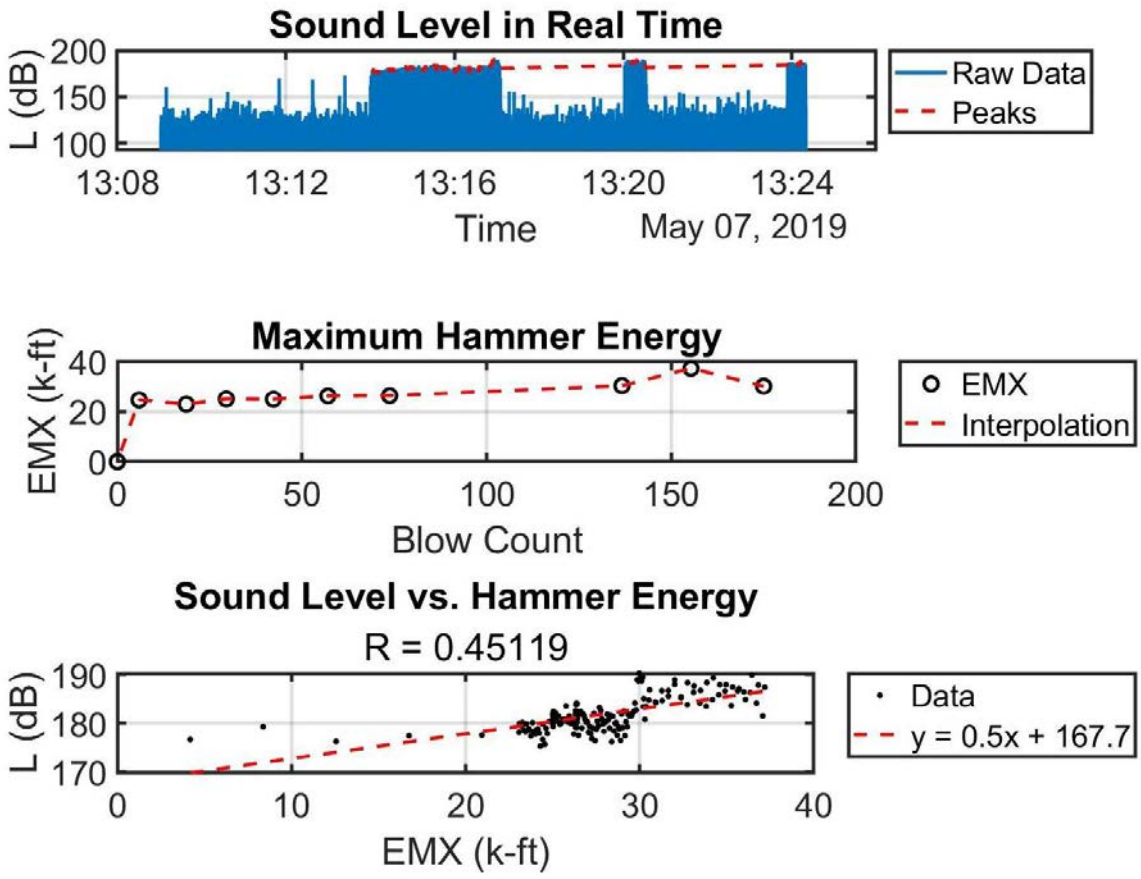

Figure 3-1. Sound Level vs. Hammer Energy (EMX)

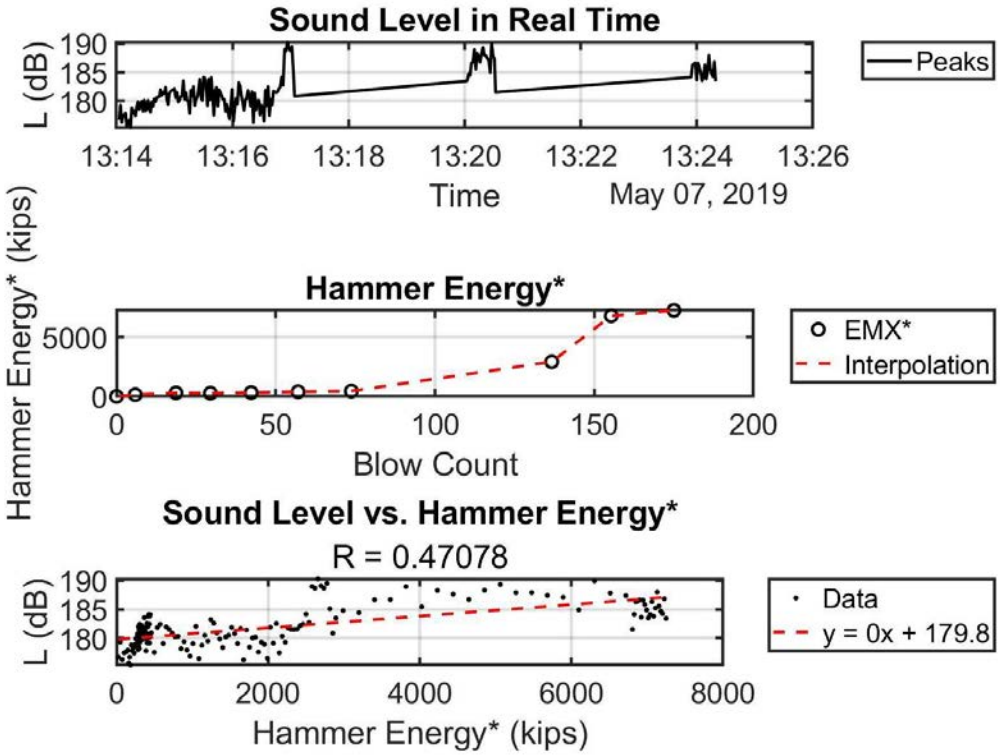

Figure 3-2. Sound Level vs. Hammer Energy normalized by Blow Count

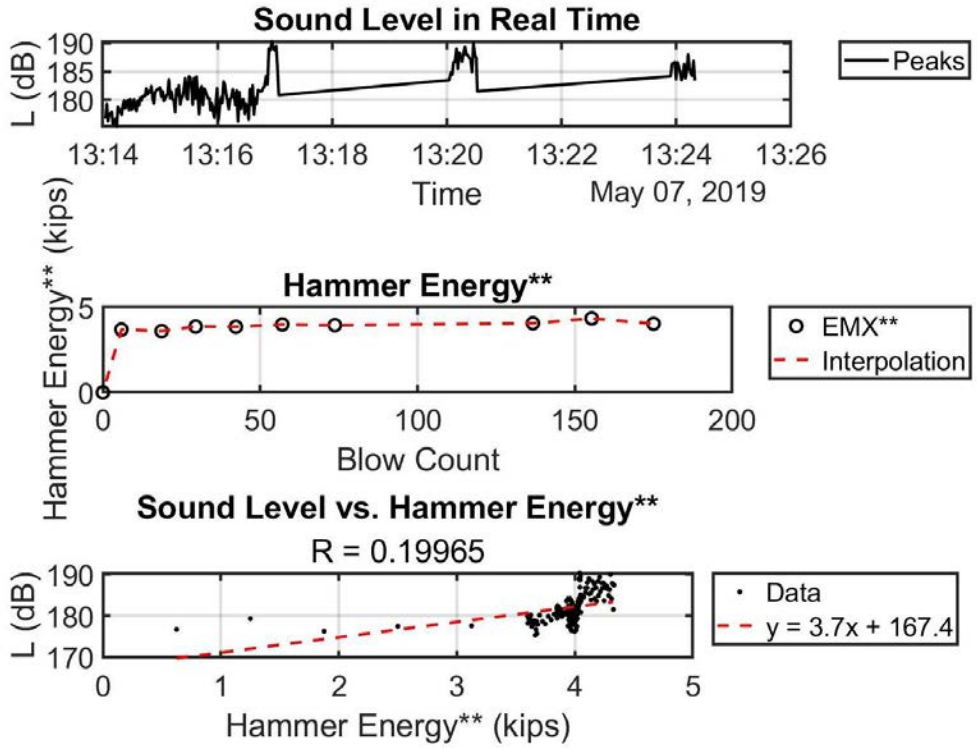

Figure 3-3. Sound Level vs. Hammer Energy normalized by Hammer Stroke Height

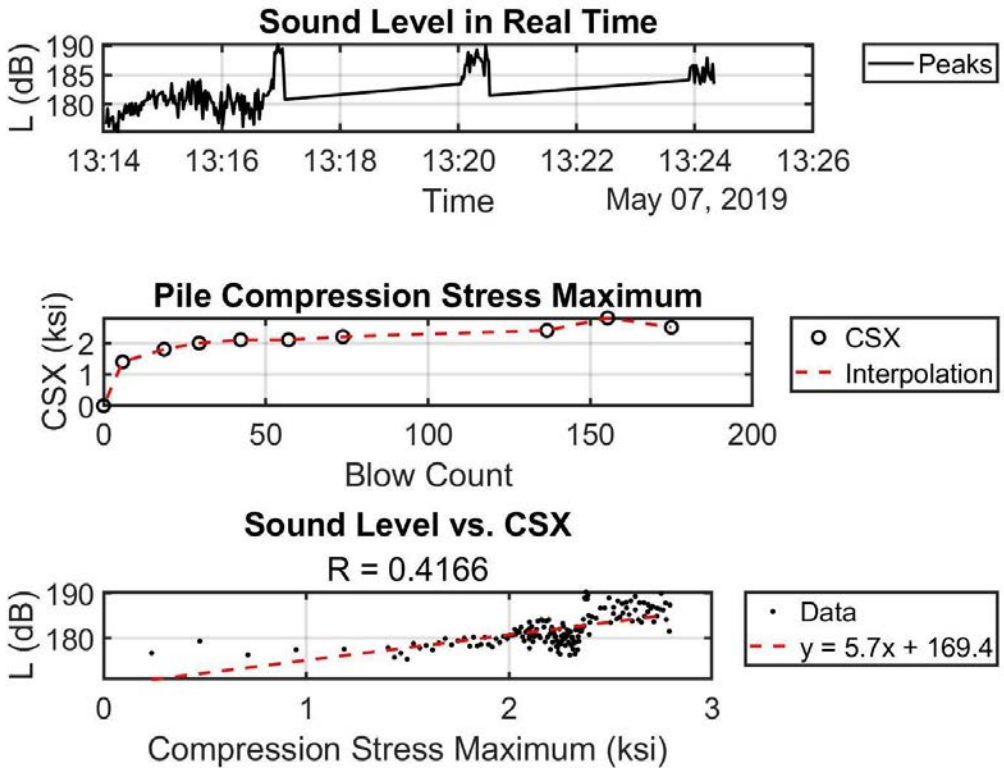

Figure 3-4. Sound Level vs. Maximum Pile Compression Stress

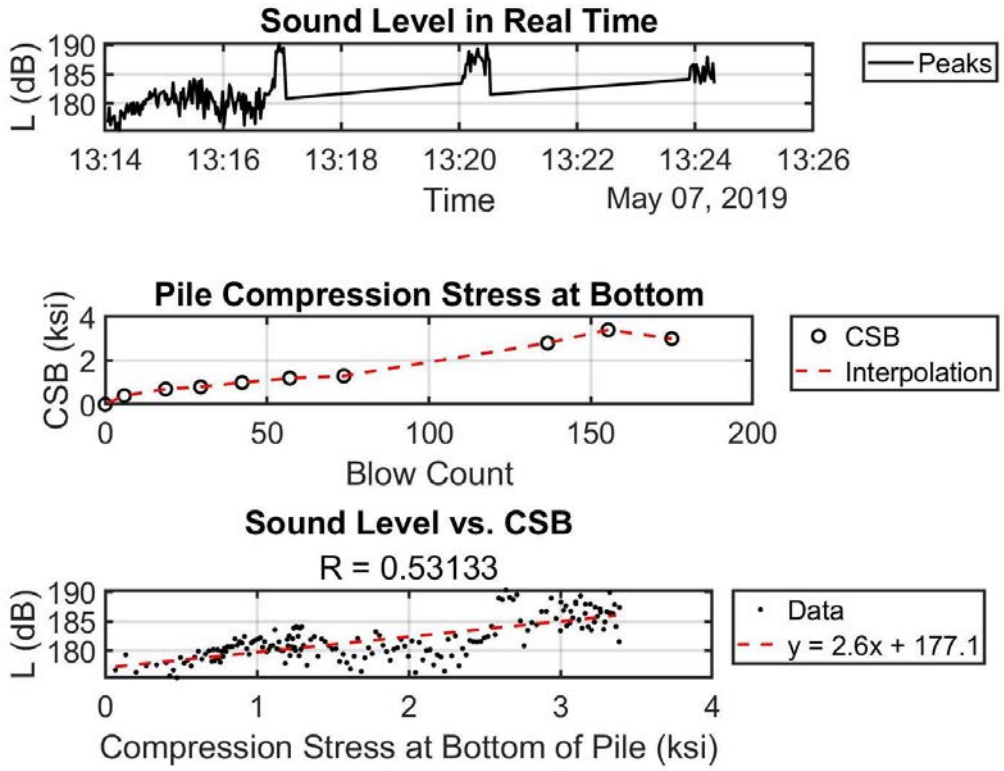

Figure 3-5. Sound Level vs. Pile Compression Stress at Bottom

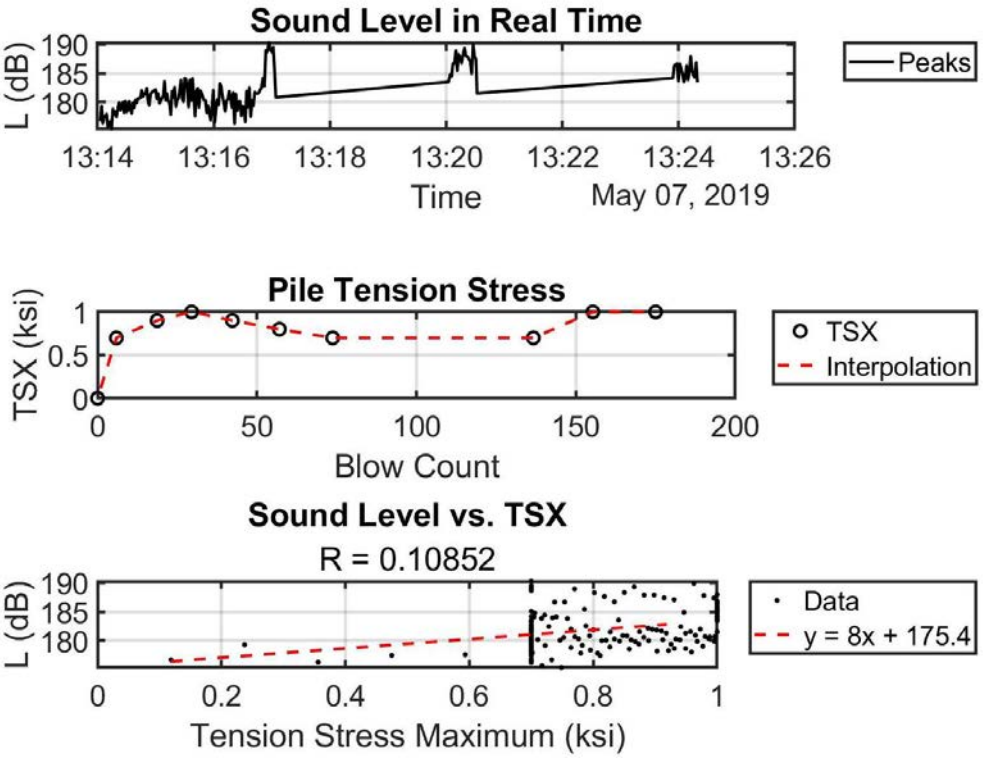

Figure 3-6. Sound Level vs. Pile Tension Stress

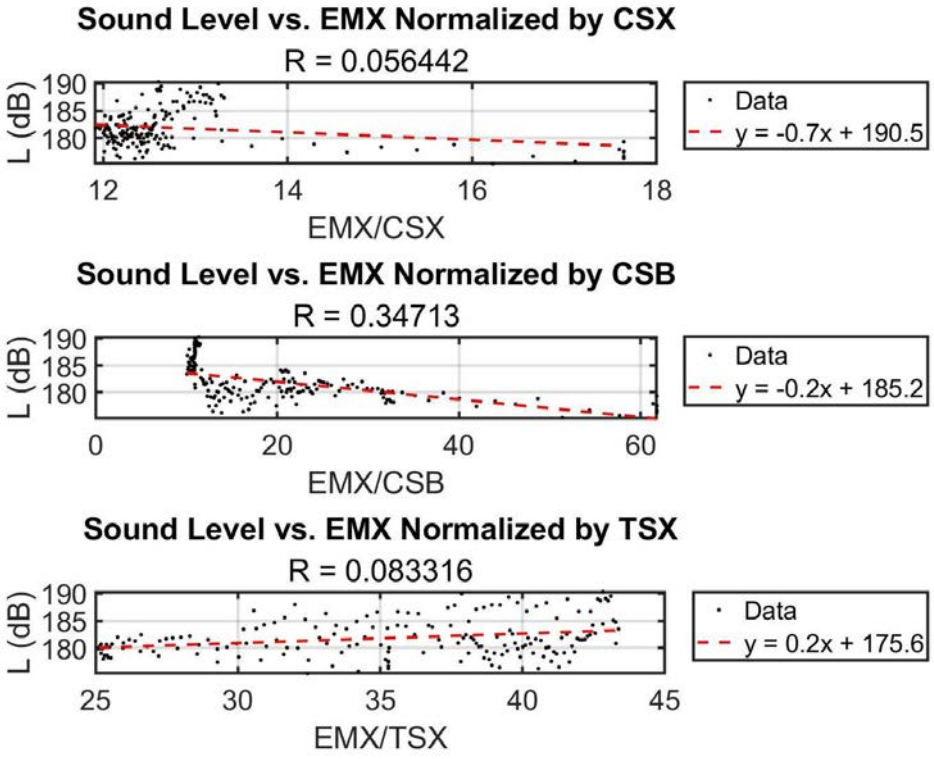

Figure 3-7. Sound Level vs. Hammer Energy normalized by Pile Stresses

3.2 CR218 over South Fork Black Creek, FL

3.2.1 CR218 over South Fork Black Creek, FL – Pile 4

- Date: 12/04/2020
- Pile: Intermediate Bent 3 Pile 4
- Dimensions: 24” x 110’ PSC Test Pile

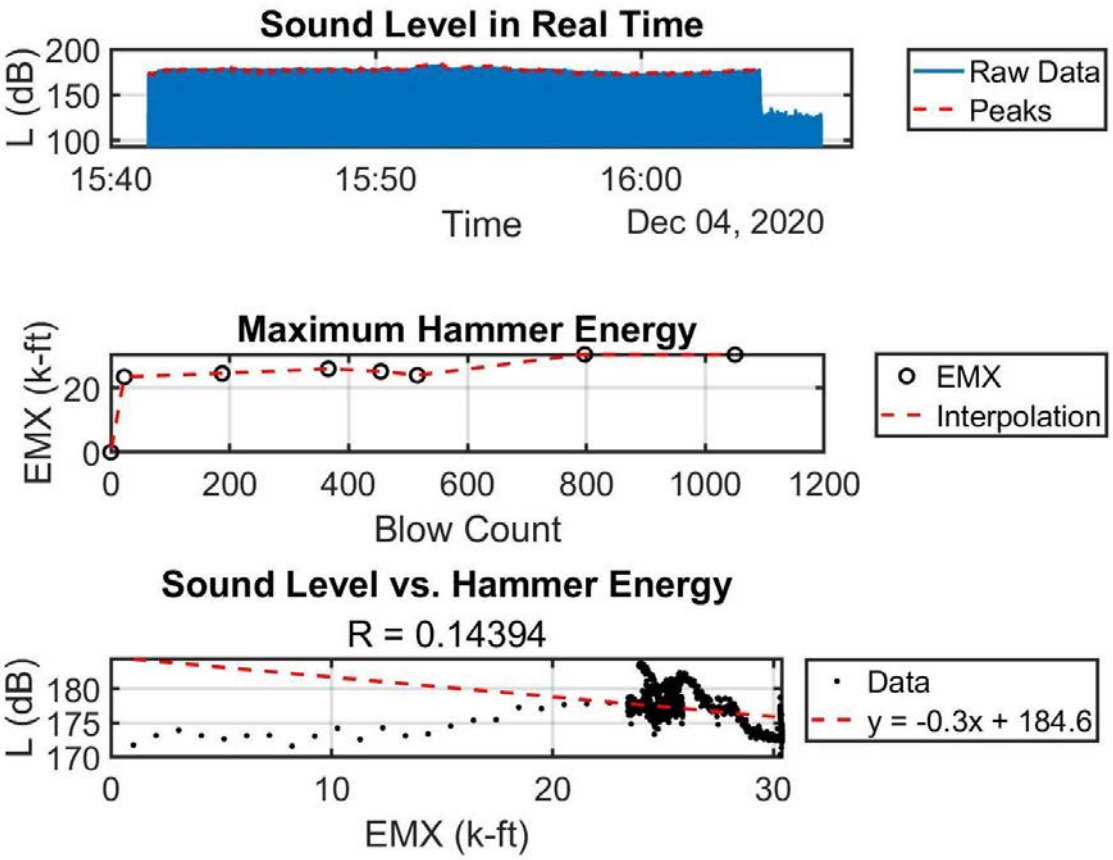

Figure 3-8. Sound Level vs. Hammer Energy (EMX)

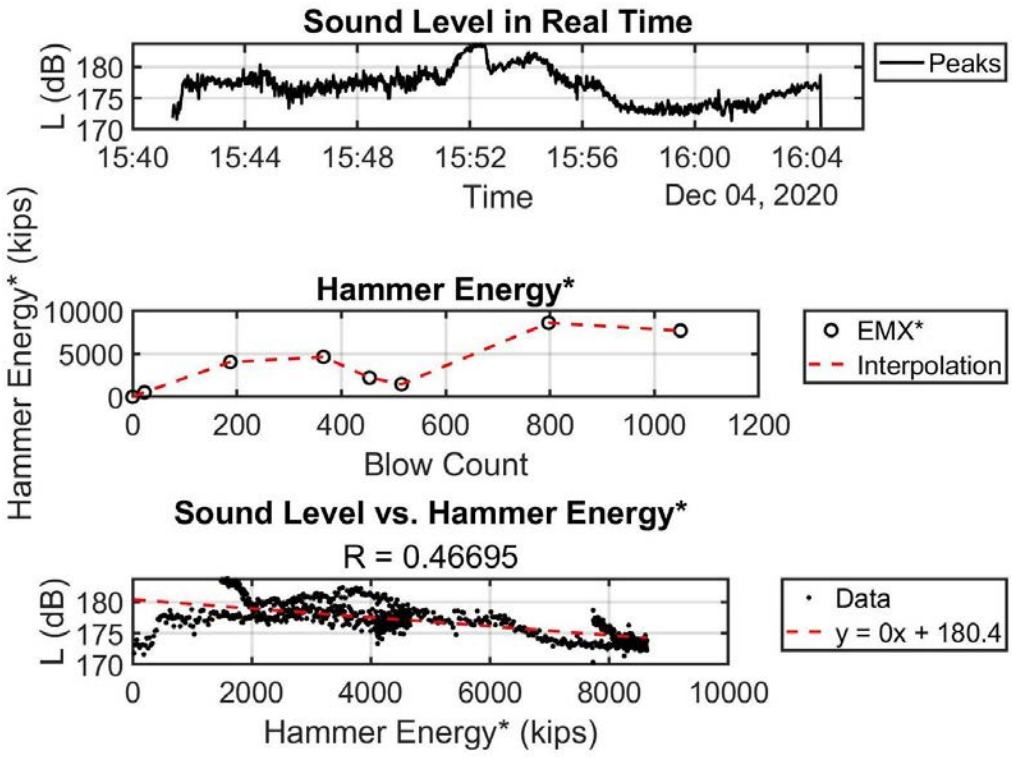

Figure 3-9. Sound Level vs. Hammer Energy normalized by Blow Count

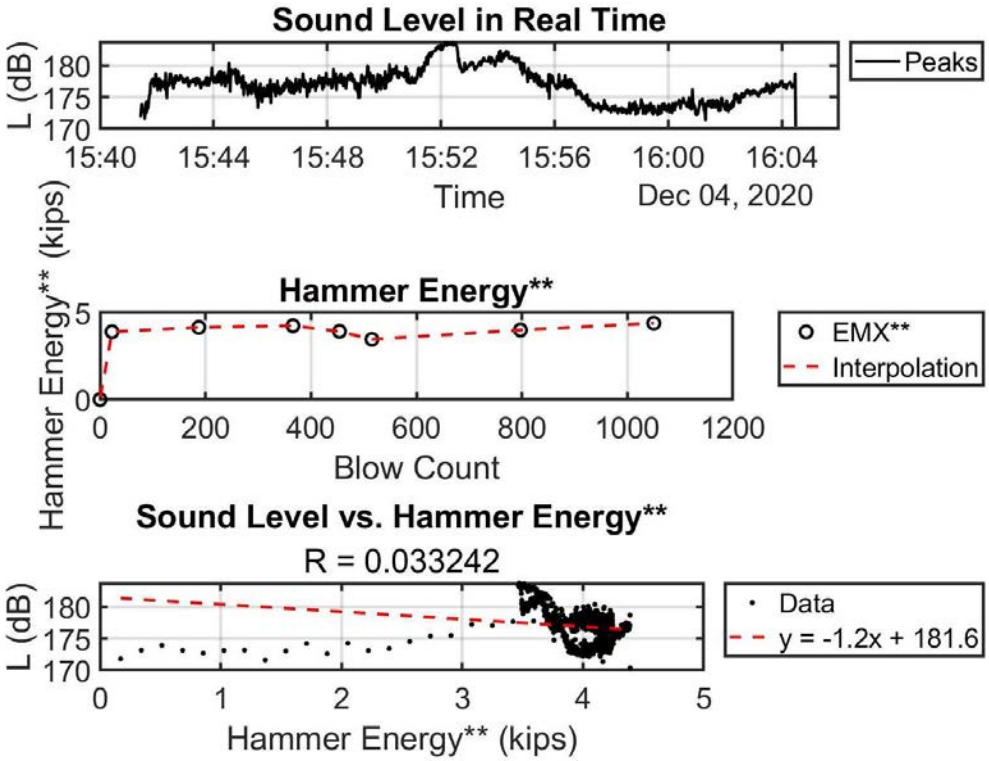

Figure 3-10. Sound Level vs. Hammer Energy normalized by Hammer Stroke Height

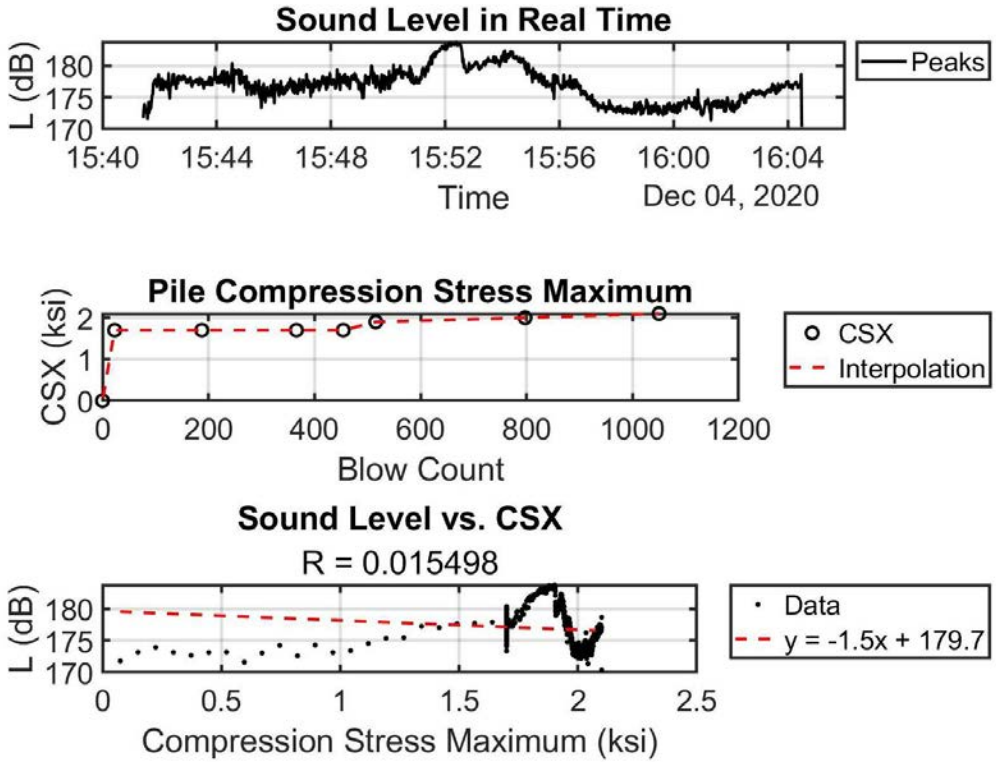

Figure 3-11. Sound Level vs. Maximum Pile Compression Stress

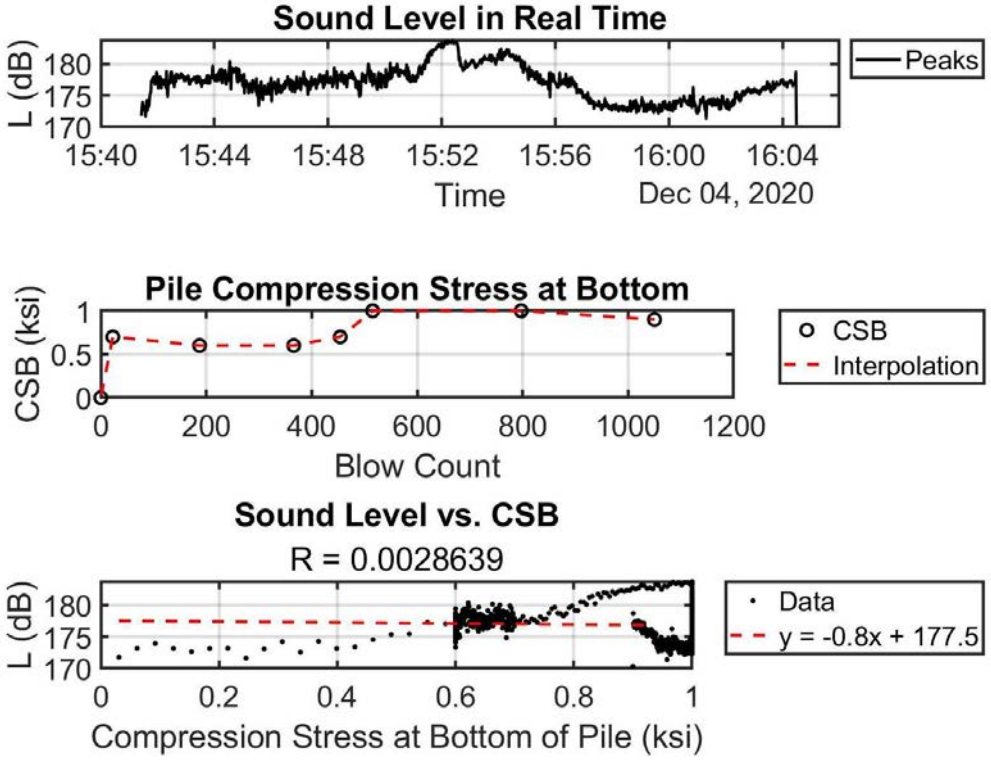

Figure 3-12. Sound Level vs. Pile Compression Stress at Bottom

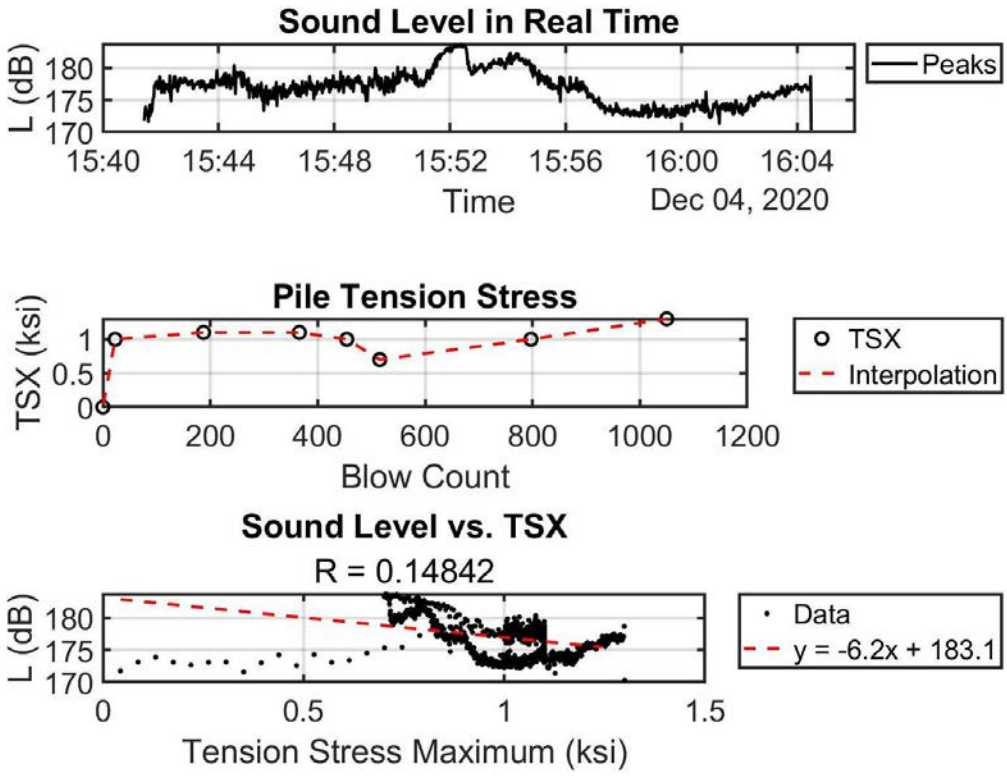

Figure 3-13. Sound Level vs. Pile Tension Stress

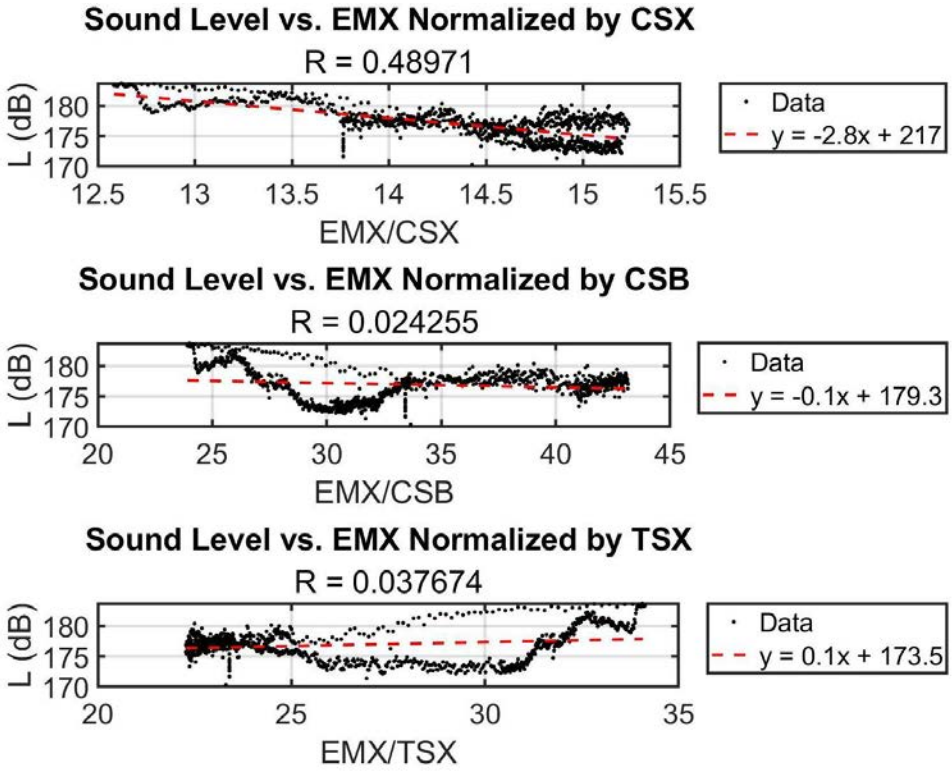

Figure 3-14. Sound Level vs. Hammer Energy normalized by Pile Stresses

3.2.2 CR218 over South Fork Black Creek, FL – Pile 5

- Date: 01/15/2021
- Pile: Intermediate Bent 3 Pile 5
- Dimensions: 24” x 80’ PSC Production Pile

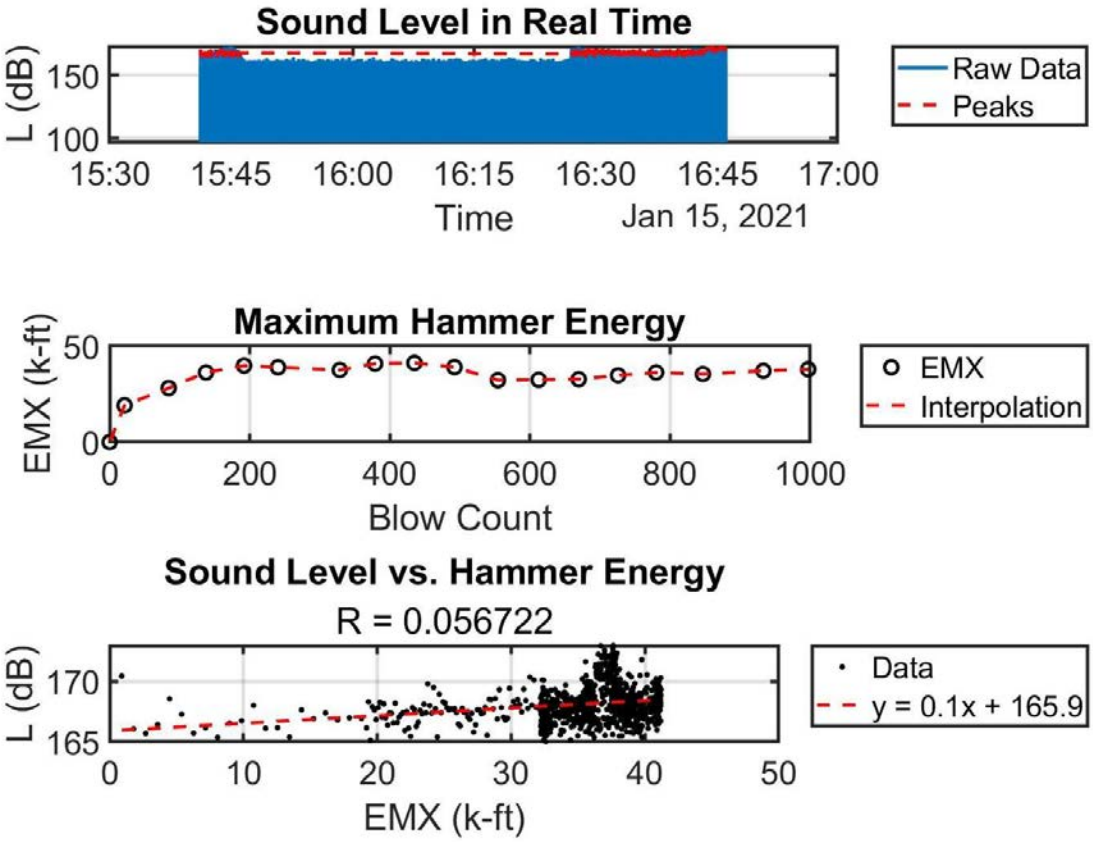

Figure 3-15. Sound Level vs. Hammer Energy (EMX)

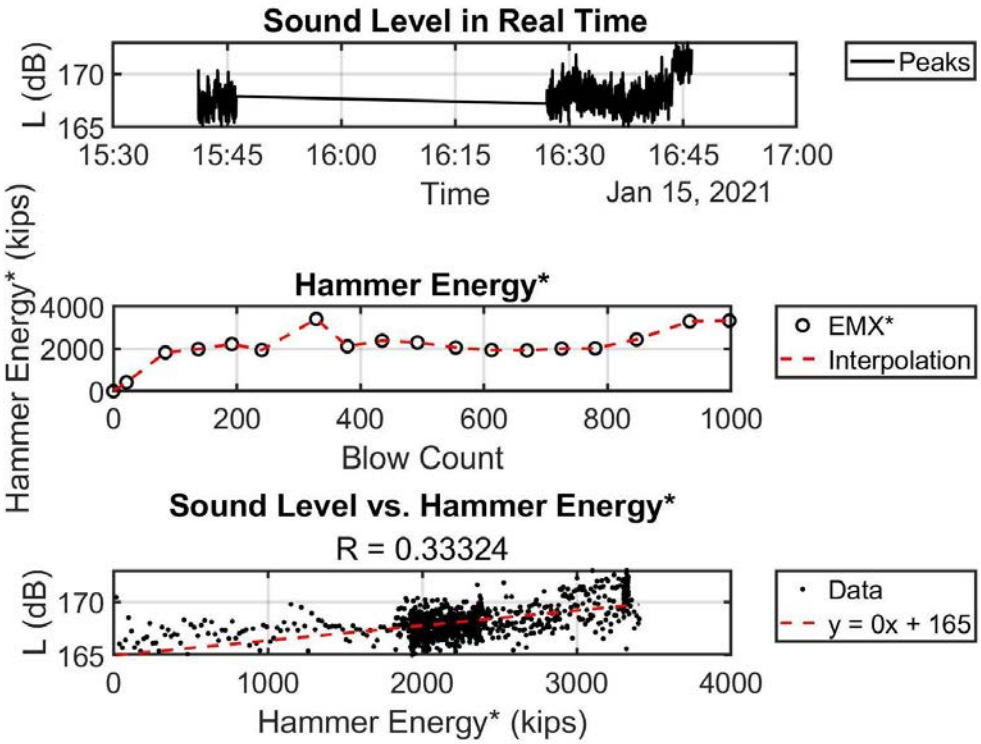

Figure 3-16. Sound Level vs. Hammer Energy normalized by Blow Count

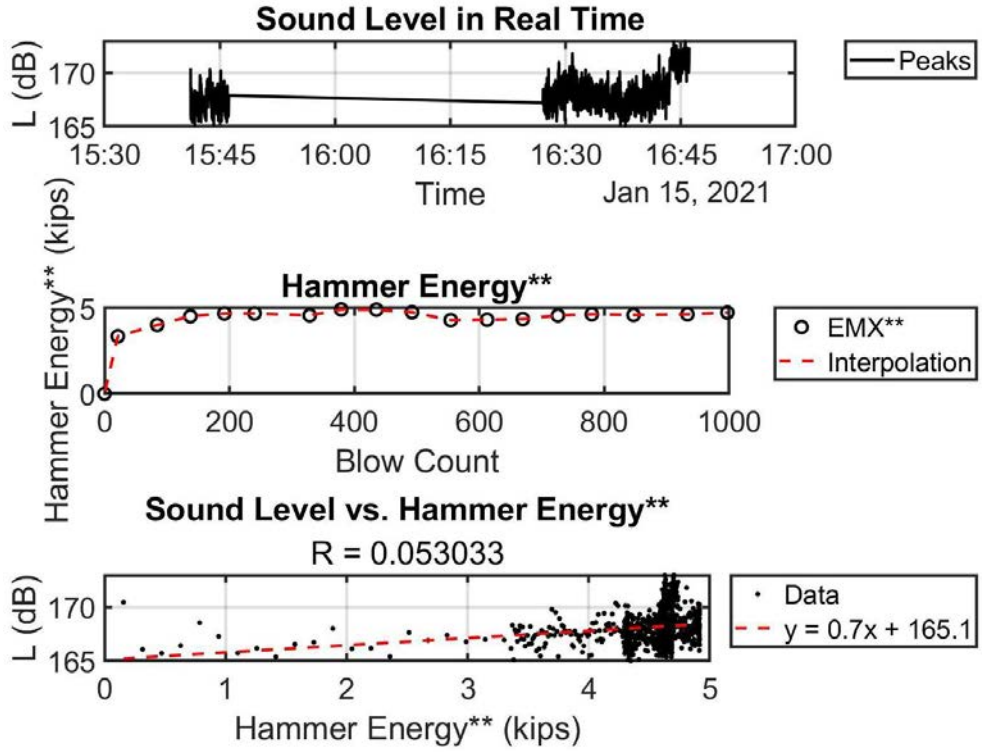

Figure 3-17. Sound Level vs. Hammer Energy normalized by Hammer Stroke Height

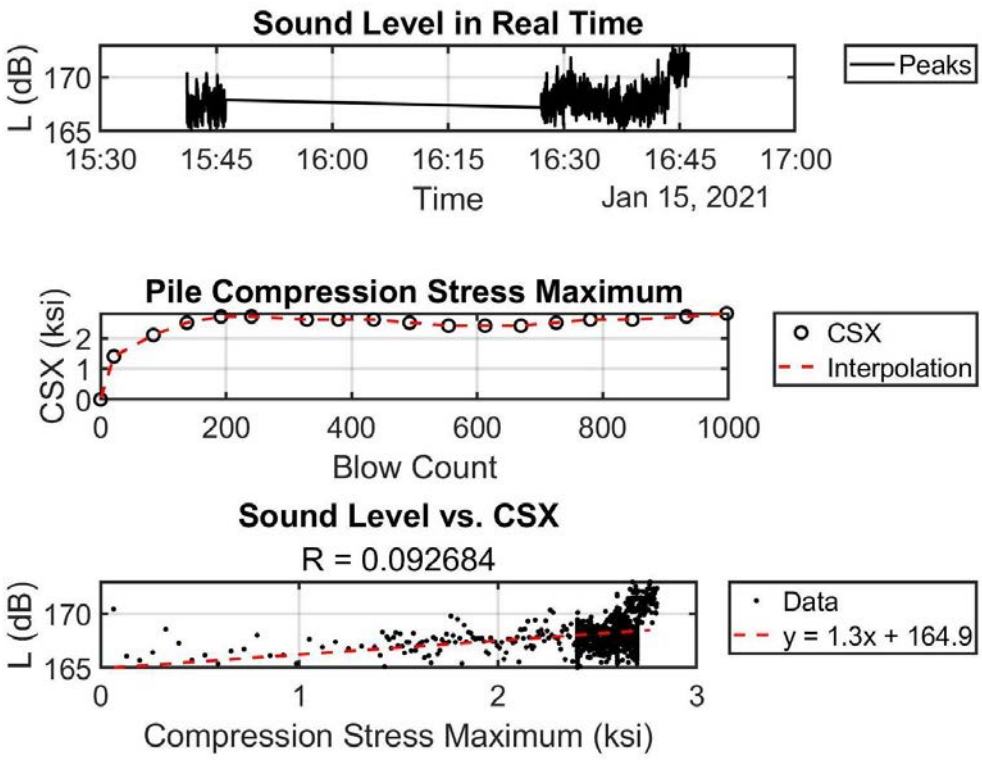

Figure 3-18. Sound Level vs. Maximum Pile Compression Stress

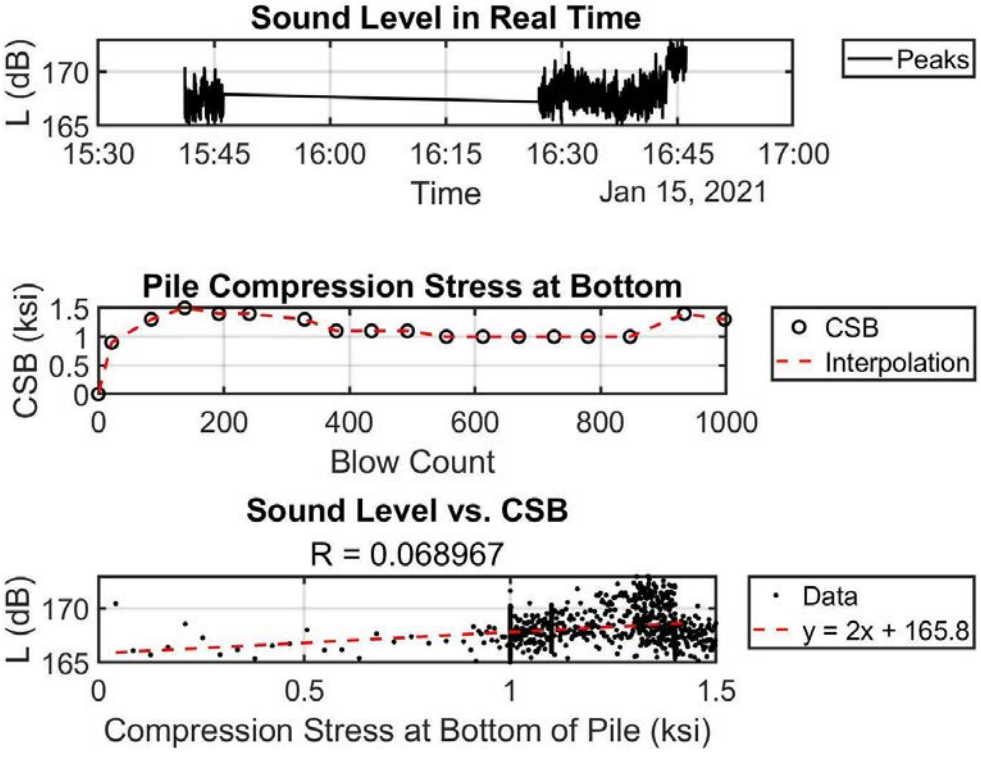

Figure 3-19. Sound Level vs. Pile Compression Stress at Bottom

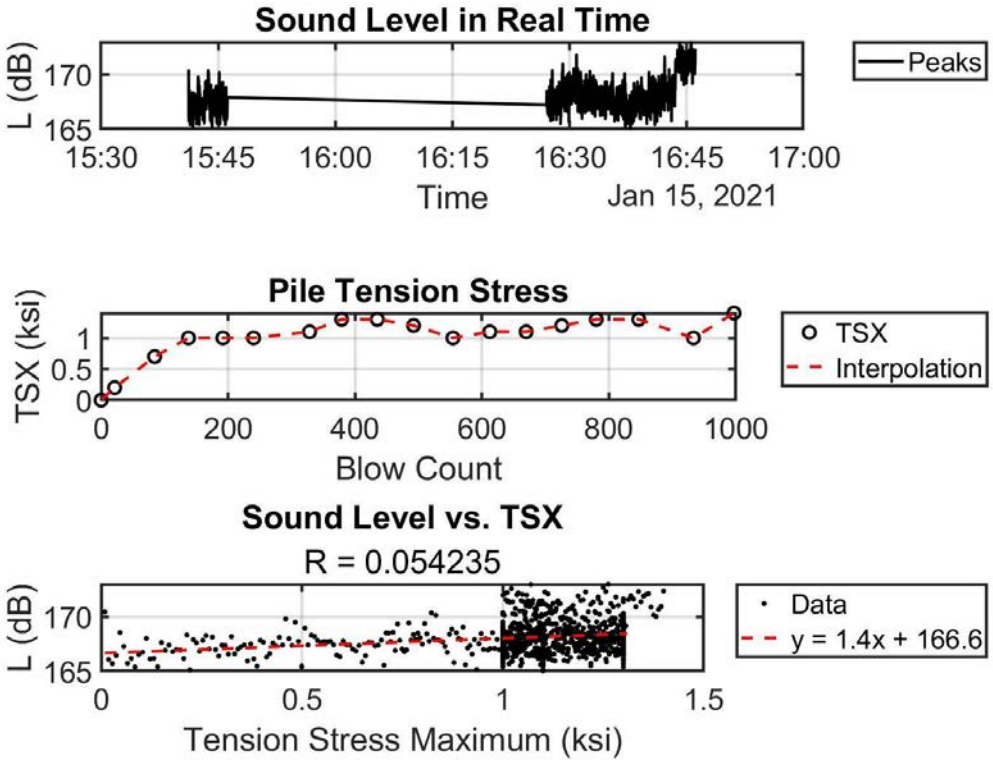

Figure 3-20. Sound Level vs. Pile Tension Stress

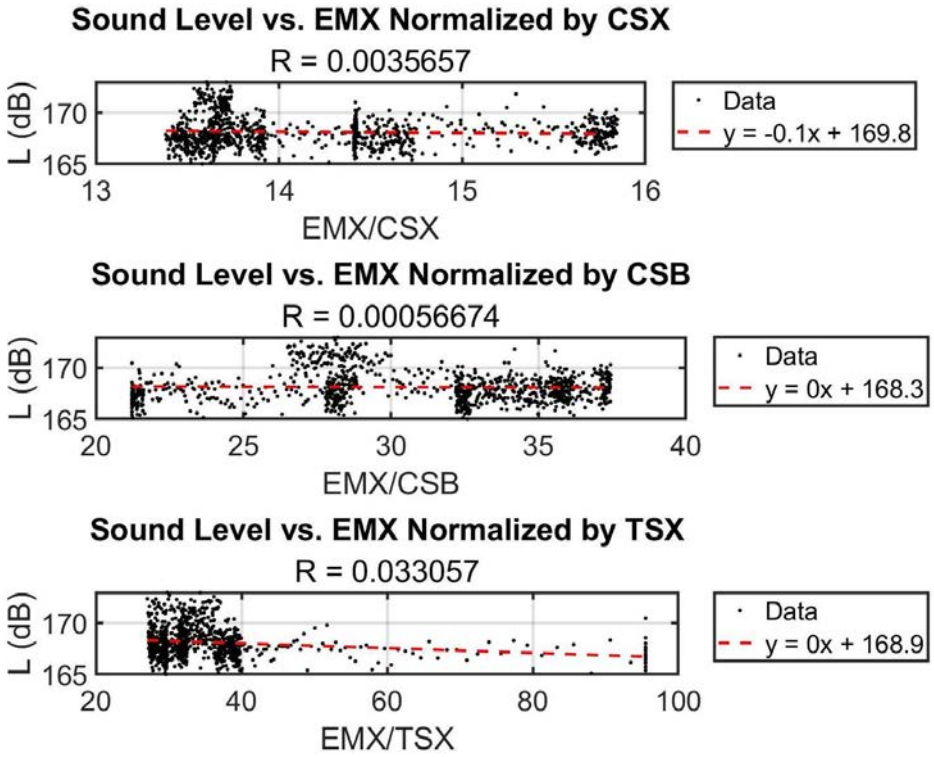

Figure 3-21. Sound Level vs. Hammer Energy normalized by Pile Stresses

3.3 SR-23 over Black Creek, FL

3.3.1 SR-23 over Black Creek, FL – Pile 1

- Date: 01/08/2021
- Pile: Intermediate Pier 4 Pile 1
- Dimensions: 24” x 90’ PSC Production Pile

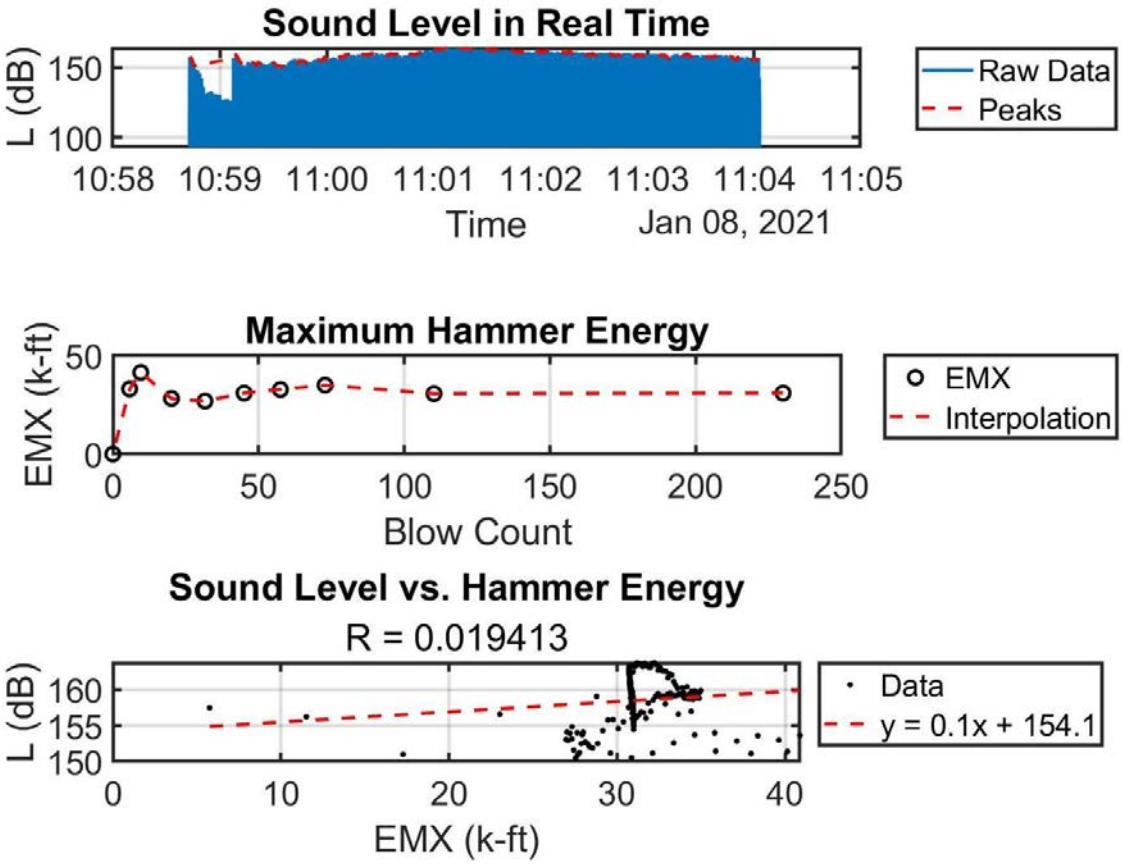

Figure 3-22. Sound Level vs. Hammer Energy (EMX)

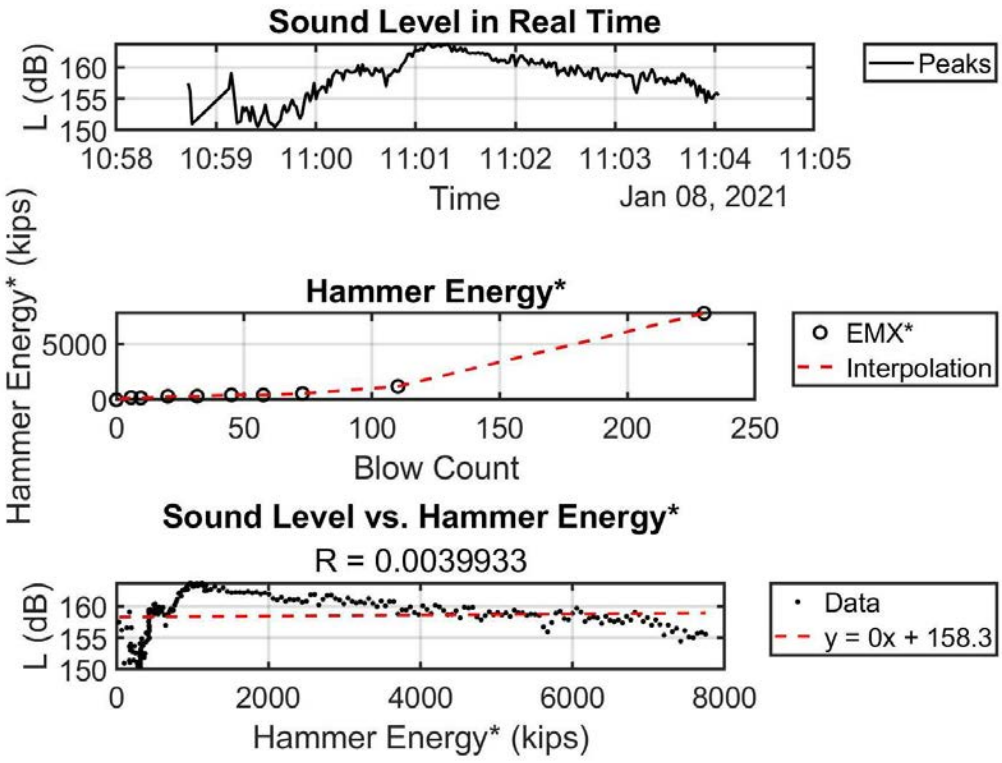

Figure 3-23. Sound Level vs. Hammer Energy normalized by Blow Count

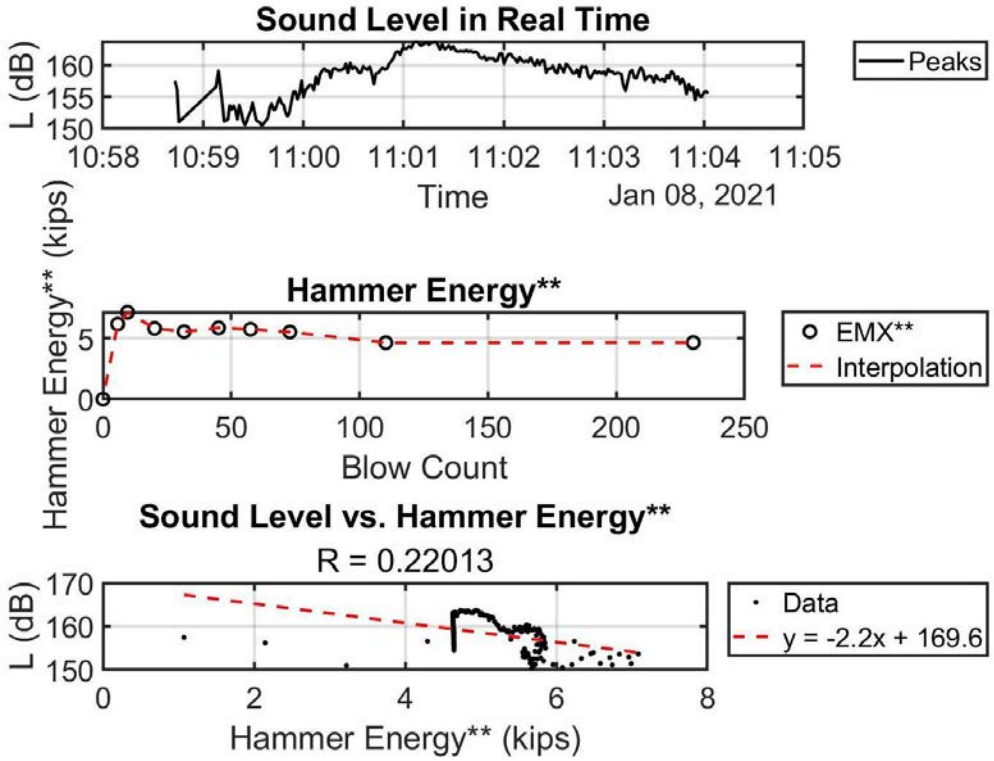

Figure 3-24. Sound Level vs. Hammer Energy normalized by Hammer Stroke Height

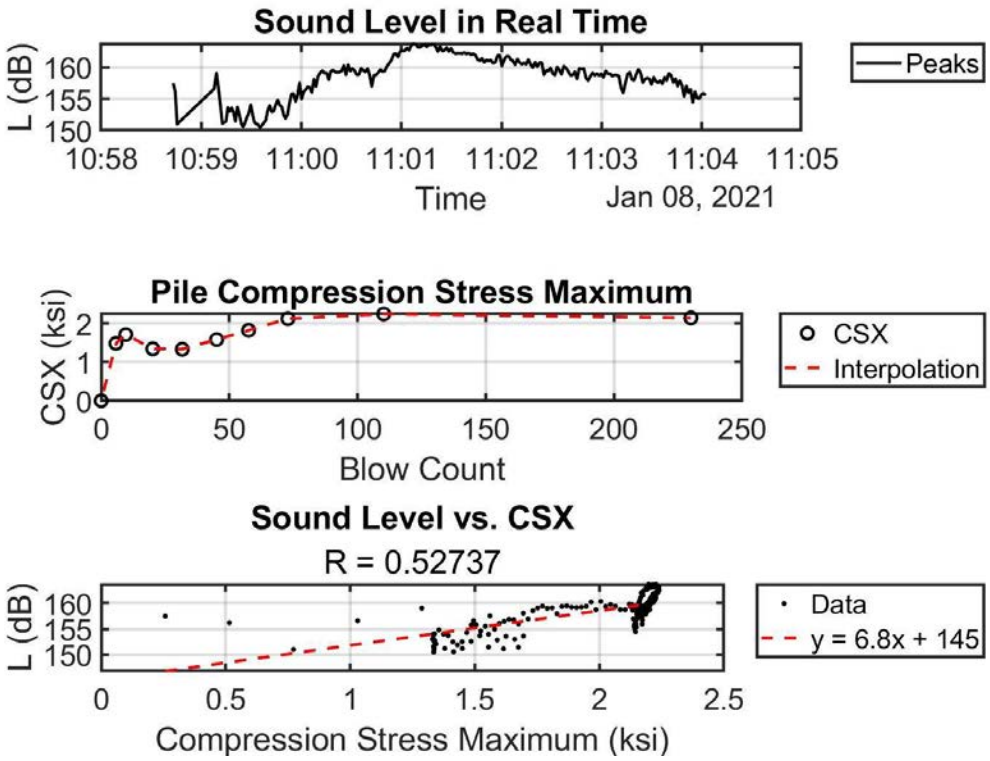

Figure 3-24. Sound Level vs. Maximum Pile Compression Stress

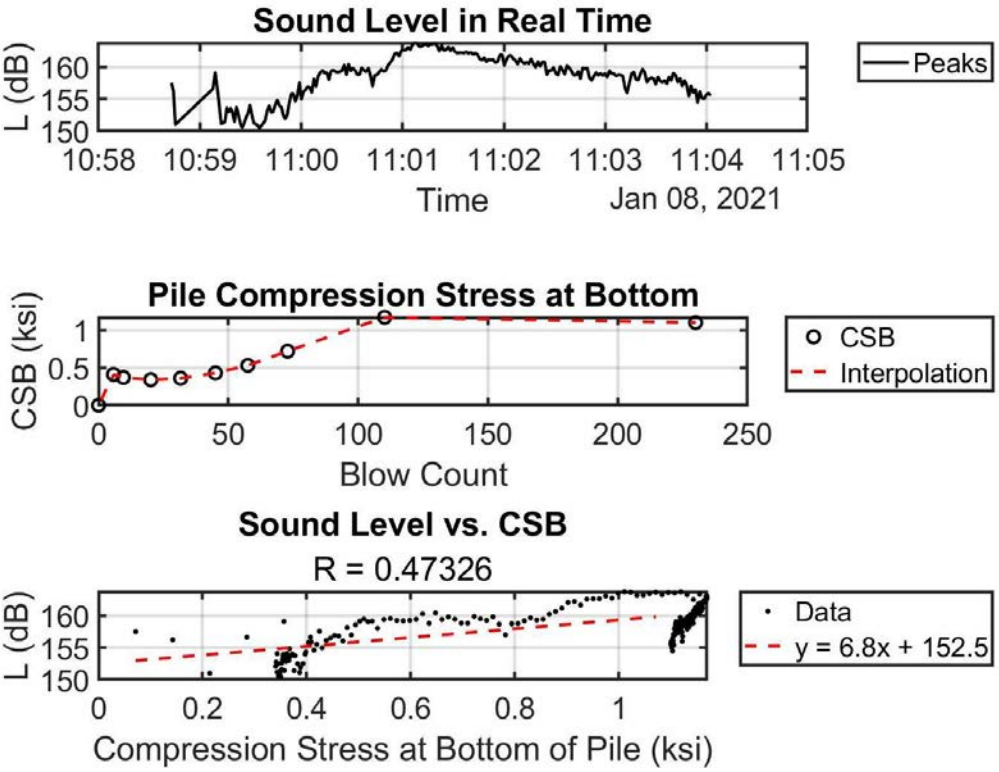

Figure 3-26. Sound Level vs. Pile Compression Stress at Bottom

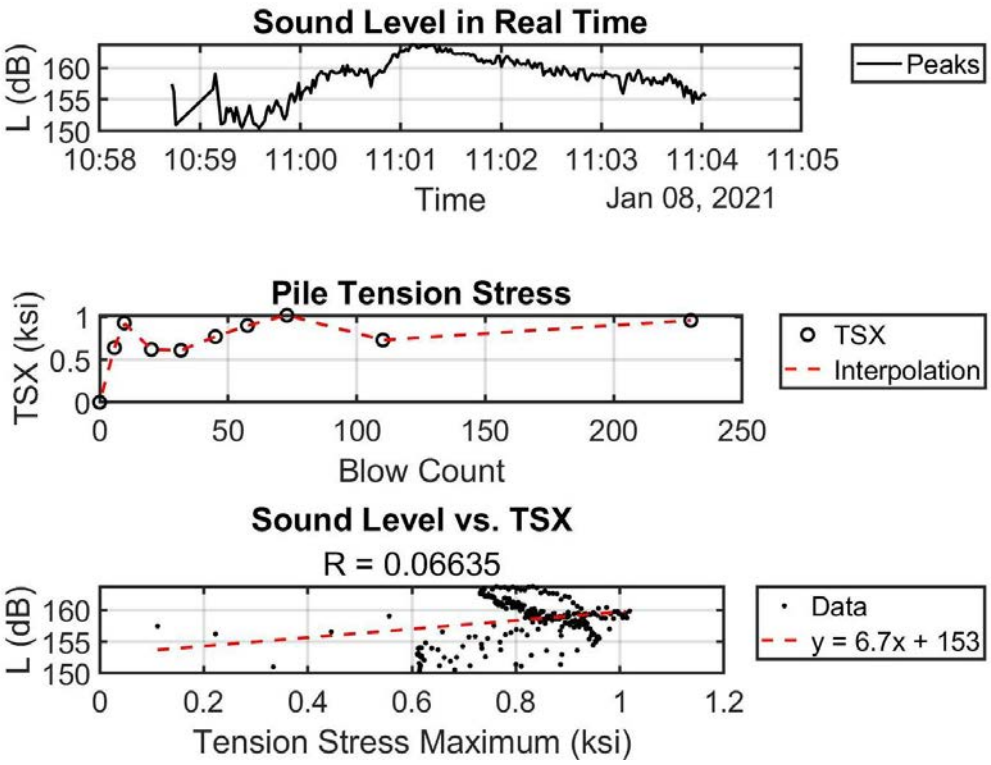

Figure 3-27. Sound Level vs. Pile Tension Stress

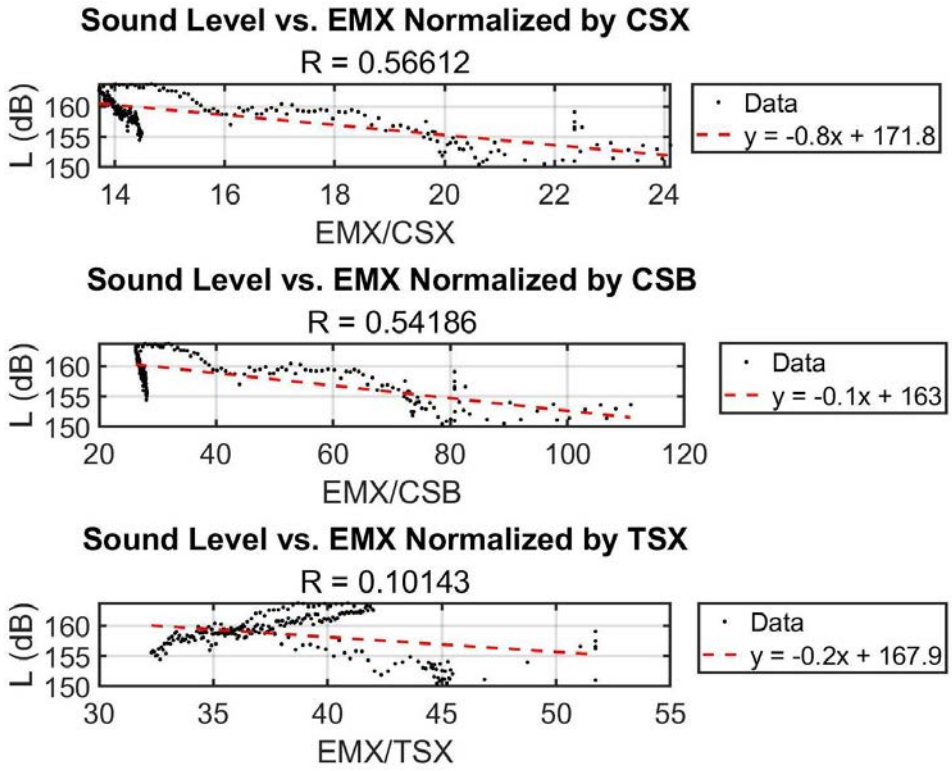

Figure 3-28. Sound Level vs. Hammer Energy normalized by Pile Stresses

3.3.2 SR-23 over Black Creek, FL – Pile 2

- Date: 01/08/2021
- Pile: Intermediate Pier 4 Pile 2
- Dimensions: 24” x 90’ PSC Production Pile

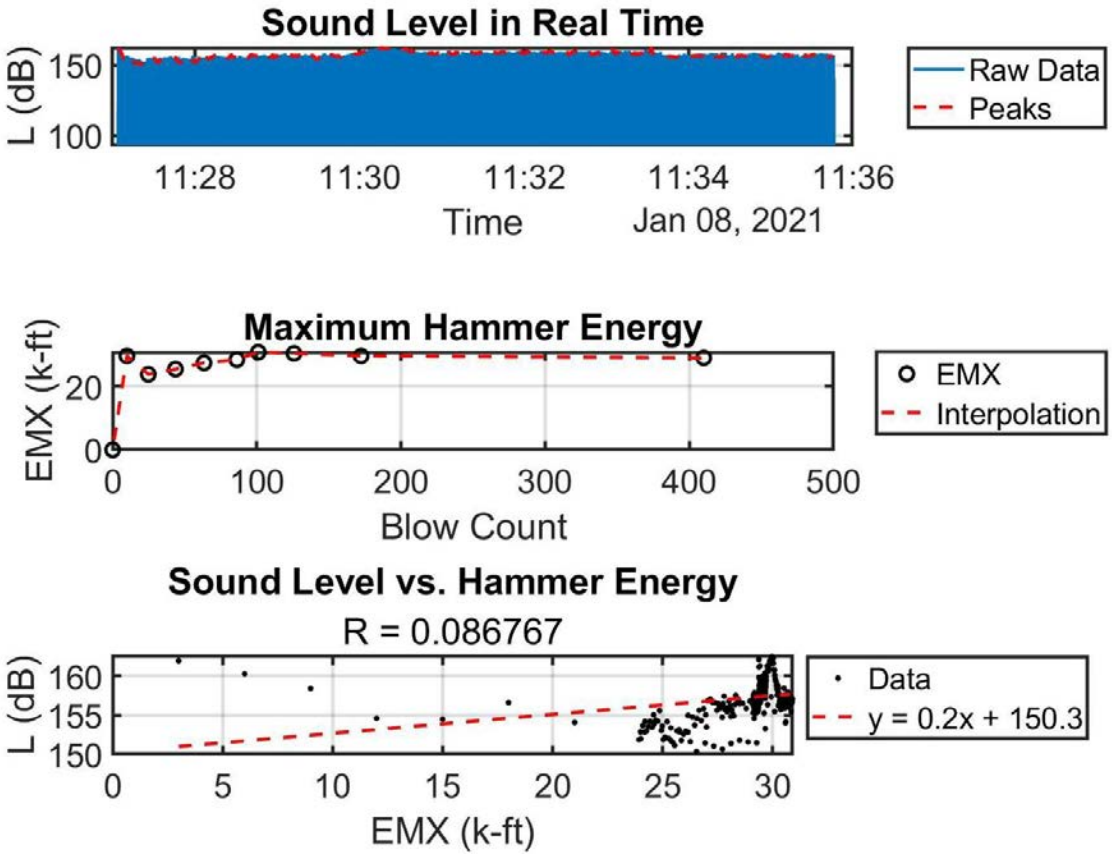

Figure 3-29. Sound Level vs. Hammer Energy (EMX)

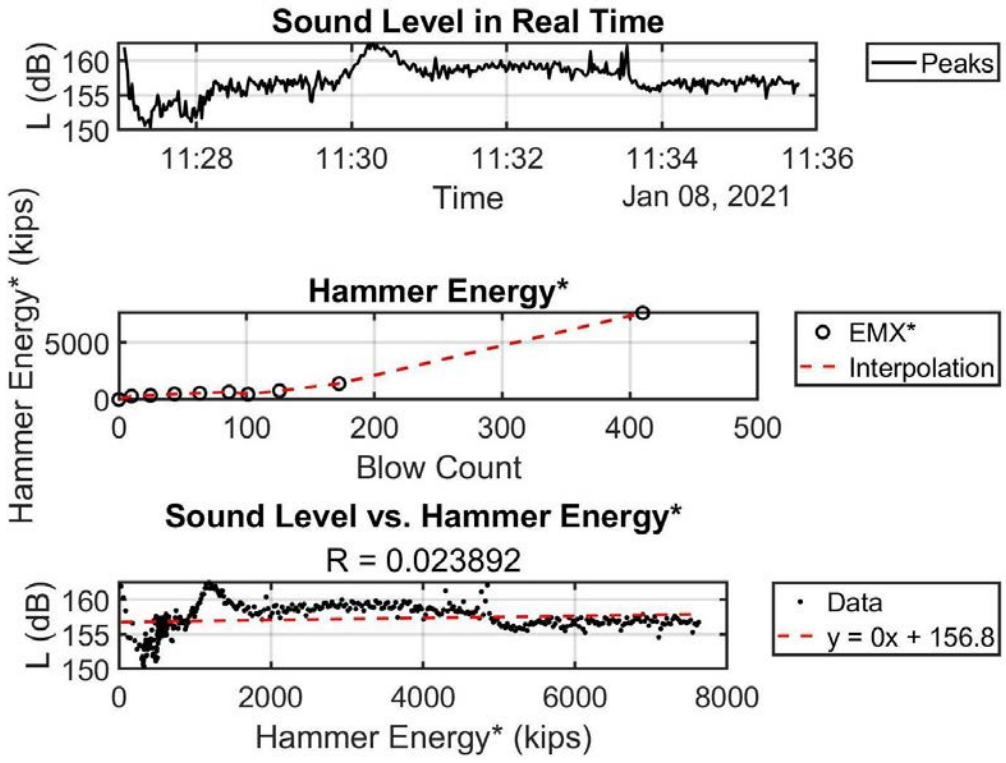

Figure 3-30. Sound Level vs. Hammer Energy normalized by Blow Count

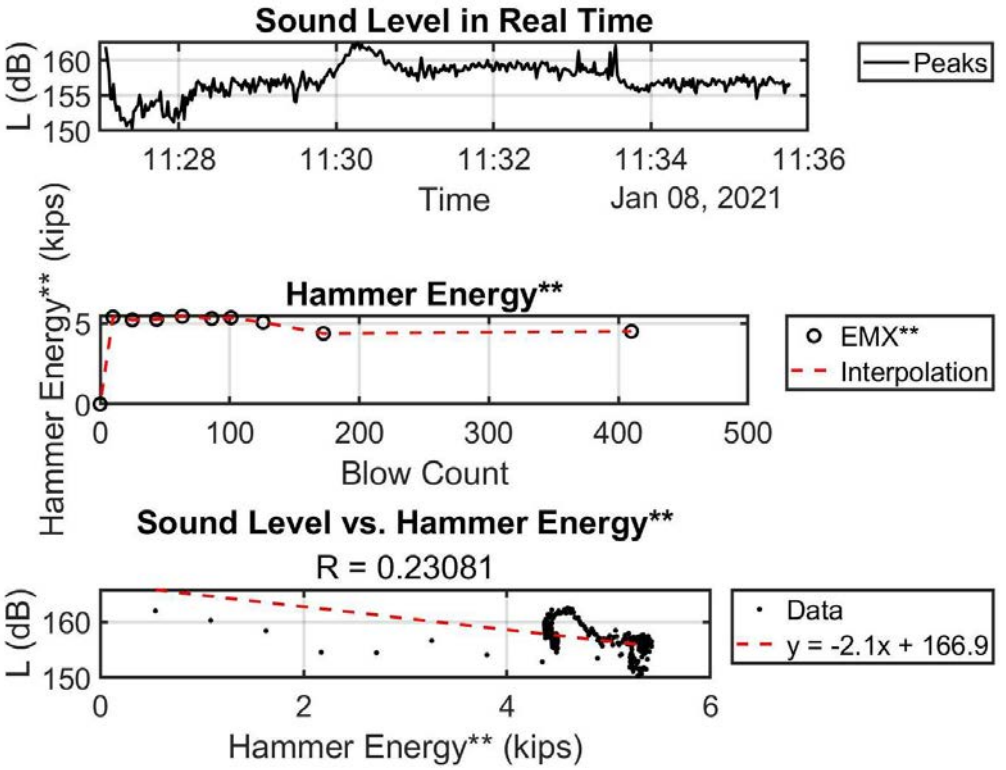

Figure 3-31. Sound Level vs. Hammer Energy normalized by Hammer Stroke Height

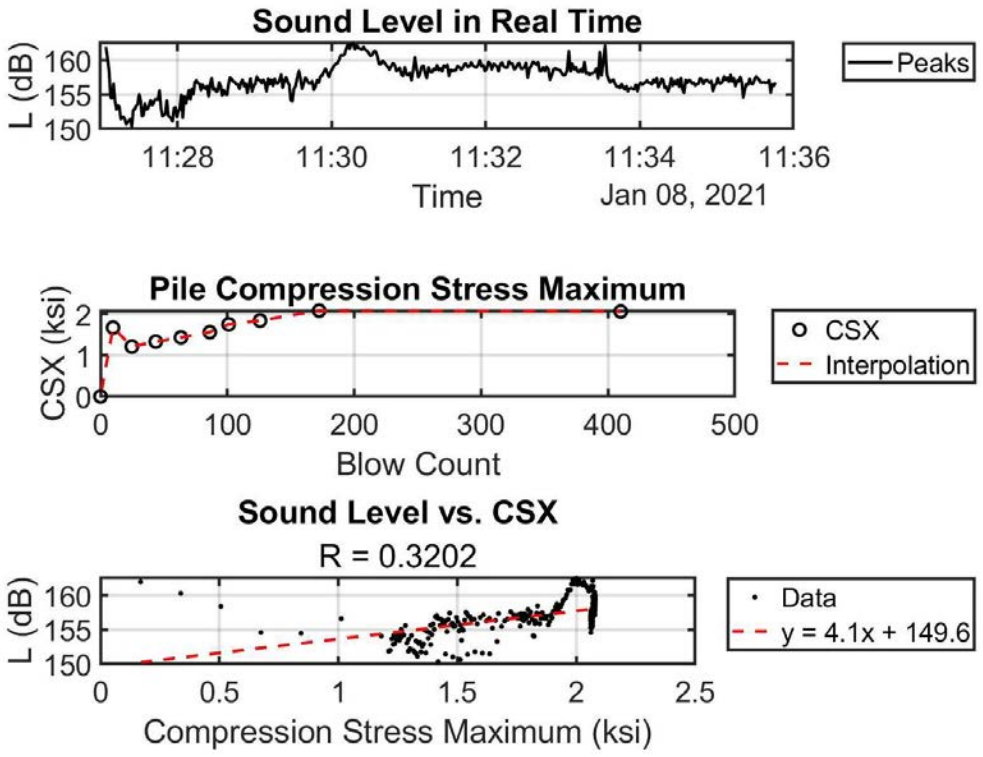

Figure 3-32. Sound Level vs. Maximum Pile Compression Stress

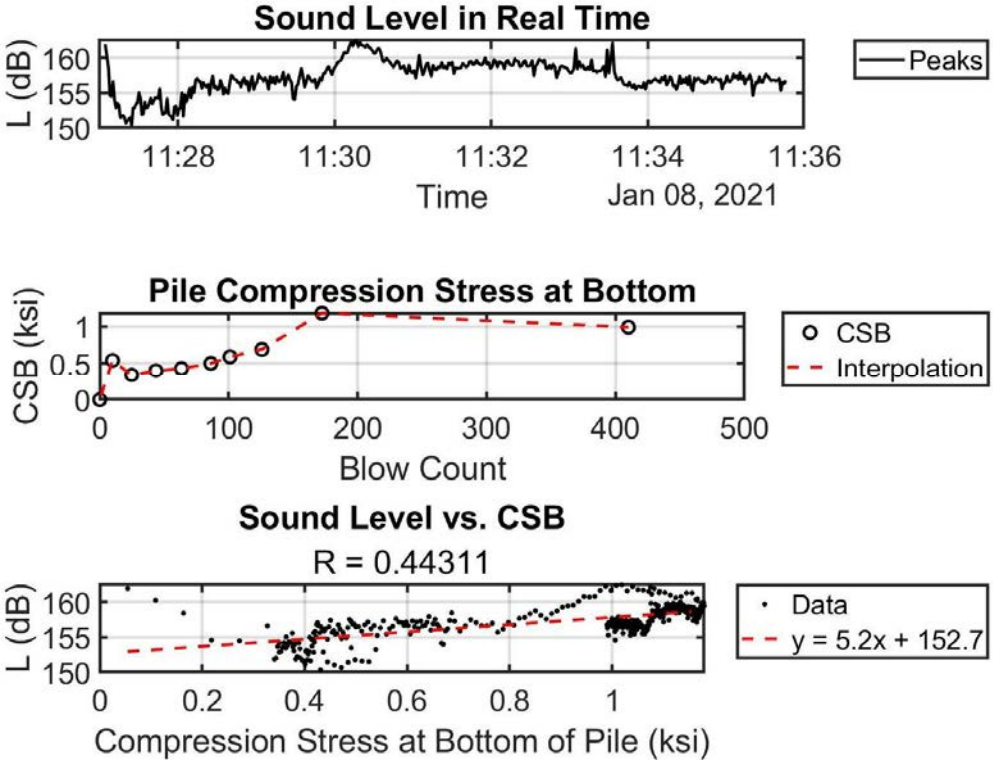

Figure 3-33. Sound Level vs. Pile Compression Stress at Bottom

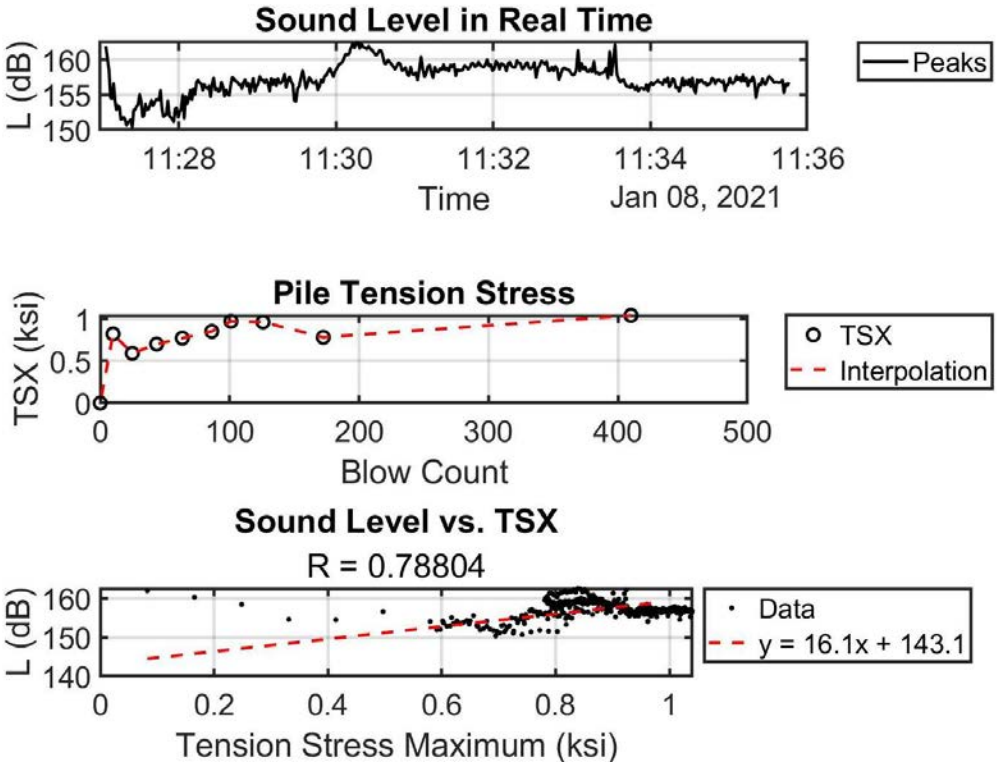

Figure 3-34. Sound Level vs. Pile Tension Stress

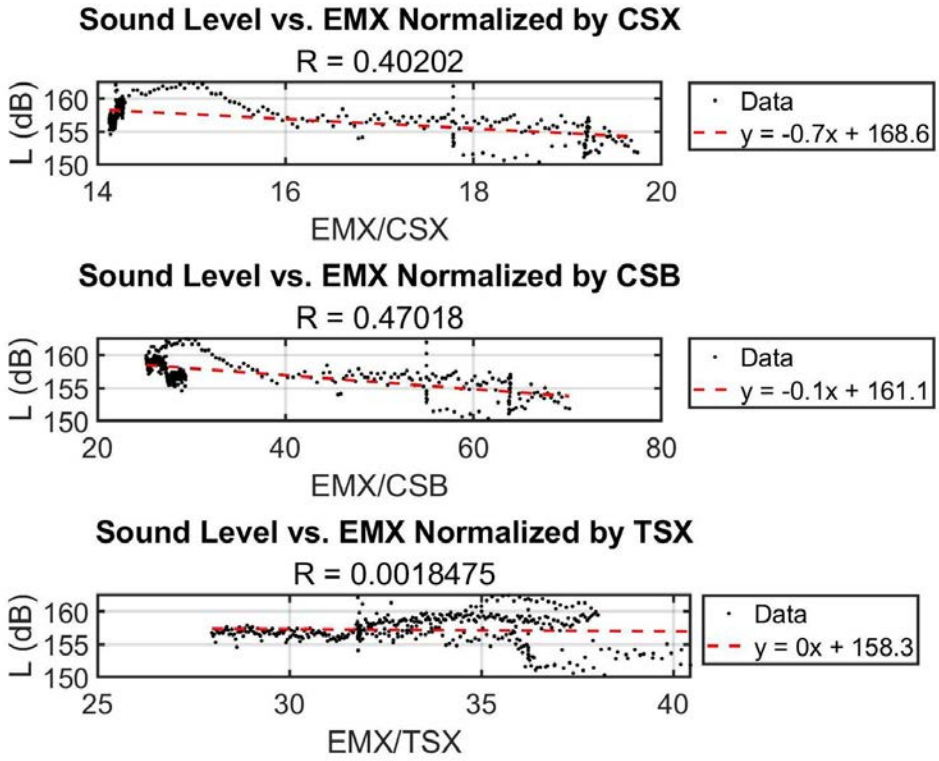

Figure 3-35. Sound Level vs. Hammer Energy normalized by Pile Stresses

3.3.3 SR-23 over Black Creek, FL – Pile 3

- Date: 01/08/2021
- Pile: Intermediate Pier 4 Pile 3
- Dimensions: 24” x 90’ PSC Production Pile

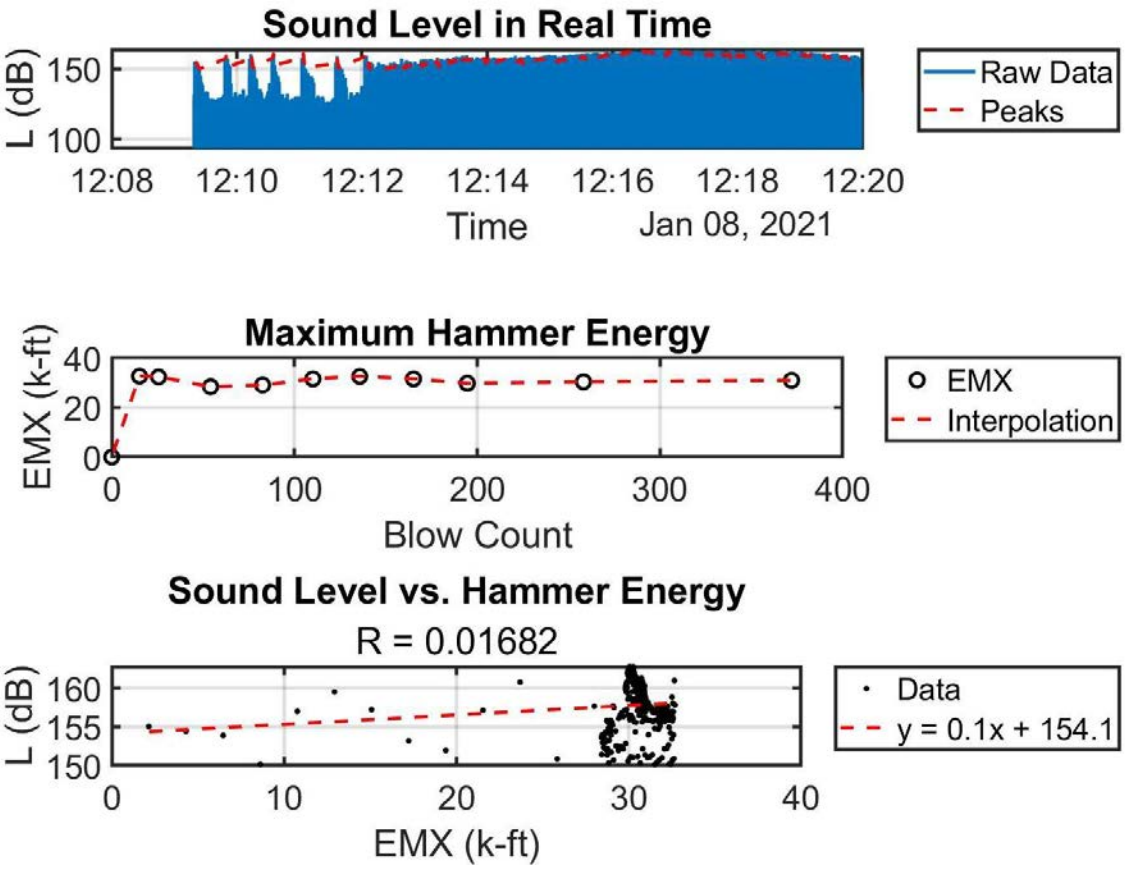

Figure 3-36. Sound Level vs. Hammer Energy (EMX)

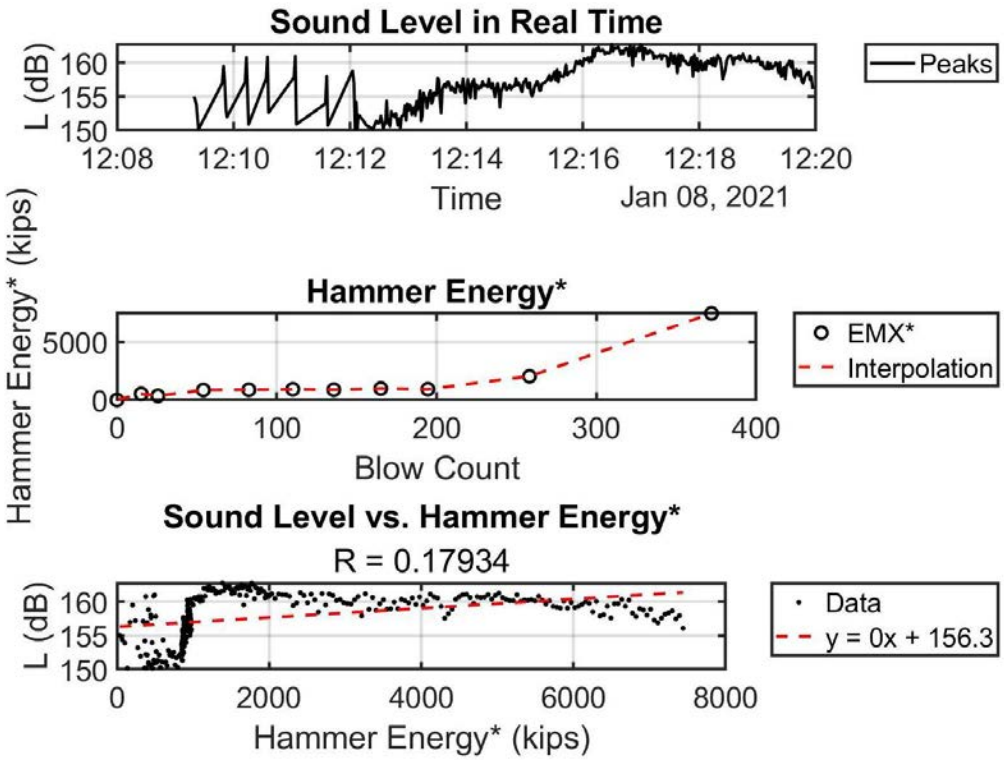

Figure 3-37. Sound Level vs. Hammer Energy normalized by Blow Count

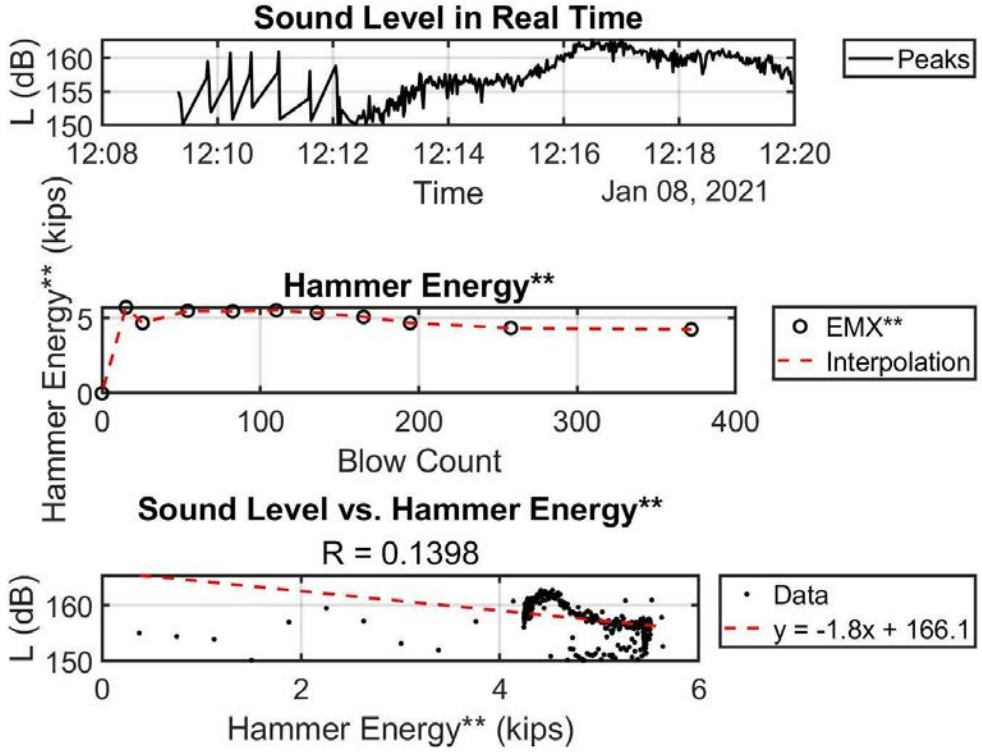

Figure 3-38. Sound Level vs. Hammer Energy normalized by Hammer Stroke Height

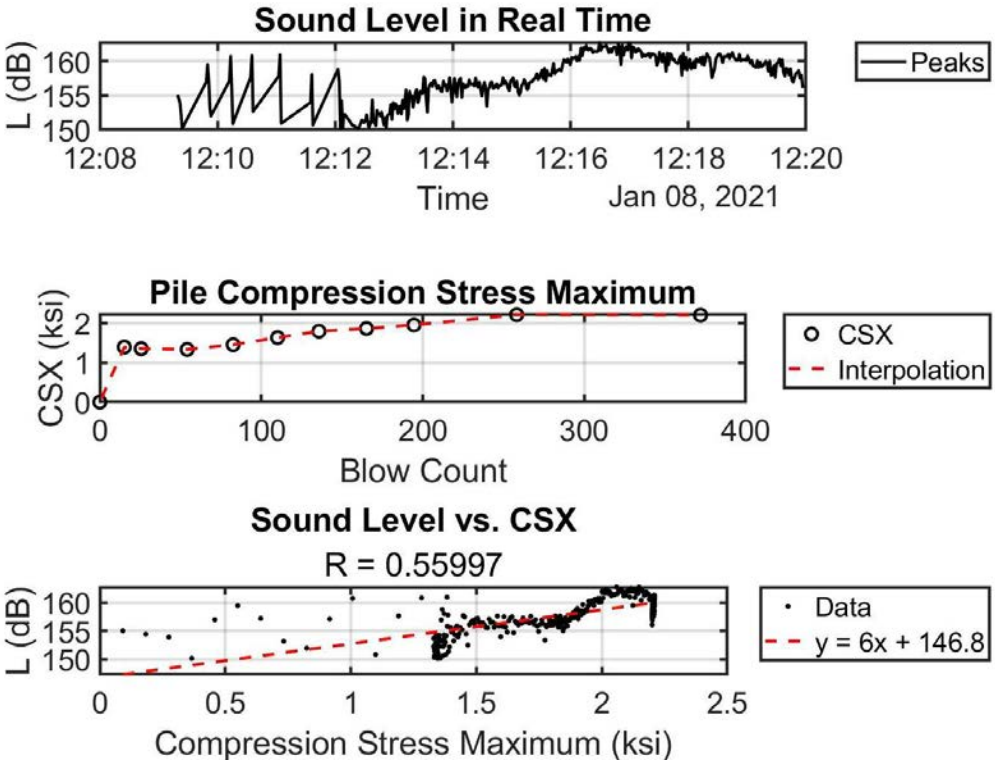

Figure 3-39. Sound Level vs. Maximum Pile Compression Stress

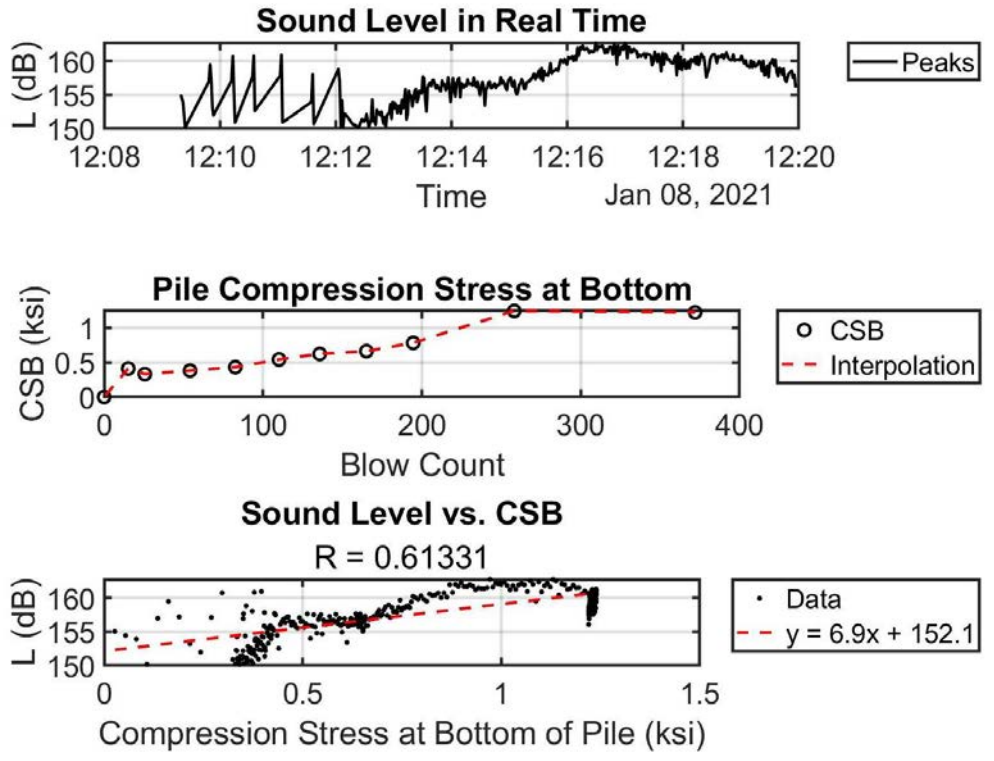

Figure 3-40. Sound Level vs. Pile Compression Stress at Bottom

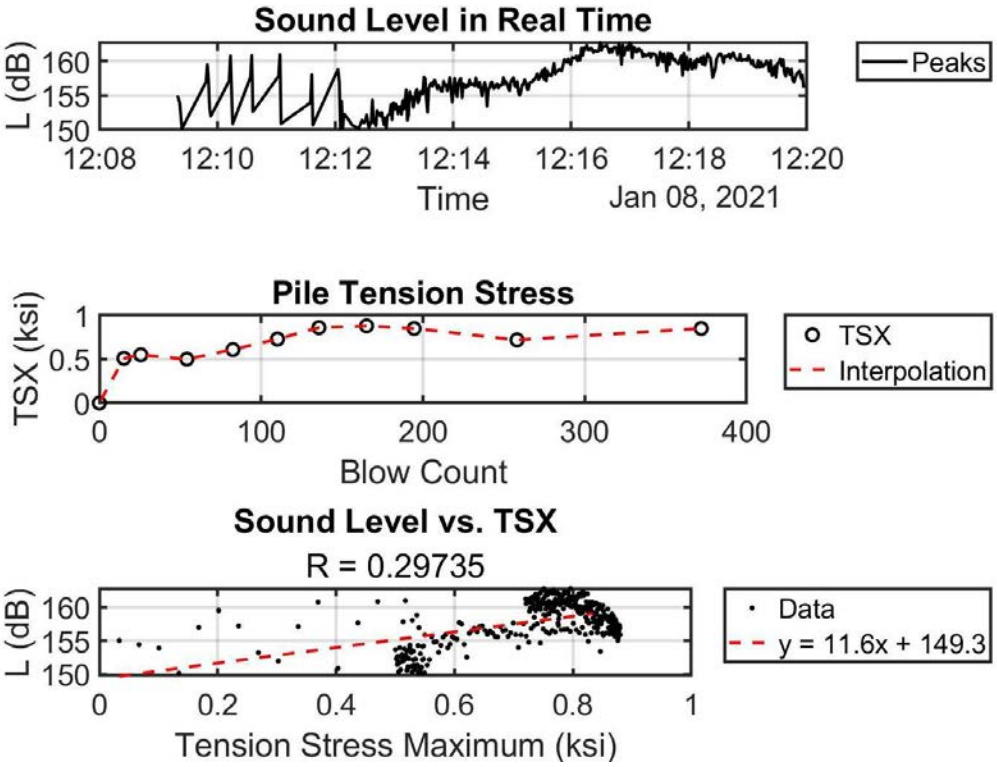

Figure 3-41. Sound Level vs. Pile Tension Stress

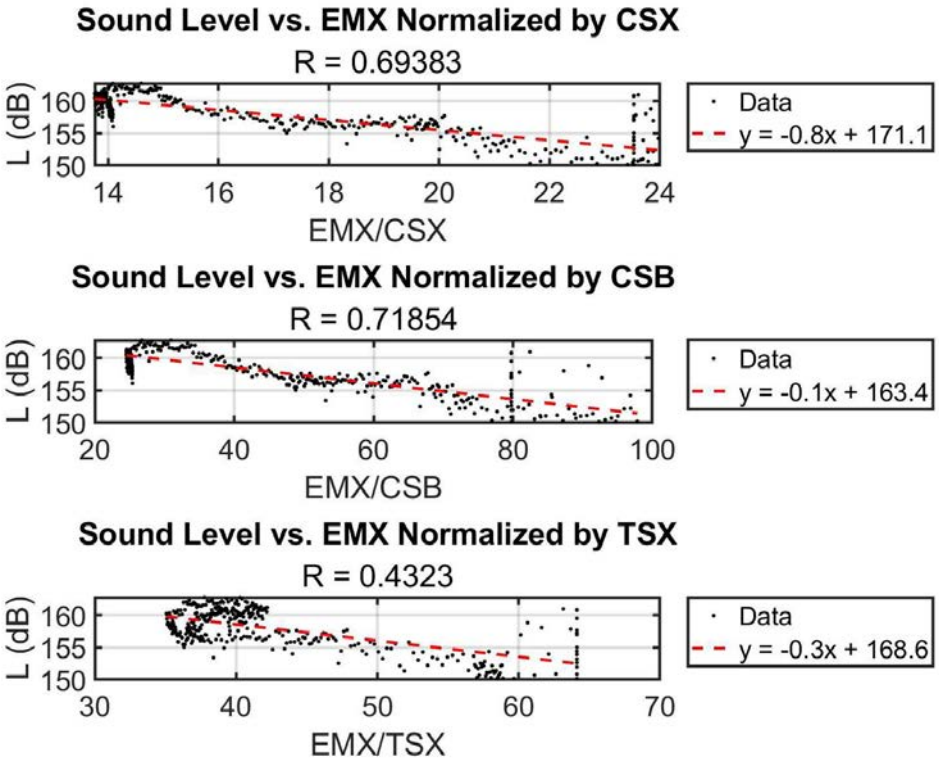

Figure 3-42. Sound Level vs. Hammer Energy normalized by Pile Stresses

3.3.4 SR-23 over Black Creek, FL – Pile 4

- Date: 01/08/2021
- Pile: Intermediate Pier 4 Pile 4
- Dimensions: 24” x 90’ PSC Production Pile

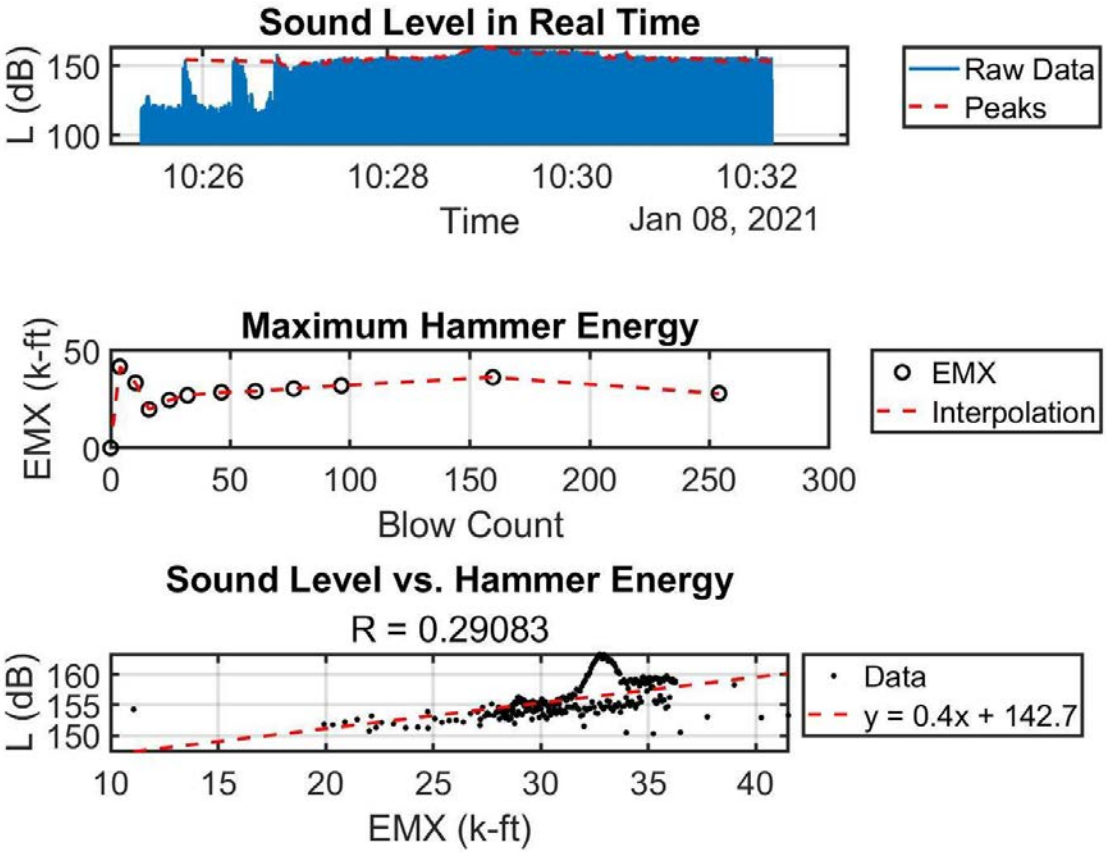

2

Figure 3-43. Sound Level vs. Hammer Energy (EMX)

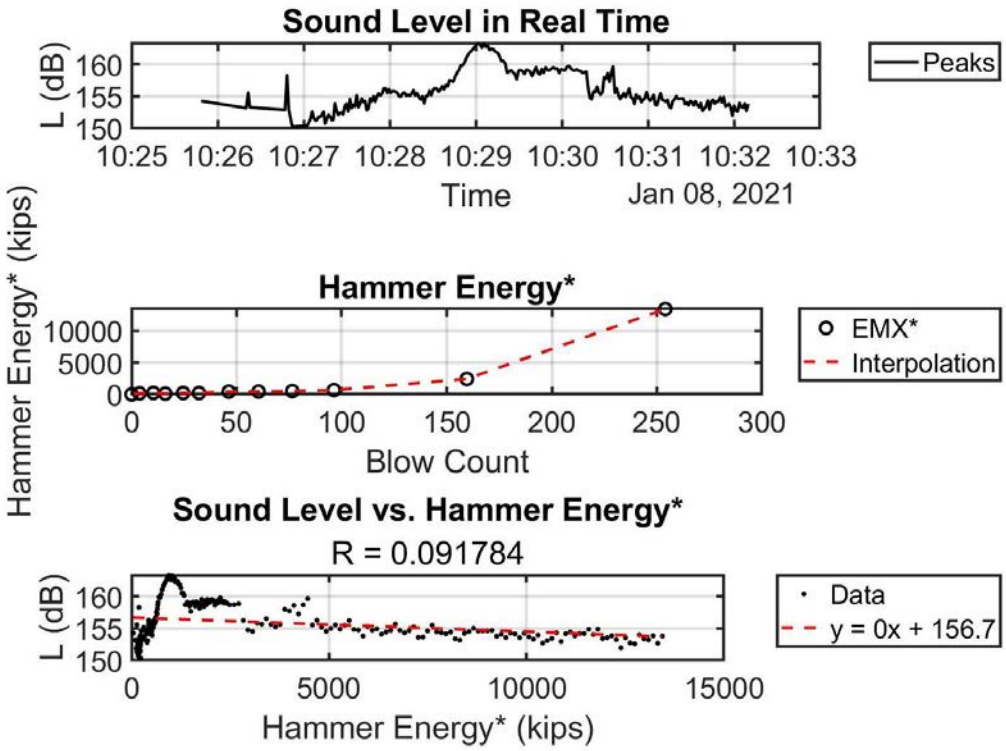

Figure 3-44. Sound Level vs. Hammer Energy normalized by Blow Count

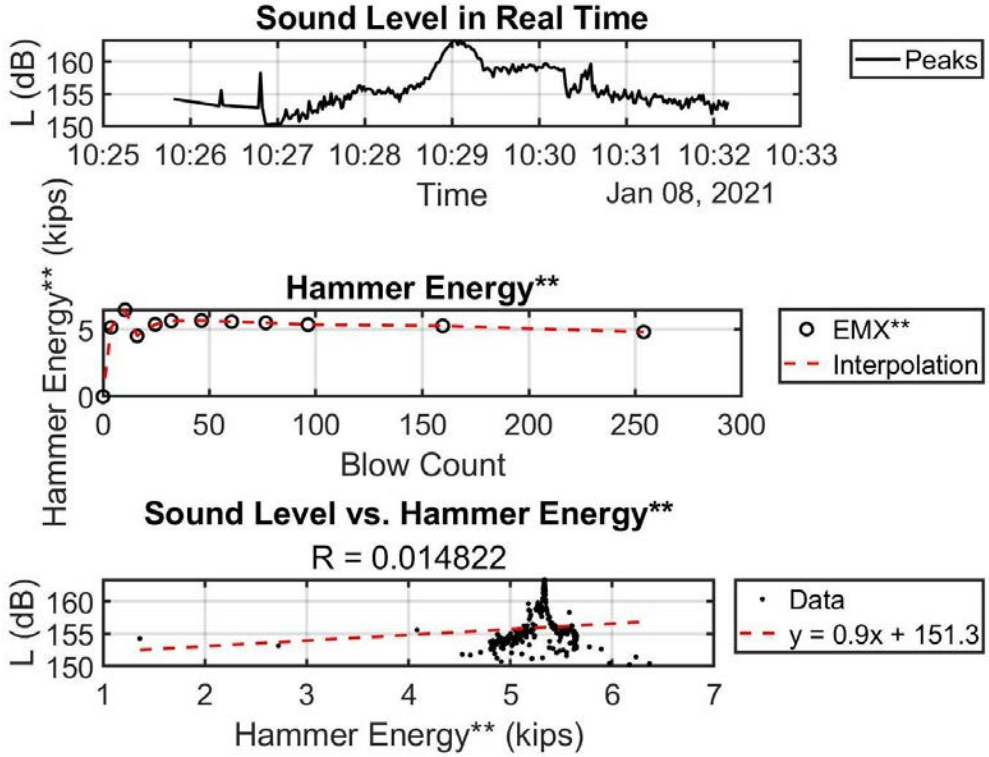

Figure 3-45. Sound Level vs. Hammer Energy normalized by Hammer Stroke Height

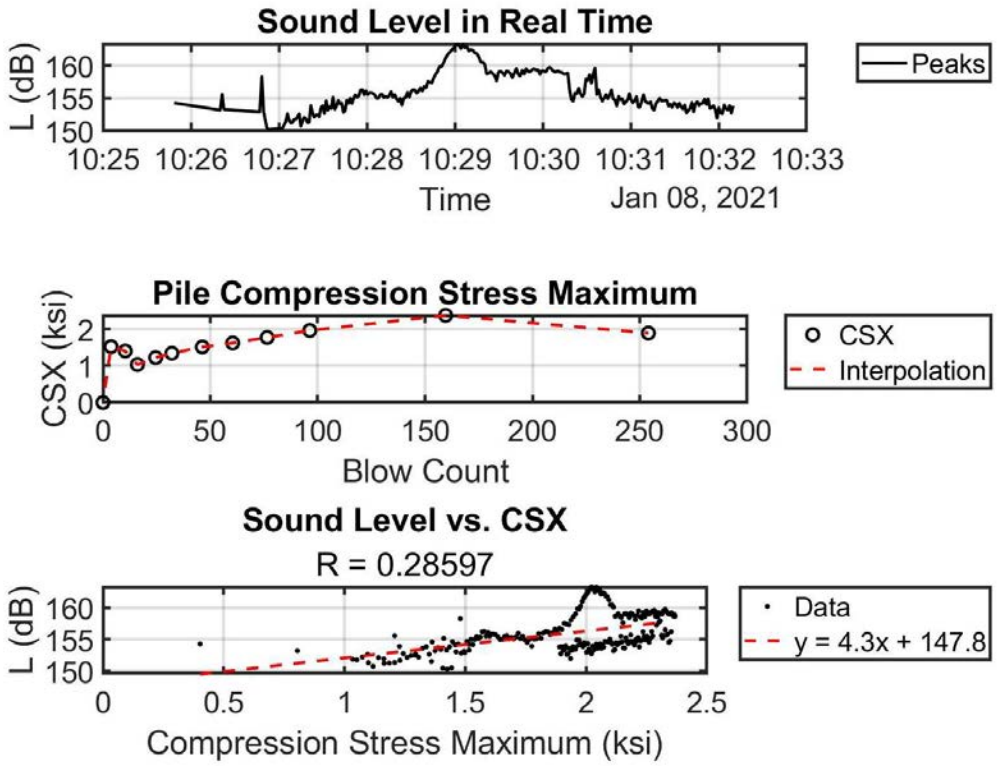

Figure 3-46. Sound Level vs. Maximum Pile Compression Stress

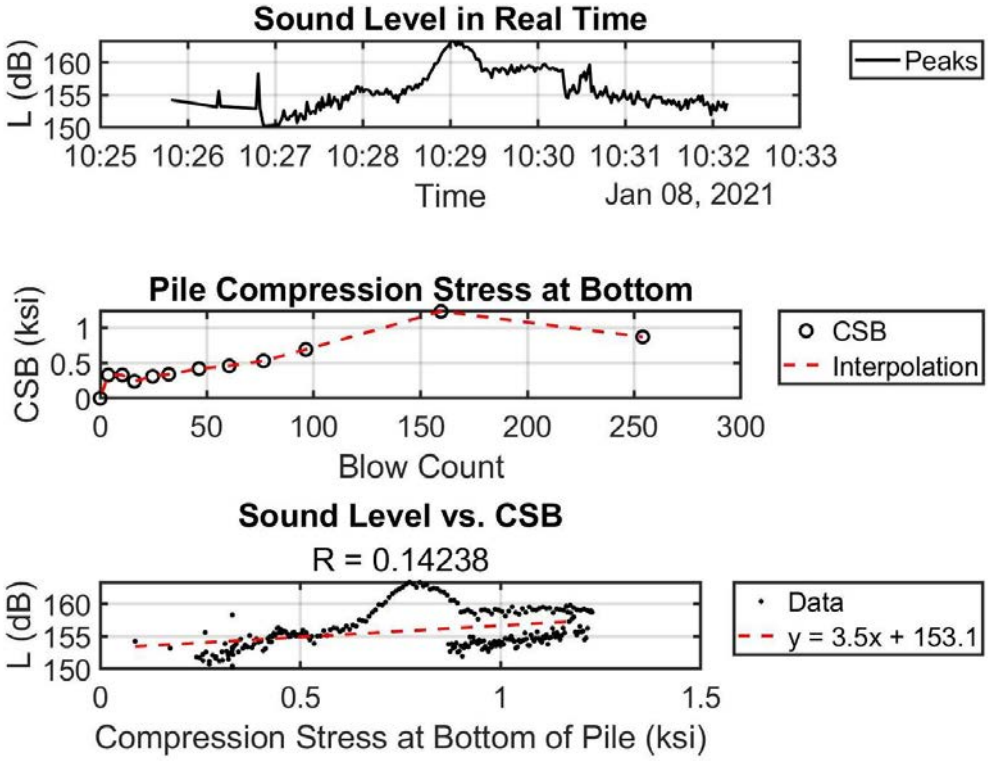

Figure 3-47. Sound Level vs. Pile Compression Stress at Bottom

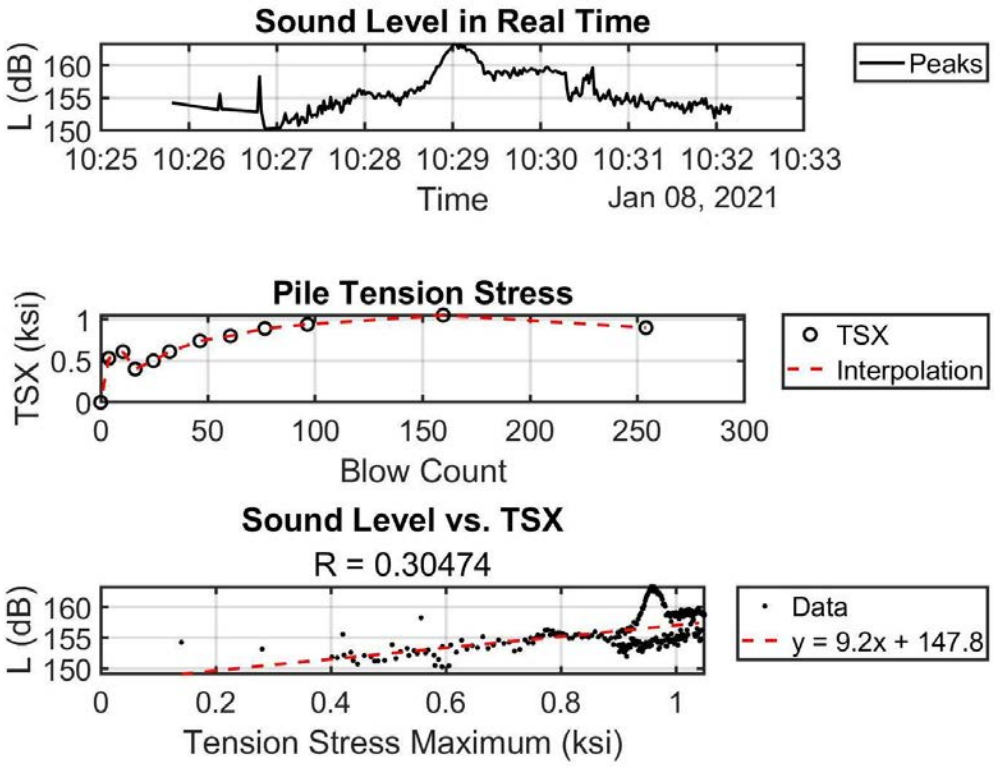

Figure 3-48. Sound Level vs. Pile Tension Stress

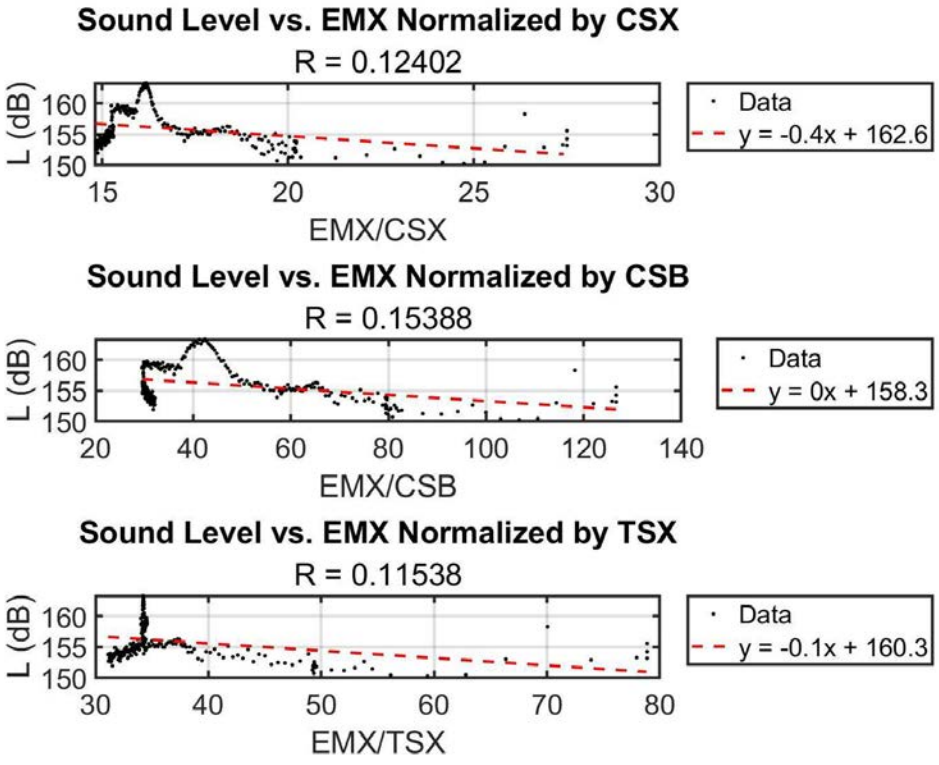

Figure 3-49. Sound Level vs. Hammer Energy normalized by Pile Stresses

3.3.5 SR-23 over Black Creek, FL – Pile 5

- Date: 01/08/2021
- Pile: Intermediate Pier 4 Pile 5
- Dimensions: 24” x 90’ PSC Production Pile

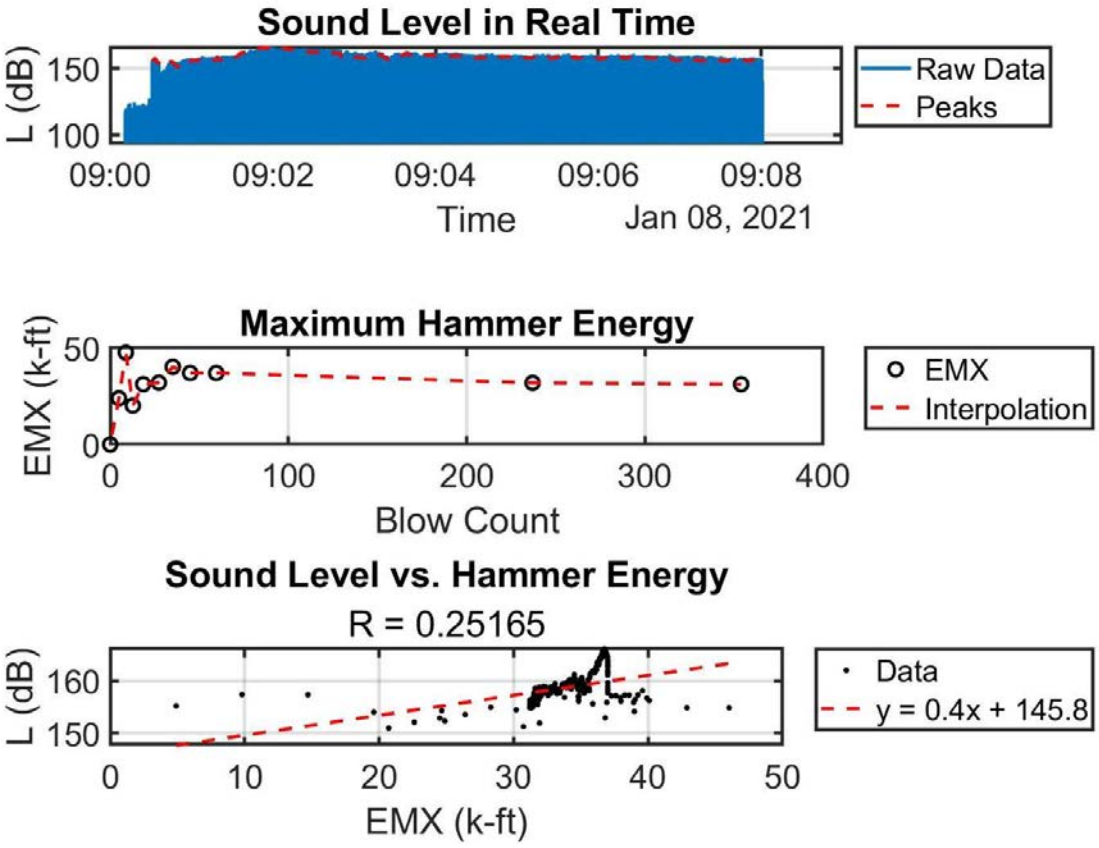

Figure 3-50. Sound Level vs. Hammer Energy (EMX)

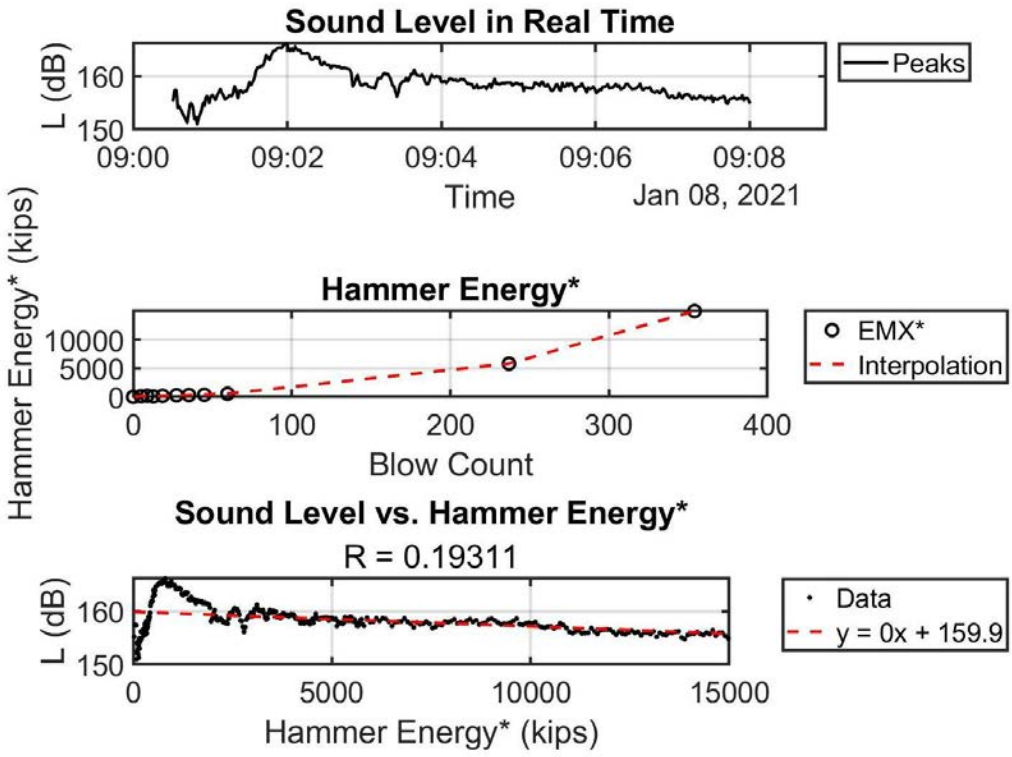

Figure 3-51. Sound Level vs. Hammer Energy normalized by Blow Count

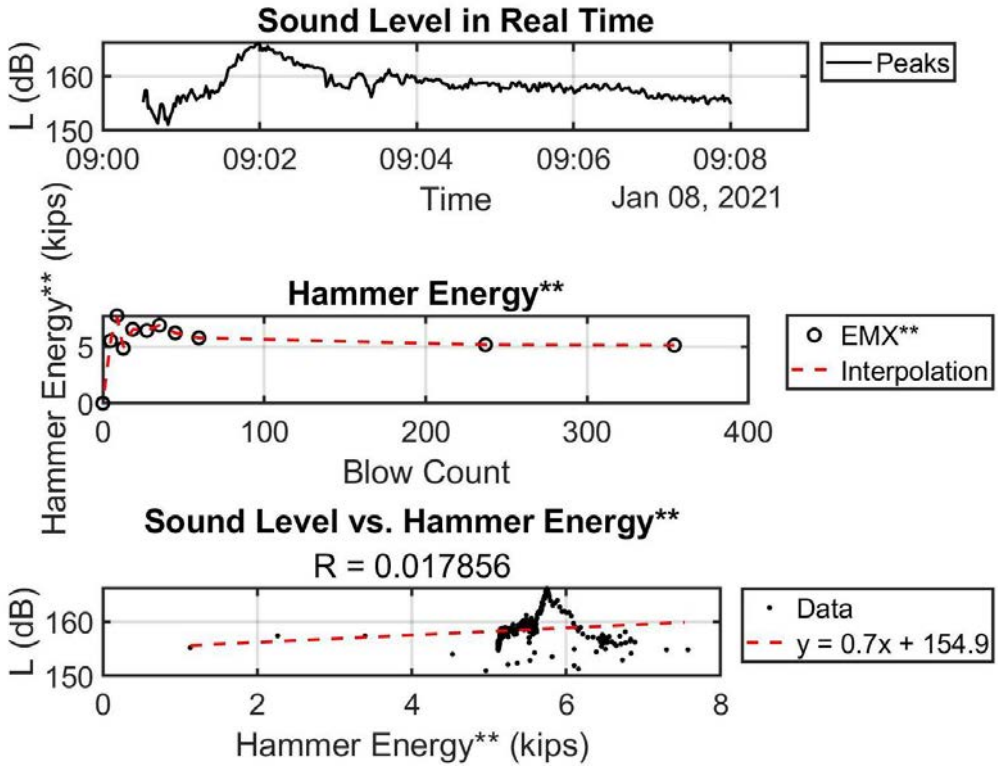

Figure 3-52. Sound Level vs. Hammer Energy normalized by Hammer Stroke Height

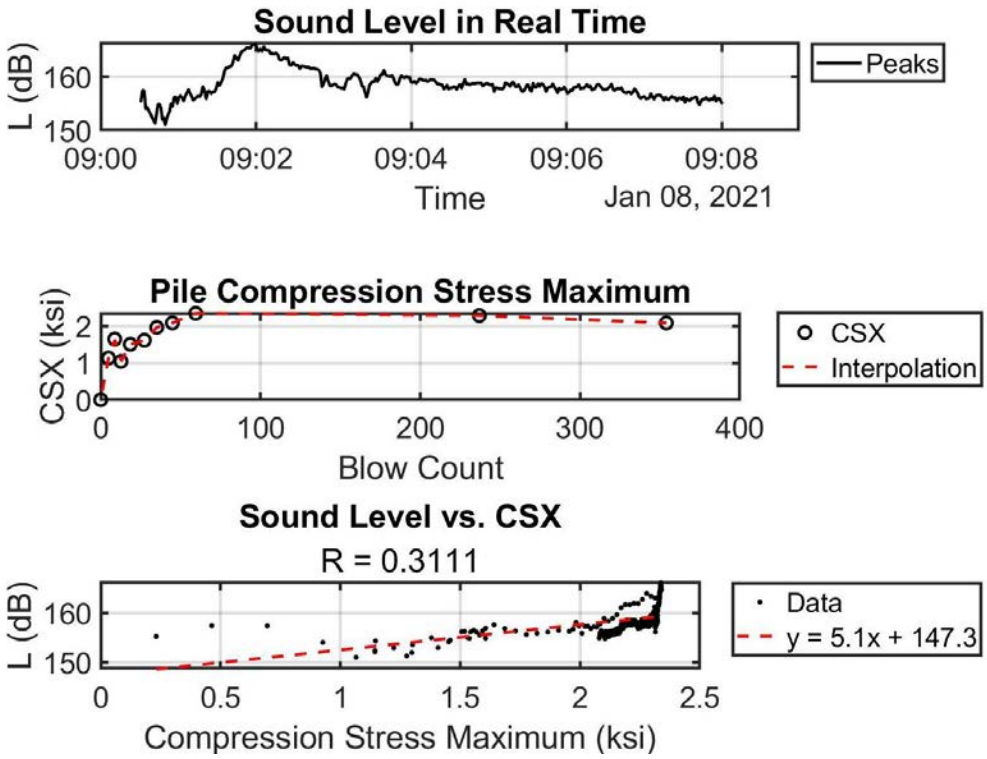

Figure 3-4. Sound Level vs. Maximum Pile Compression Stress

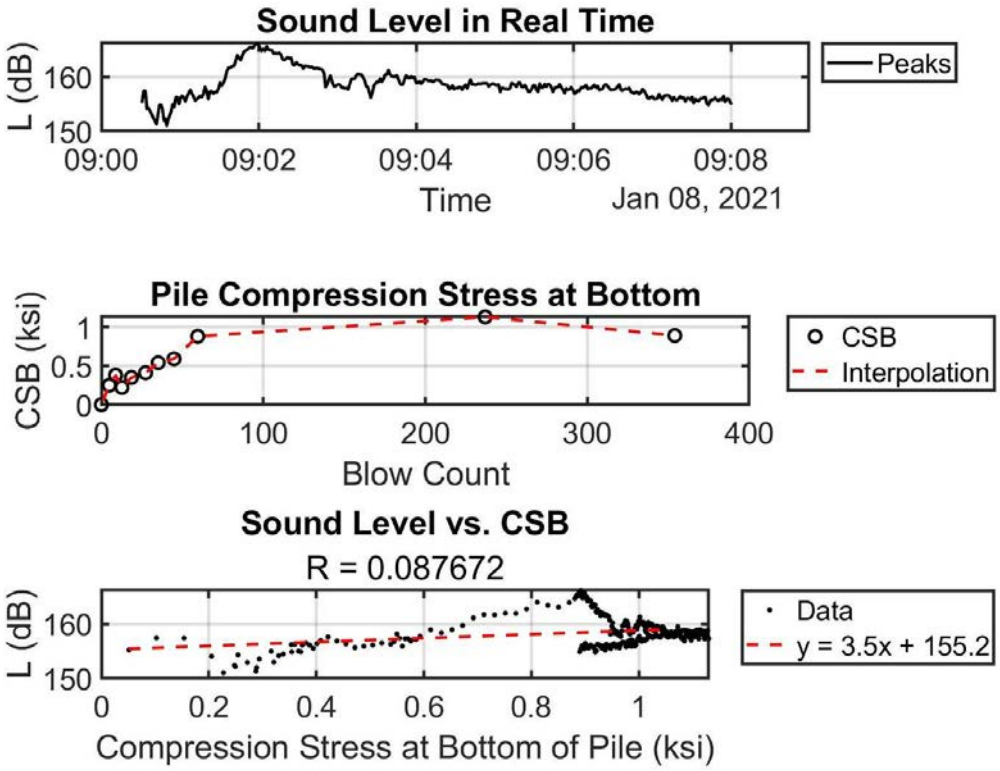

Figure 3-53. Sound Level vs. Pile Compression Stress at Bottom

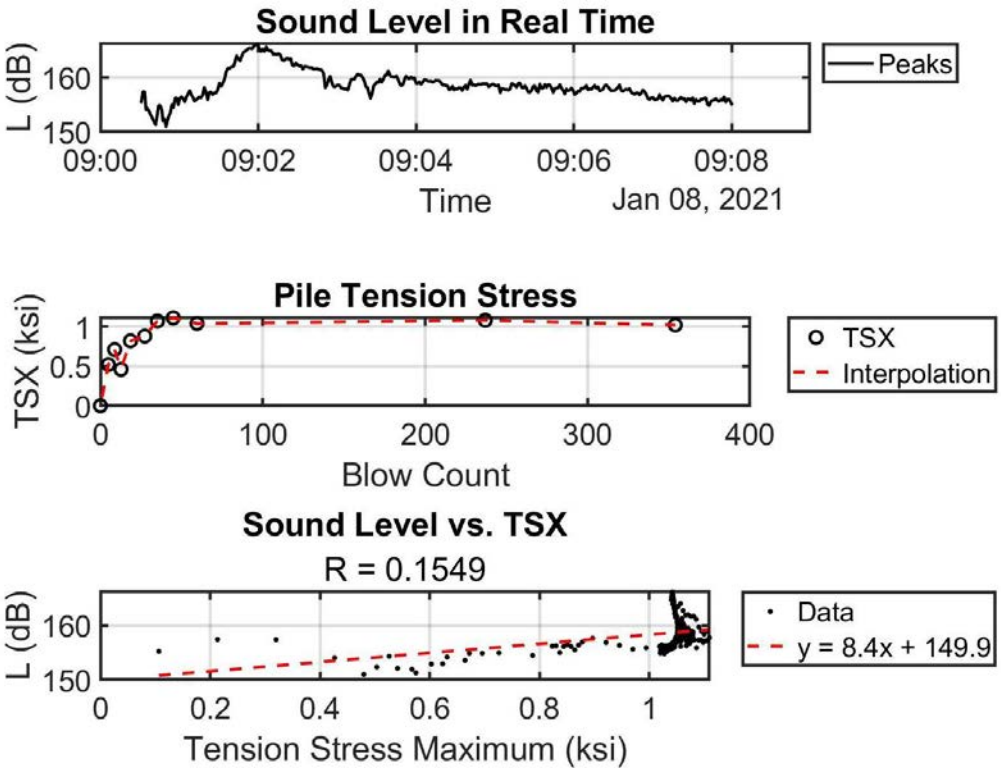

Figure 3-54. Sound Level vs. Pile Tension Stress

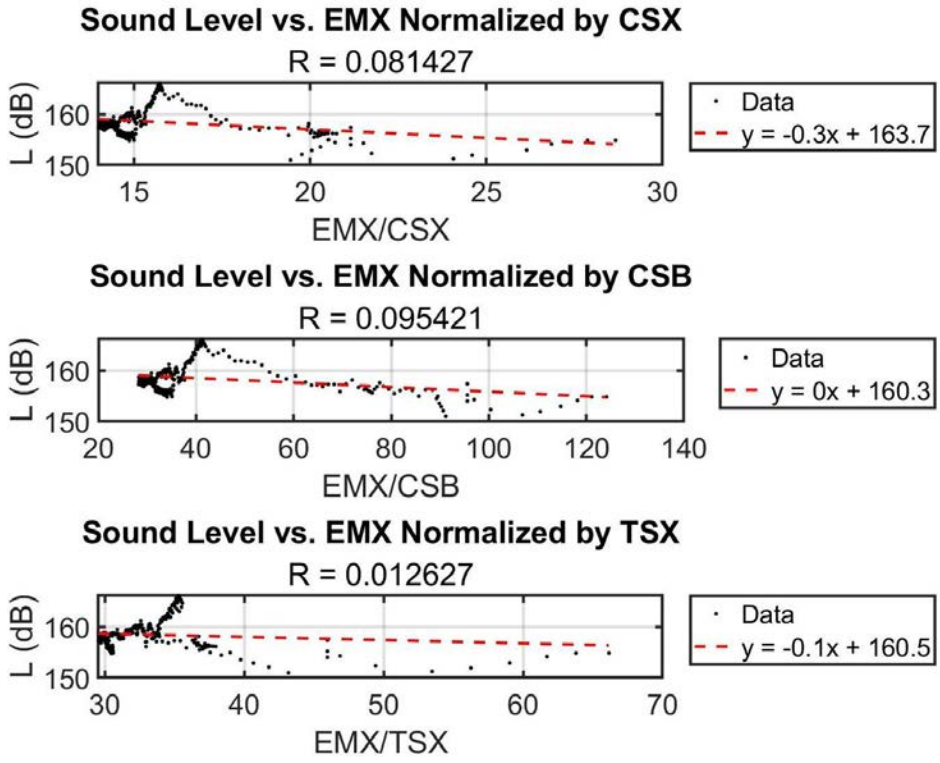

Figure 3-55. Sound Level vs. Hammer Energy normalized by Pile Stresses

3.3.6 SR-23 over Black Creek, FL – Pile 6

- Date: 01/08/2021
- Pile: Intermediate Pier 4 Pile 6
- Dimensions: 24” x 90’ PSC Production Pile

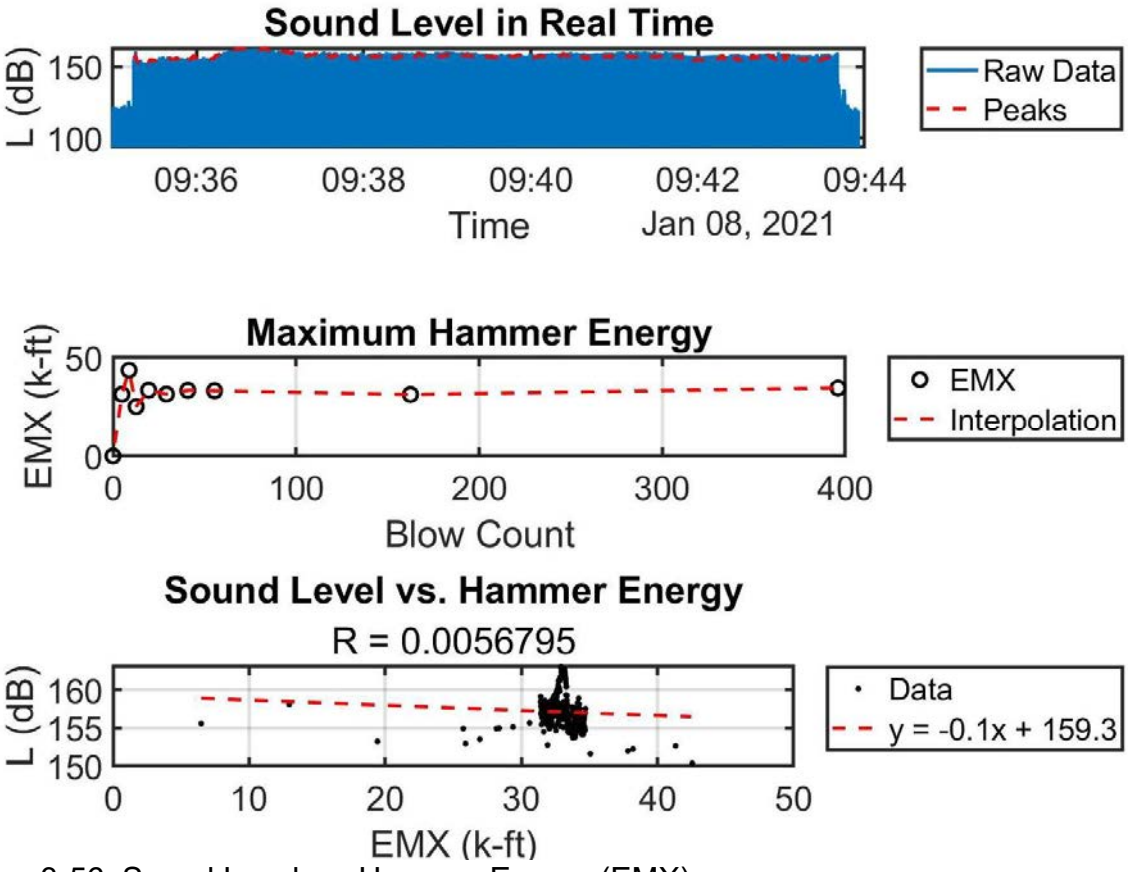

Figure 3-56. Sound Level vs. Hammer Energy (EMX)

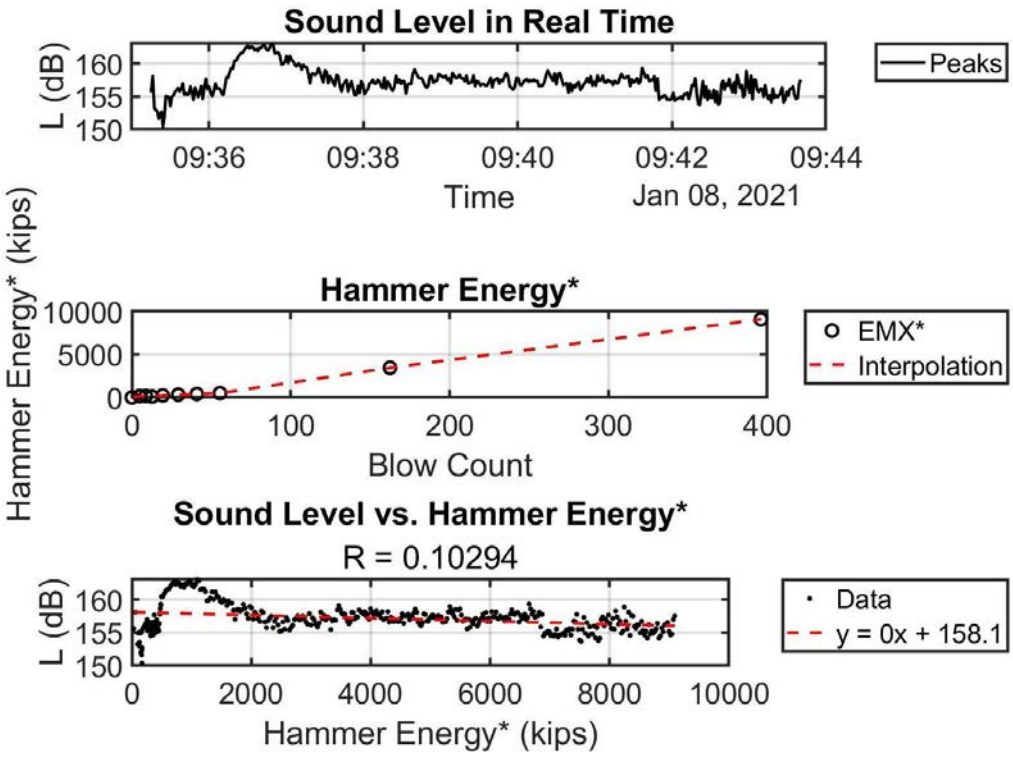

Figure 3-57. Sound Level vs. Hammer Energy normalized by Blow Count

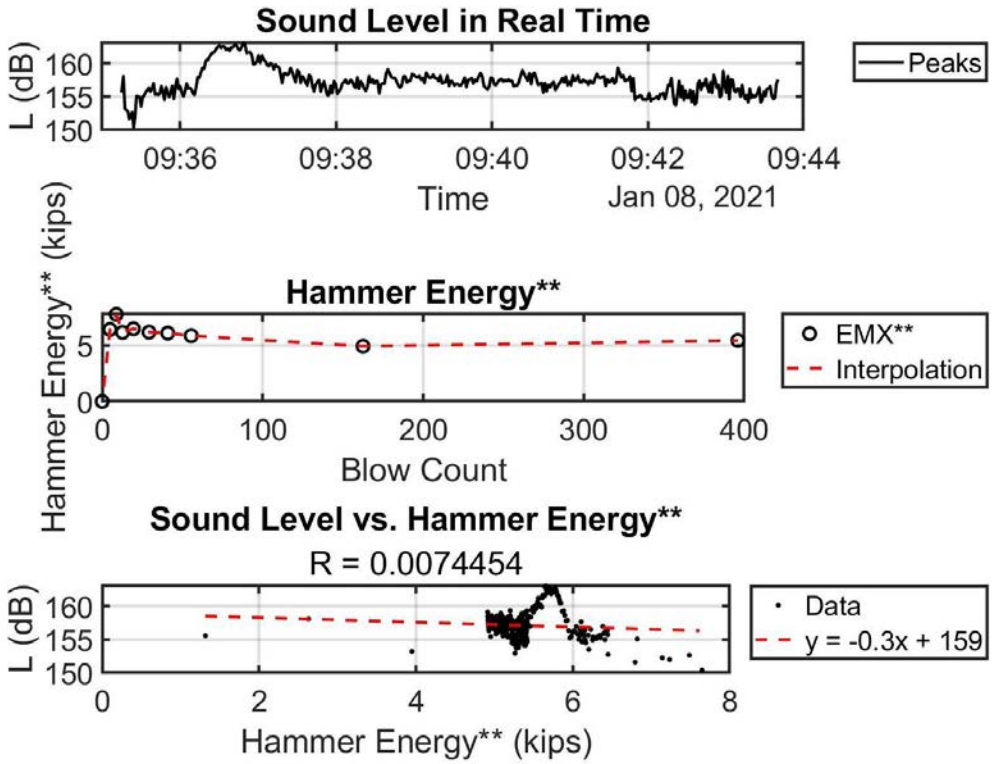

Figure 3-58. Sound Level vs. Hammer Energy normalized by Hammer Stroke Height

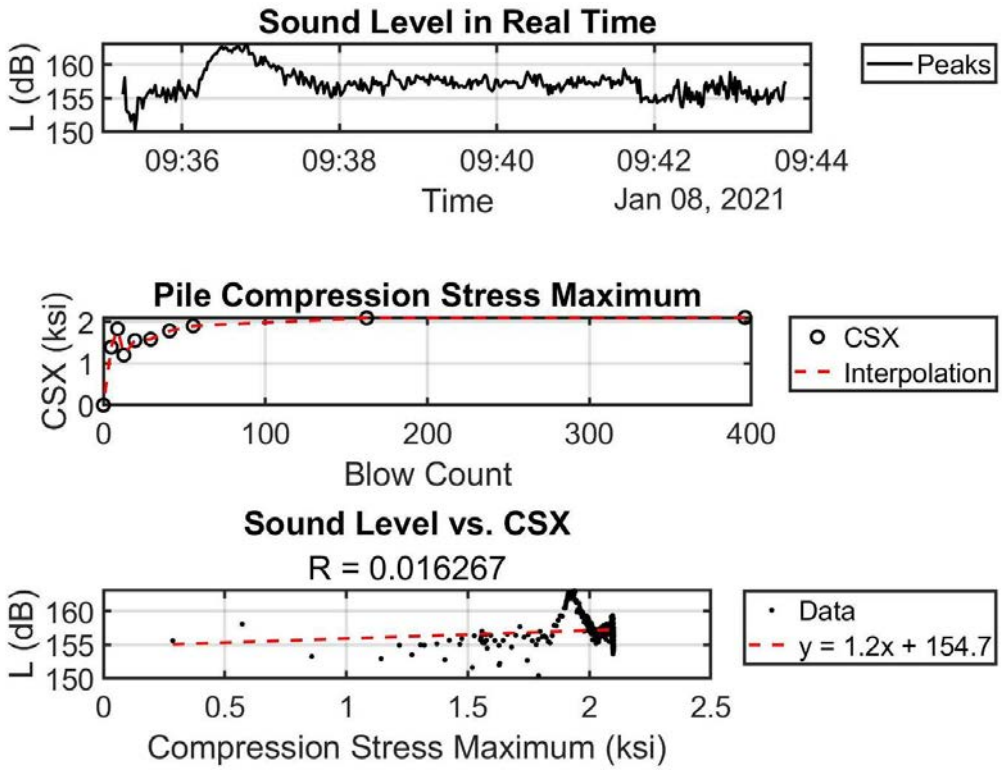

Figure 3-59. Sound Level vs. Maximum Pile Compression Stress

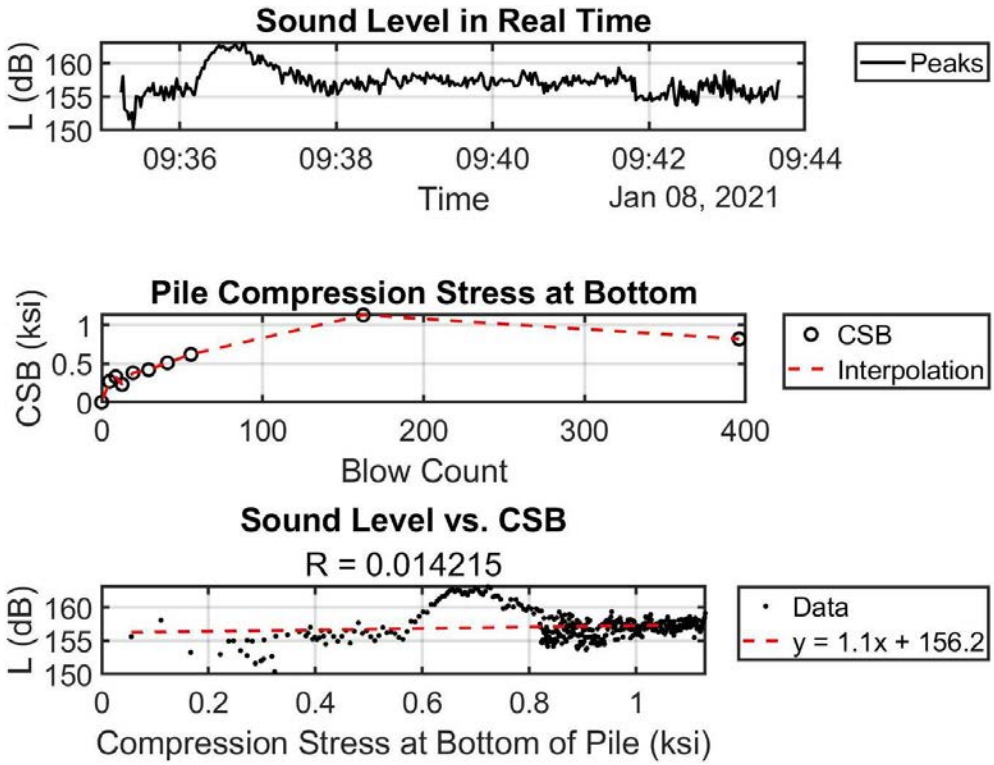

Figure 3-60. Sound Level vs. Pile Compression Stress at Bottom

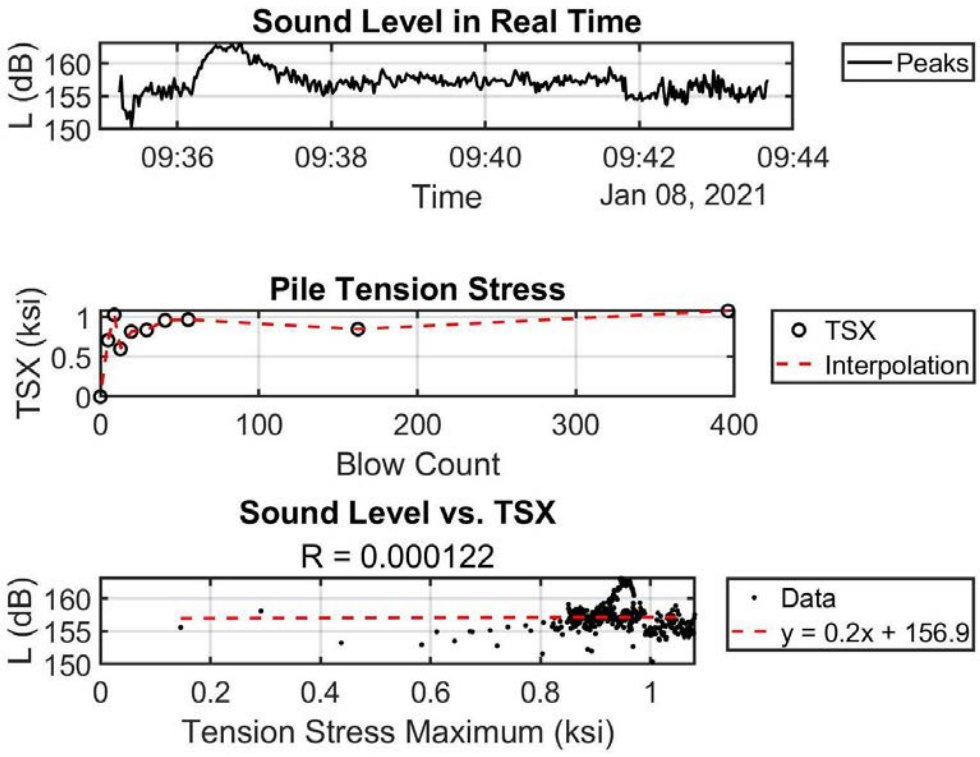

Figure 3-61. Sound Level vs. Pile Tension Stress

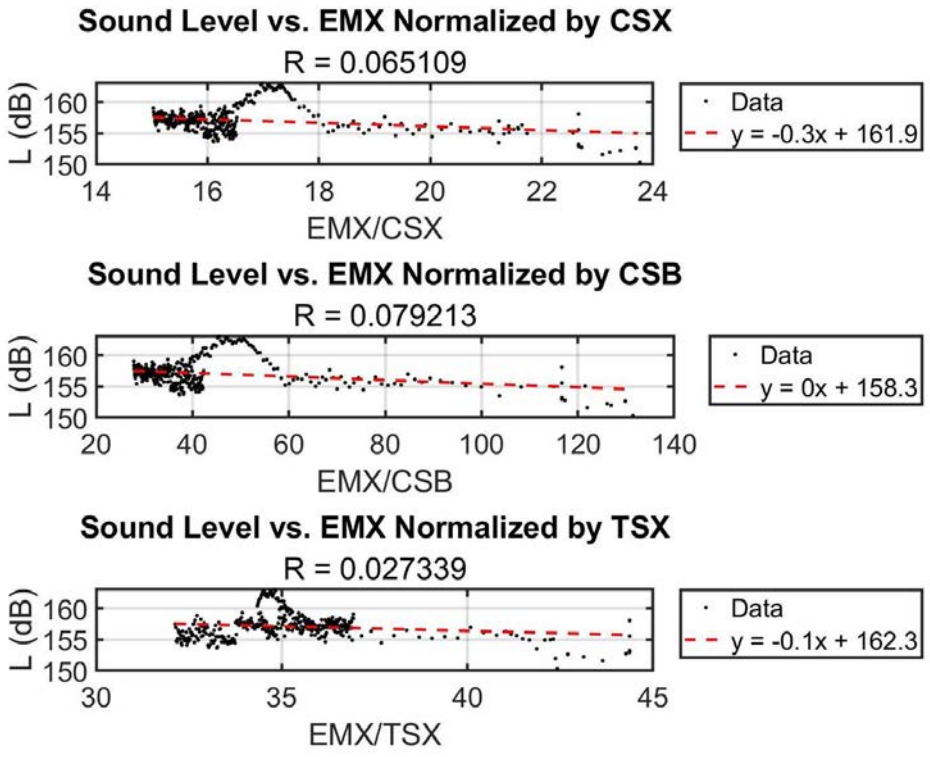

Figure 3-62. Sound Level vs. Hammer Energy normalized by Pile Stresses

3.3.7 SR-23 over Black Creek, FL – Pile 7

- Date: 01/21/2021
- Pile: Intermediate Pier 4 Pile 7
- Dimensions: 24” x 90’ PSC Production Pile

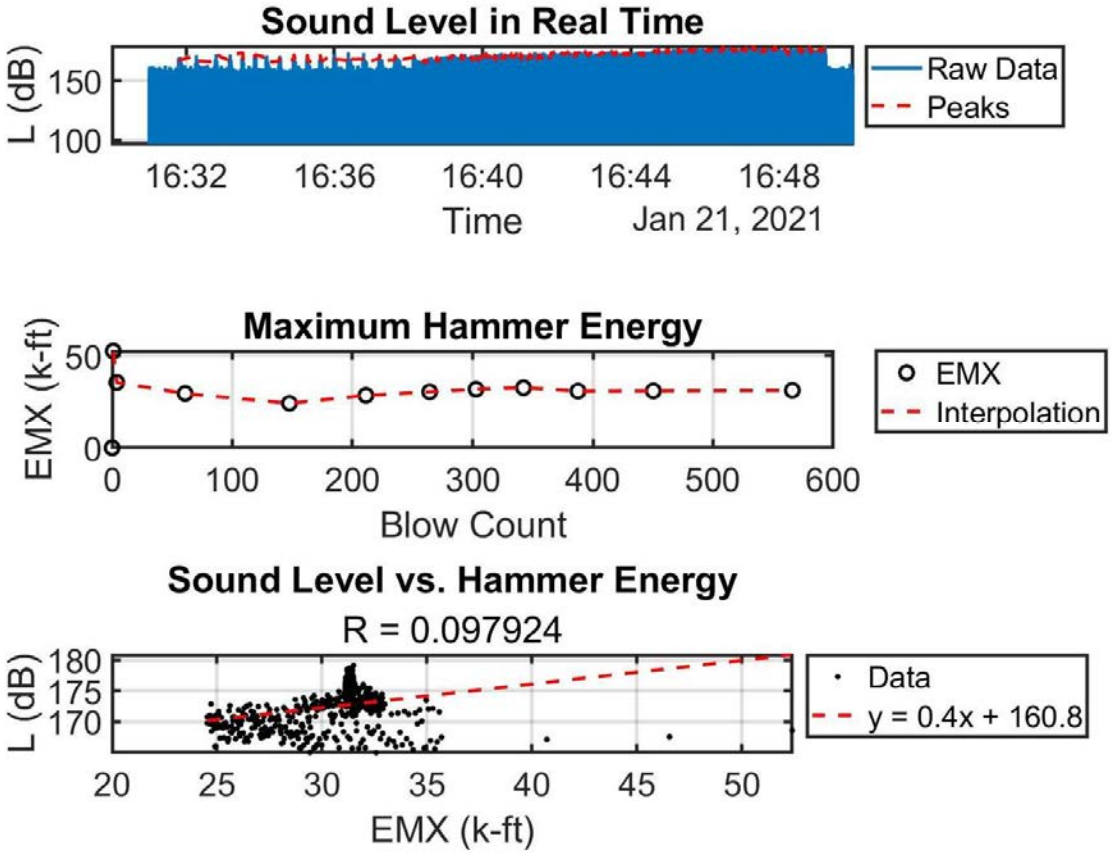

Figure 3-63. Sound Level vs. Hammer Energy (EMX)

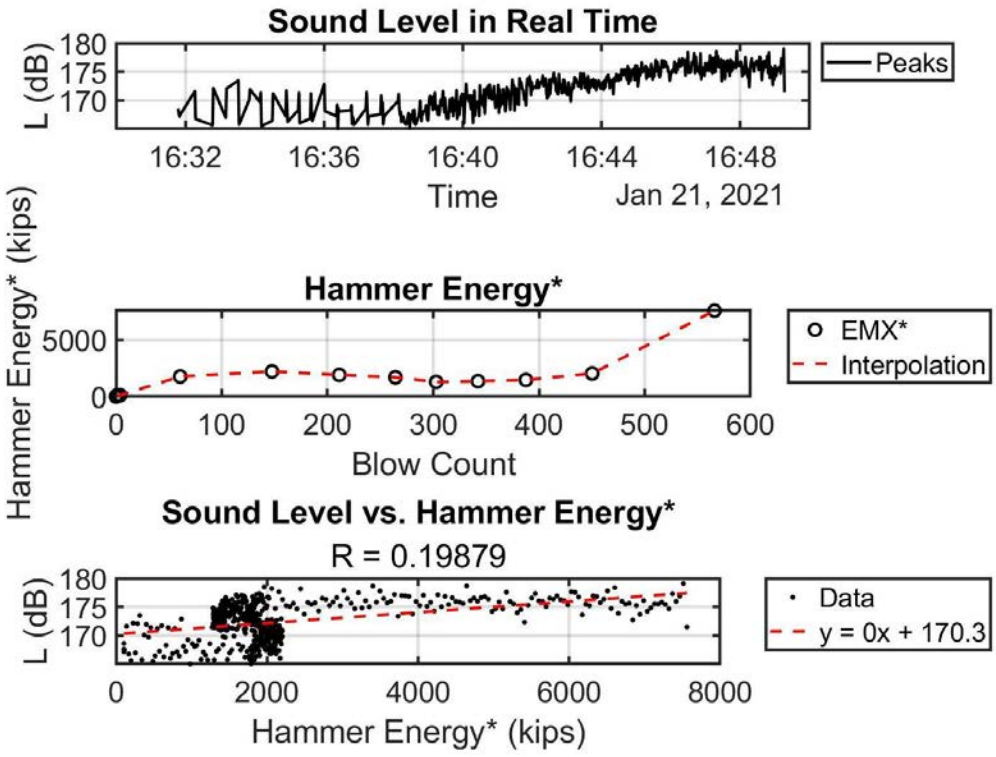

Figure 3-64. Sound Level vs. Hammer Energy normalized by Blow Count

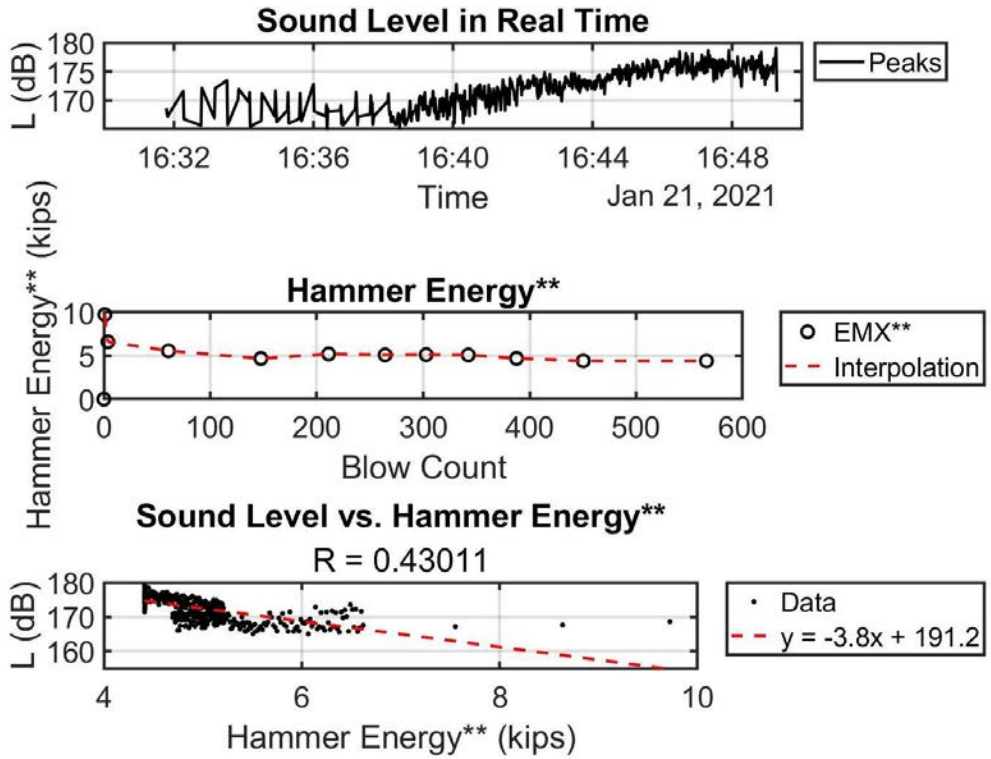

Figure 3-65. Sound Level vs. Hammer Energy normalized by Hammer Stroke Height

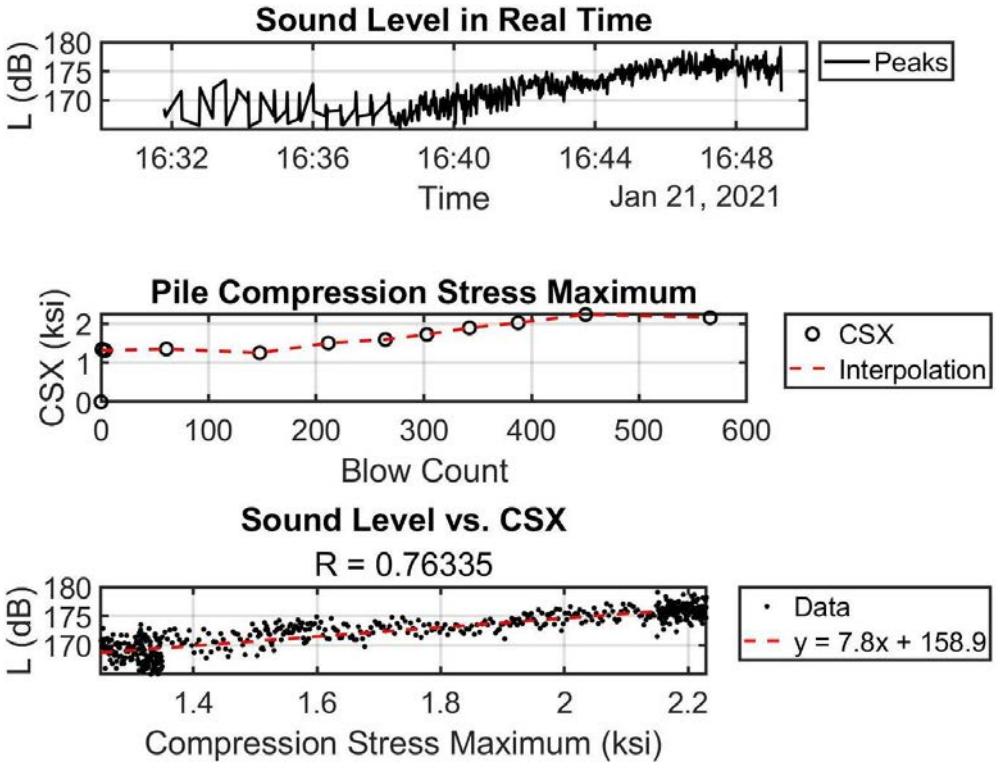

Figure 3-66. Sound Level vs. Maximum Pile Compression Stress

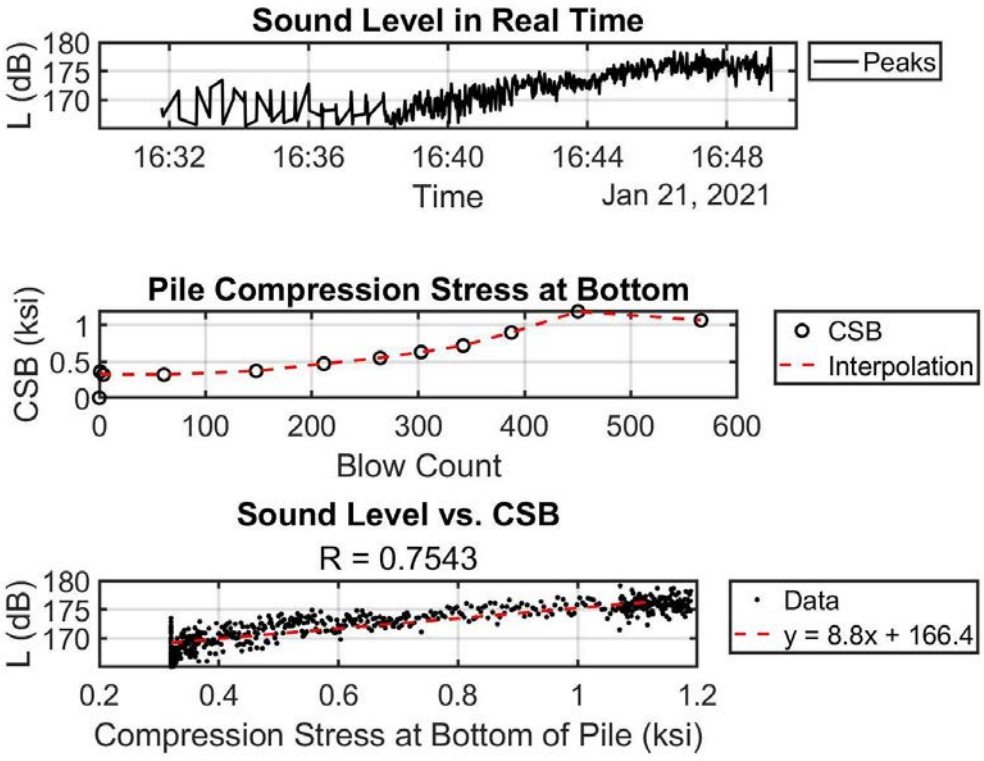

Figure 3-67. Sound Level vs. Pile Compression Stress at Bottom

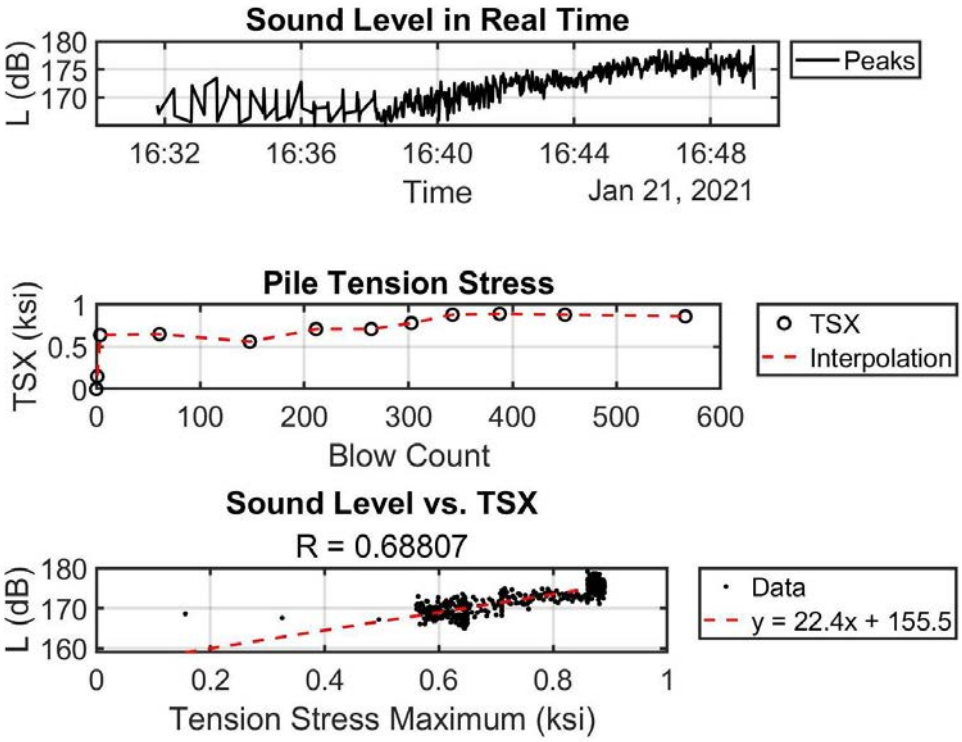

Figure 3-68. Sound Level vs. Pile Tension Stress

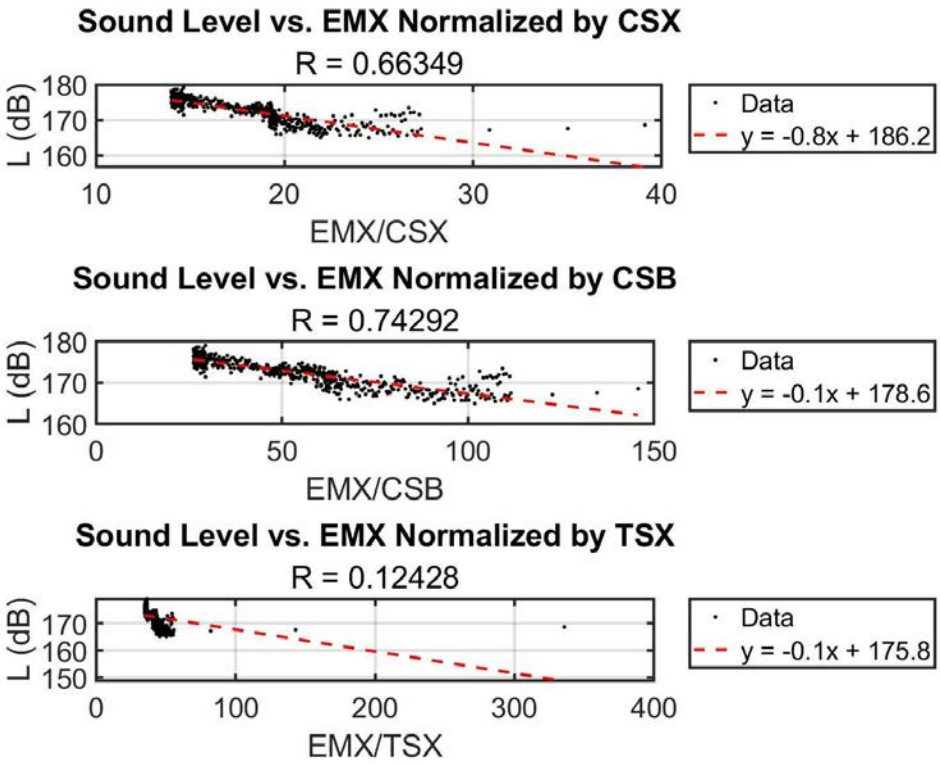

Figure 3-69. Sound Level vs. Hammer Energy normalized by Pile Stresses

3.3.8 SR-23 over Black Creek, FL – Pile 9

- Date: 01/21/2021
- Pile: Intermediate Pier 4 Pile 9
- Dimensions: 24” x 90’ PSC Production Pile

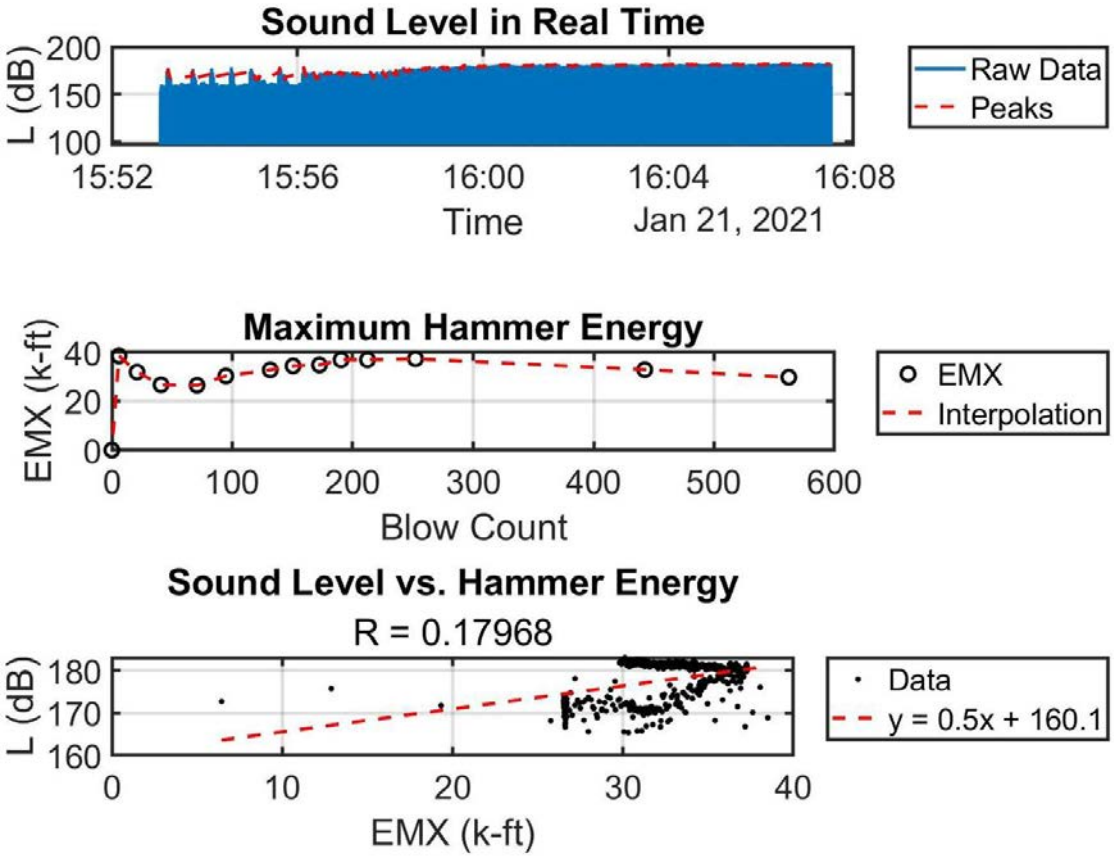

Figure 3-70. Sound Level vs. Hammer Energy (EMX)

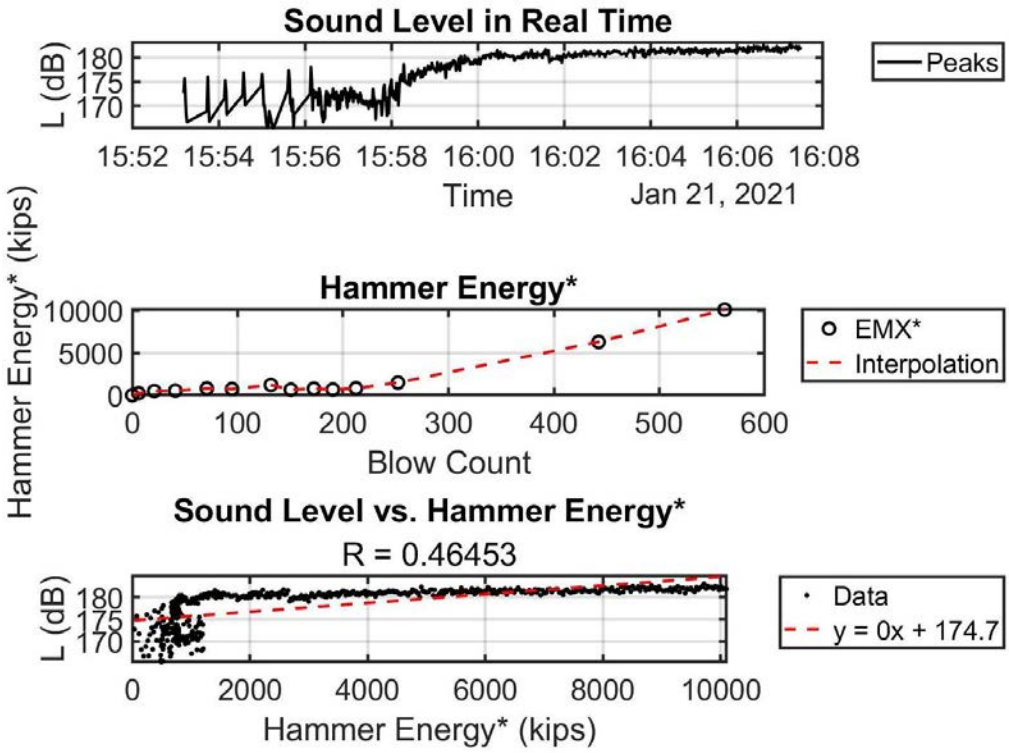

Figure 3-71. Sound Level vs. Hammer Energy normalized by Blow Count

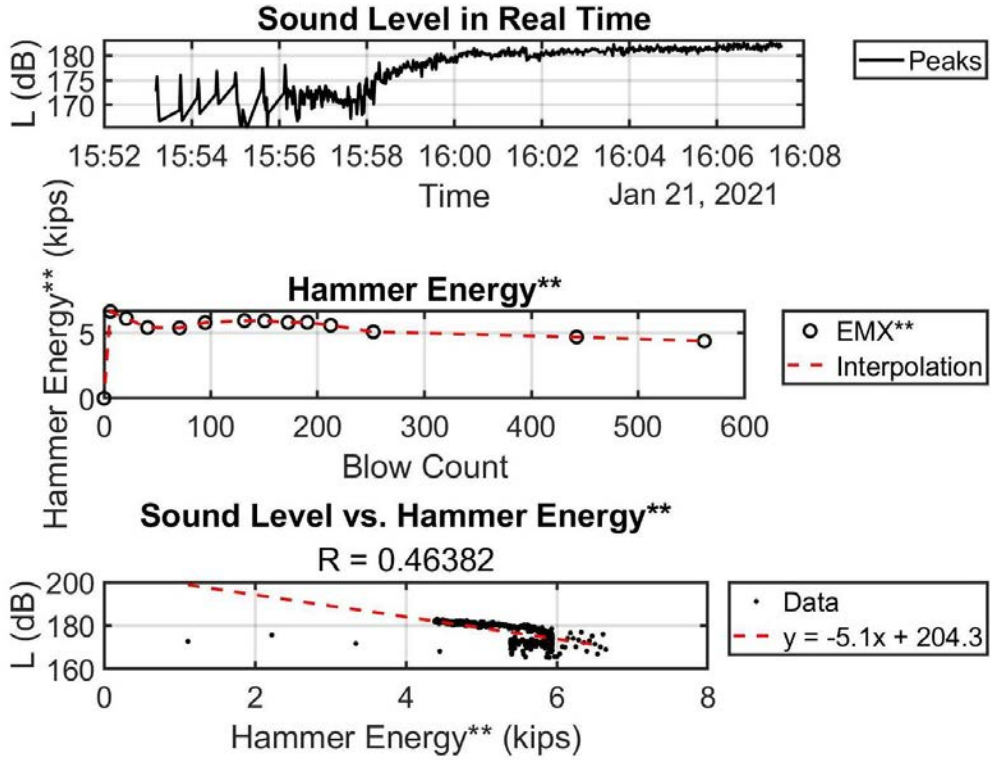

Figure 3-72. Sound Level vs. Hammer Energy normalized by Hammer Stroke Height

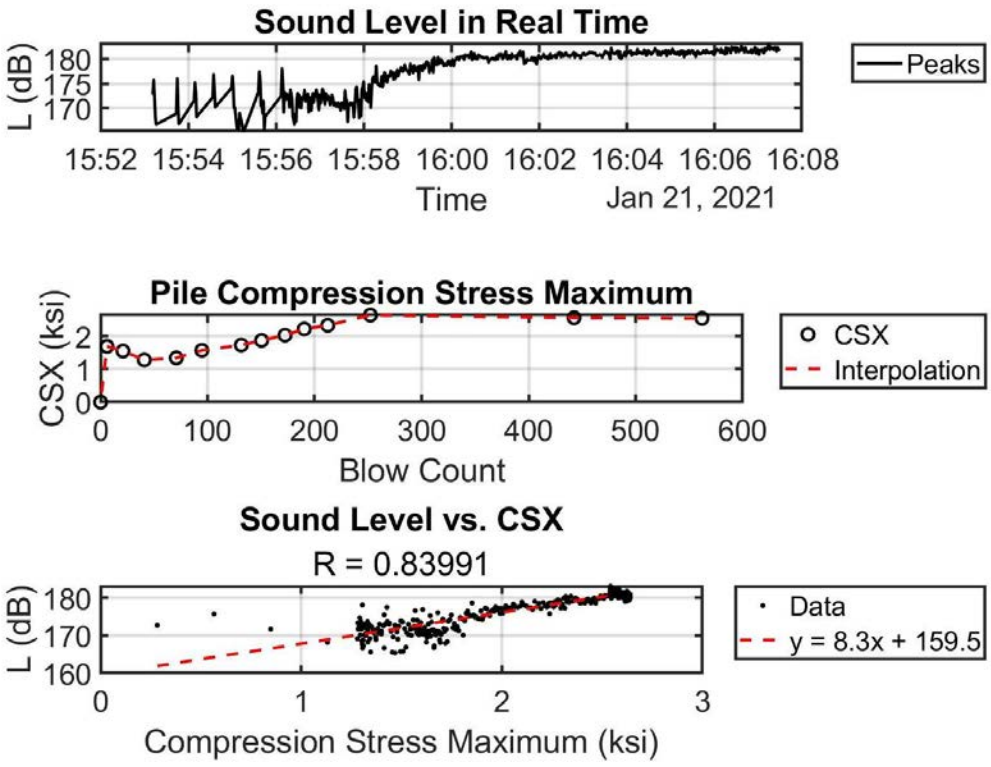

Figure 3-73. Sound Level vs. Maximum Pile Compression Stress

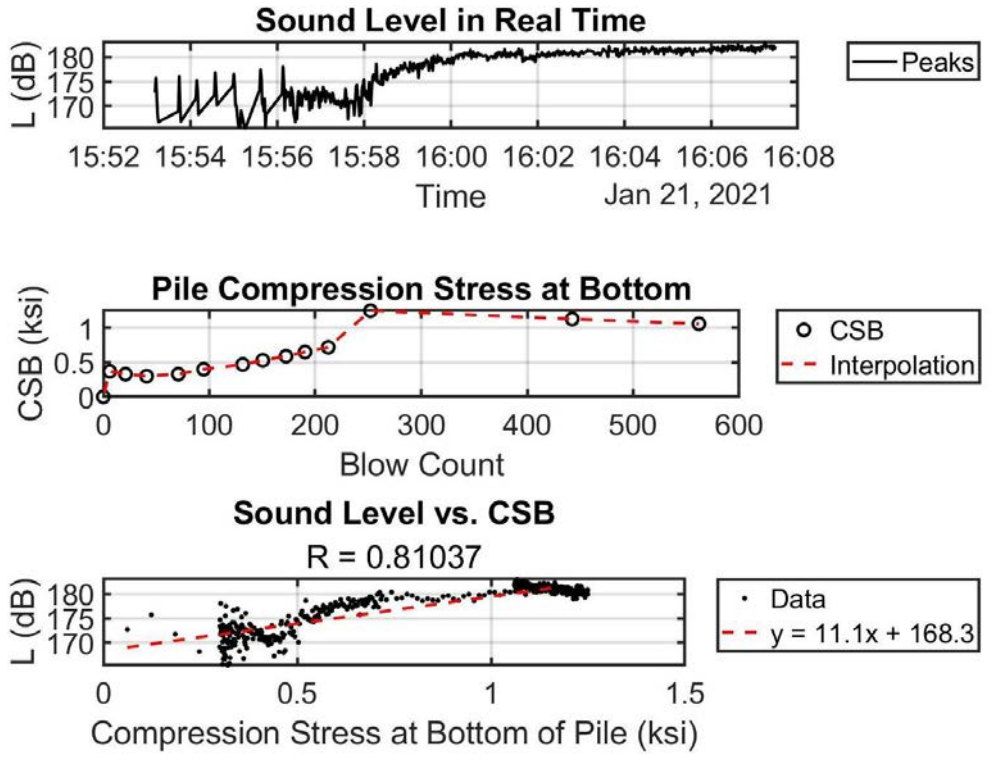

Figure 3-74. Sound Level vs. Pile Compression Stress at Bottom

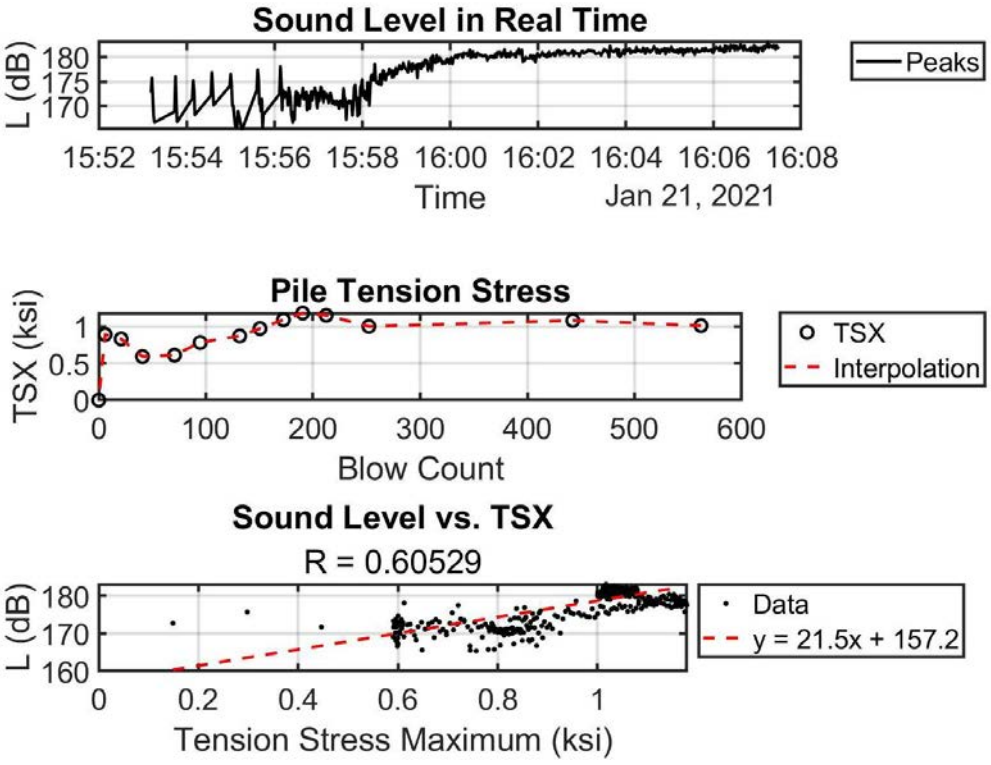

Figure 3-75. Sound Level vs. Pile Tension Stress

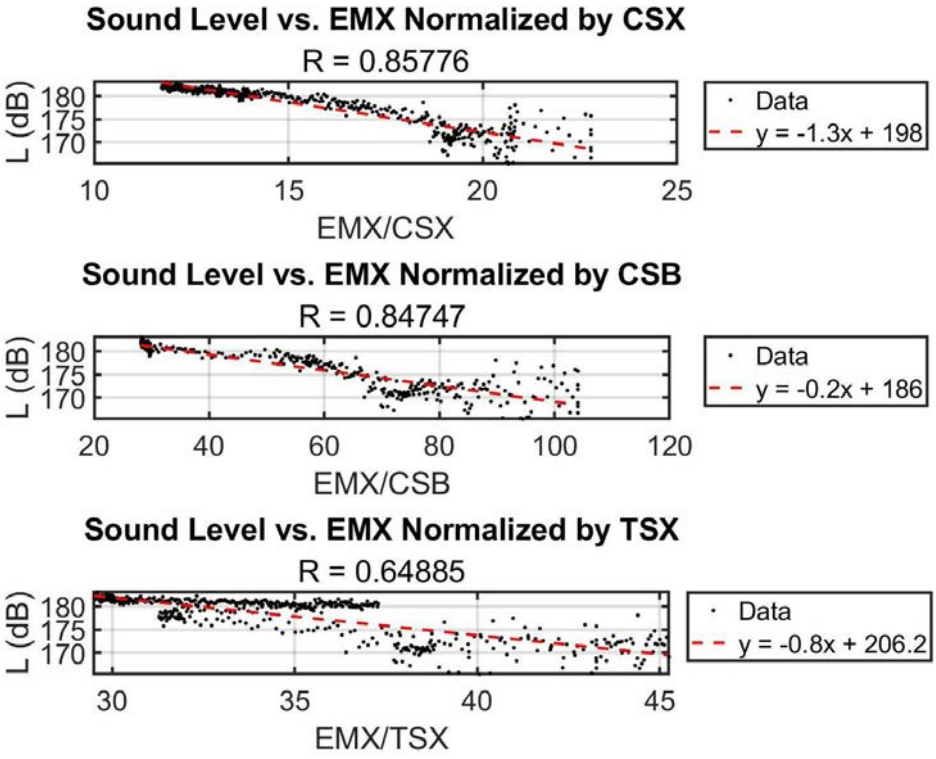

Figure 3-76. Sound Level vs. Hammer Energy normalized by Pile Stresses

3.3.9 SR-23 over Black Creek, FL – Pile 10

- Date: 01/21/2021
- Pile: Intermediate Pier 4 Pile 10
- Dimensions: 24” x 90’ PSC Production Pile

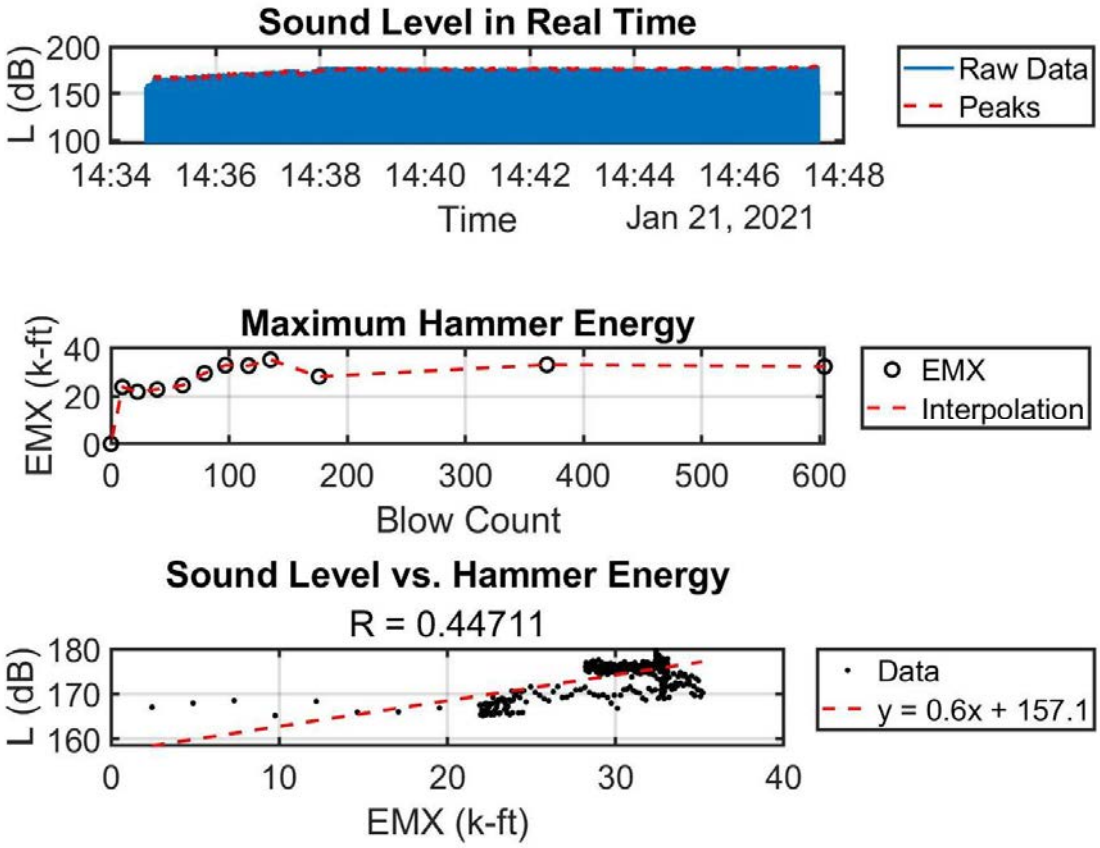

Figure 3-77. Sound Level vs. Hammer Energy (EMX)

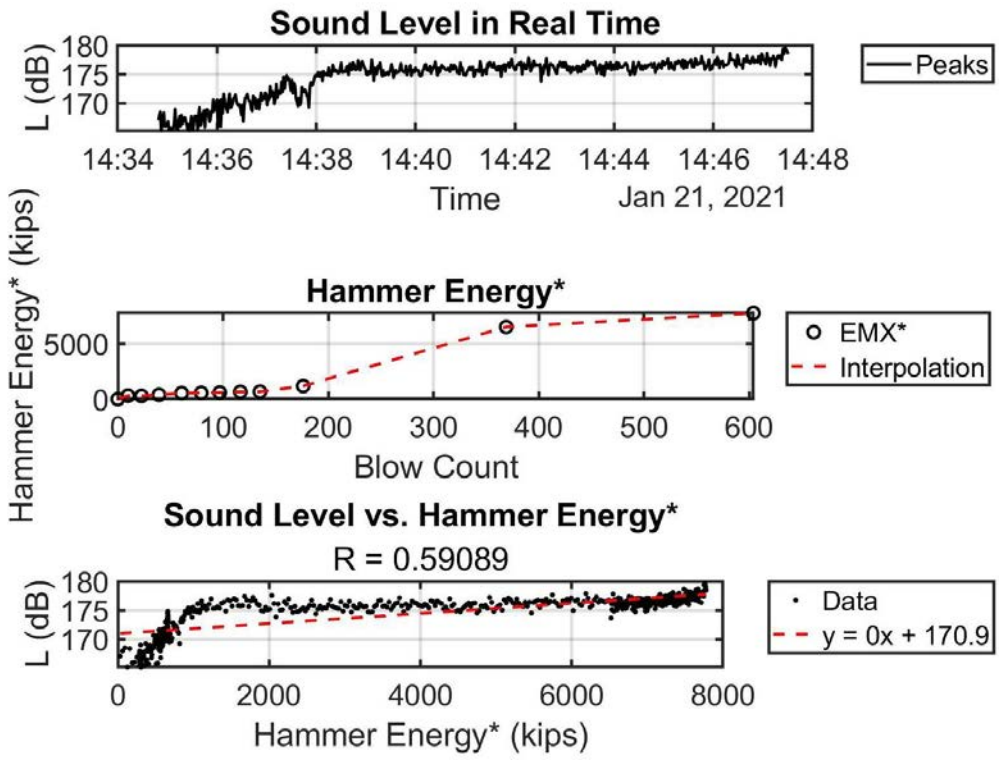

Figure 3-78. Sound Level vs. Hammer Energy normalized by Blow Count

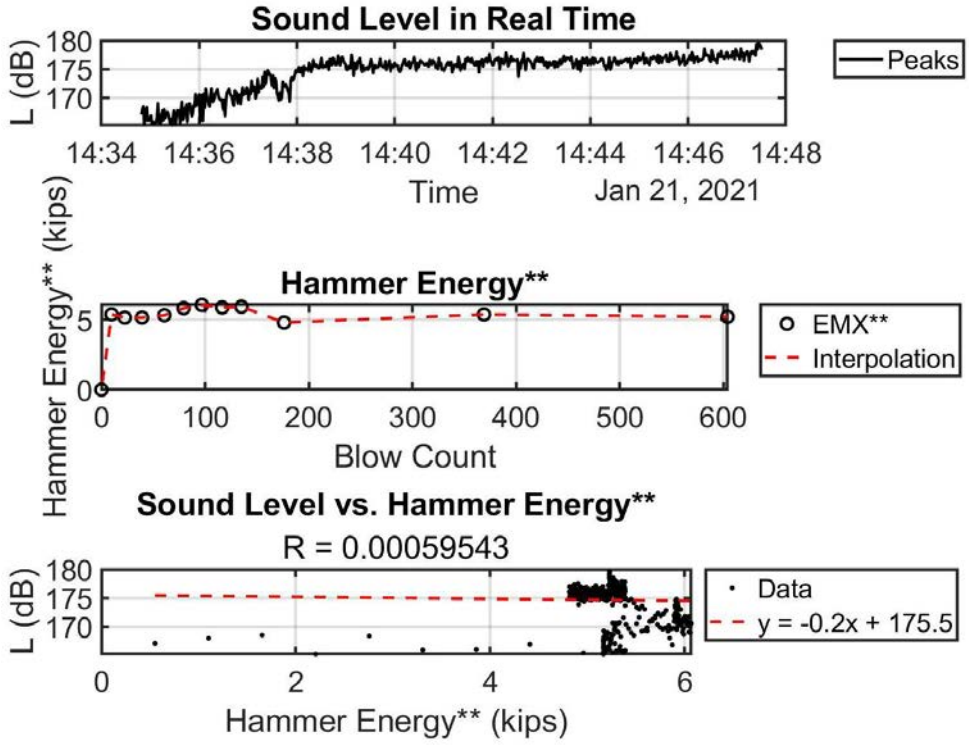

Figure 3-79. Sound Level vs. Hammer Energy normalized by Hammer Stroke Height

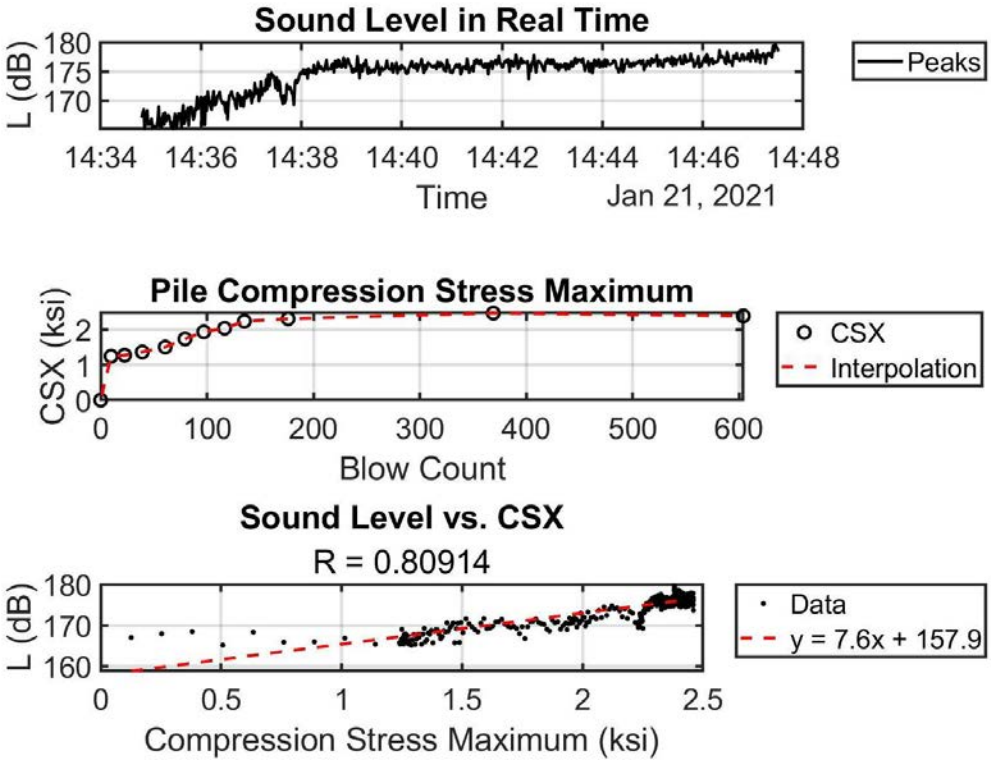

Figure 3-80. Sound Level vs. Maximum Pile Compression Stress

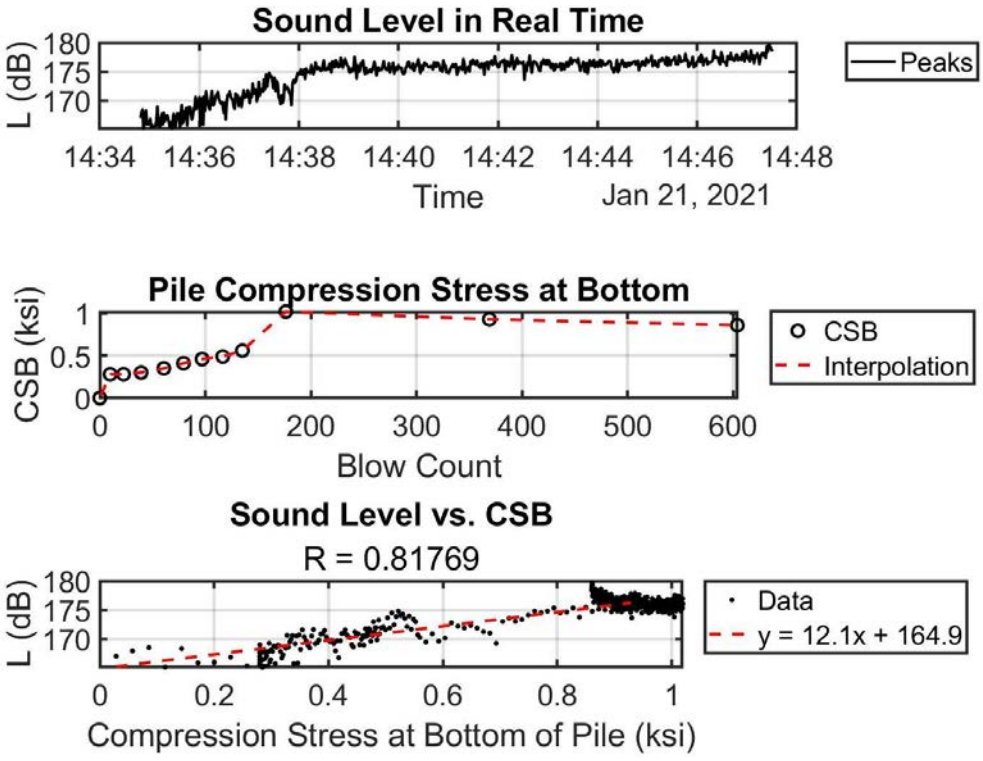

Figure 3-81. Sound Level vs. Pile Compression Stress at Bottom

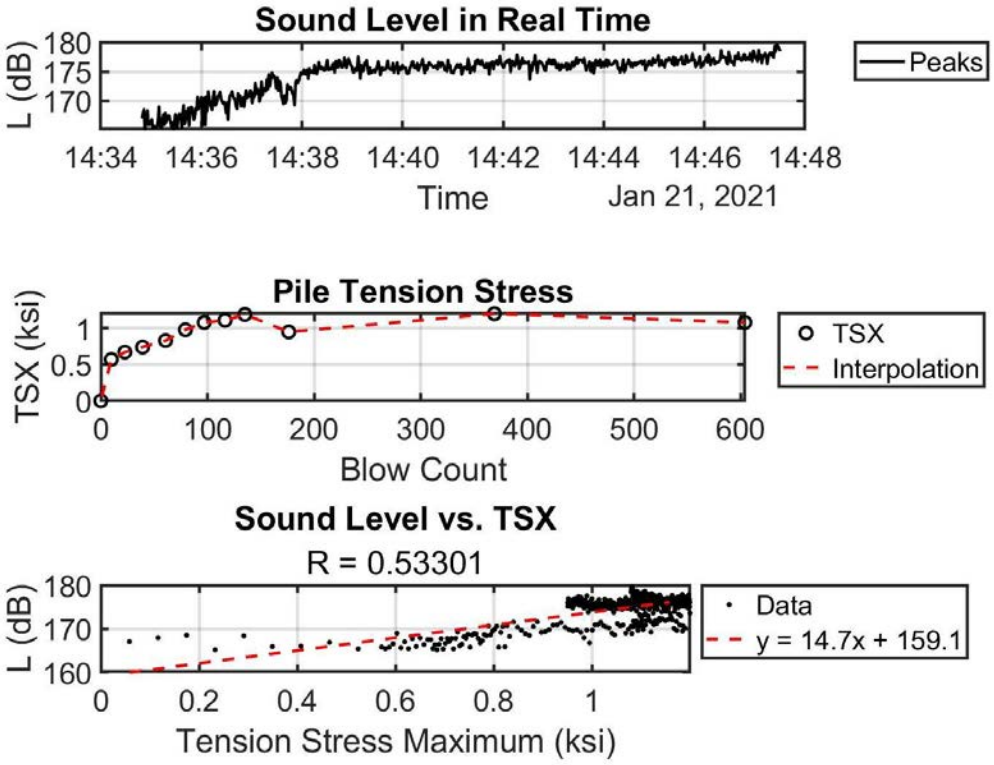

Figure 3-82. Sound Level vs. Pile Tension Stress

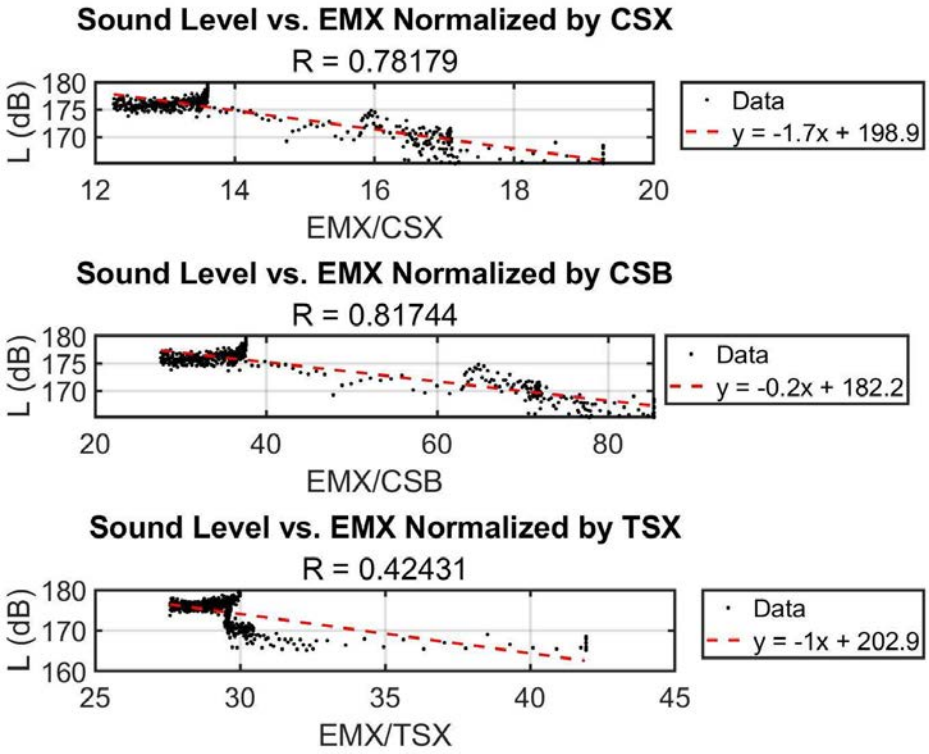

Figure 3-83. Sound Level vs. Hammer Energy normalized by Pile Stresses

3.3.10 SR-23 over Black Creek, FL – Pile 11

- Date: 01/21/2021
- Pile: Intermediate Pier 4 Pile 11
- Dimensions: 24” x 90’ PSC Production Pile

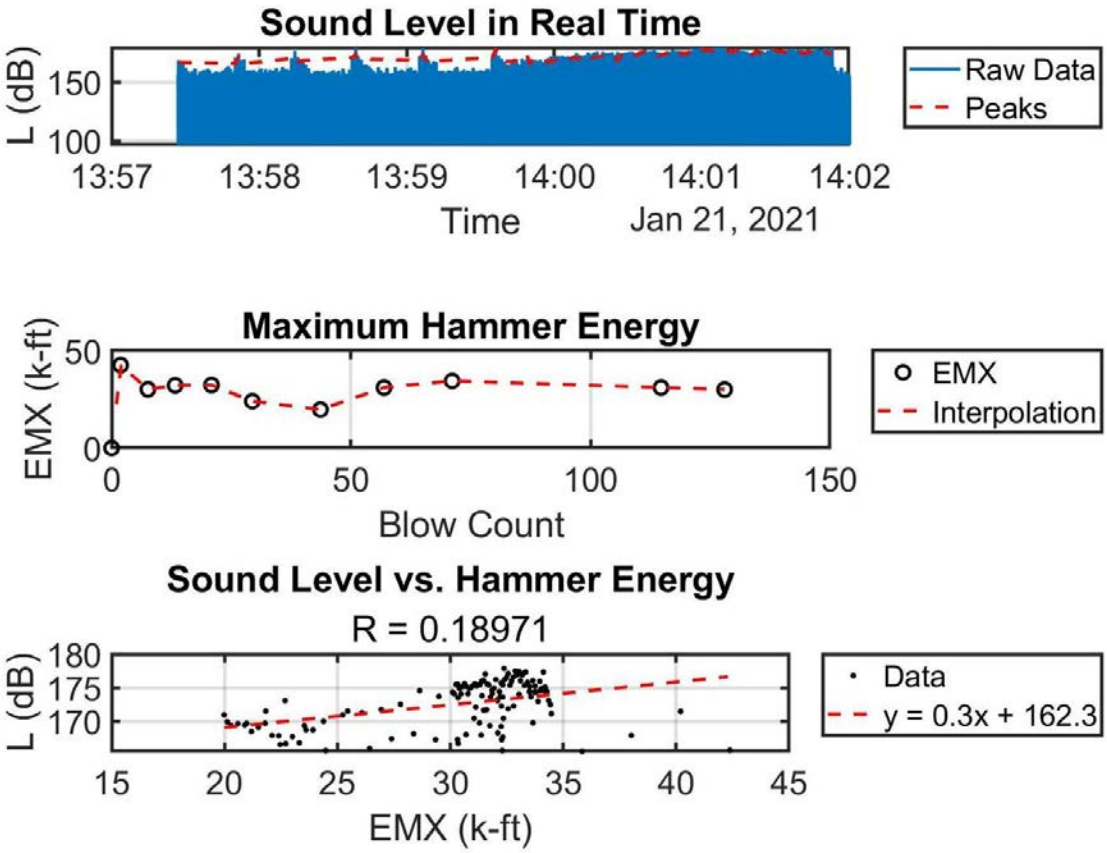

Figure 3-84. Sound Level vs. Hammer Energy (EMX)

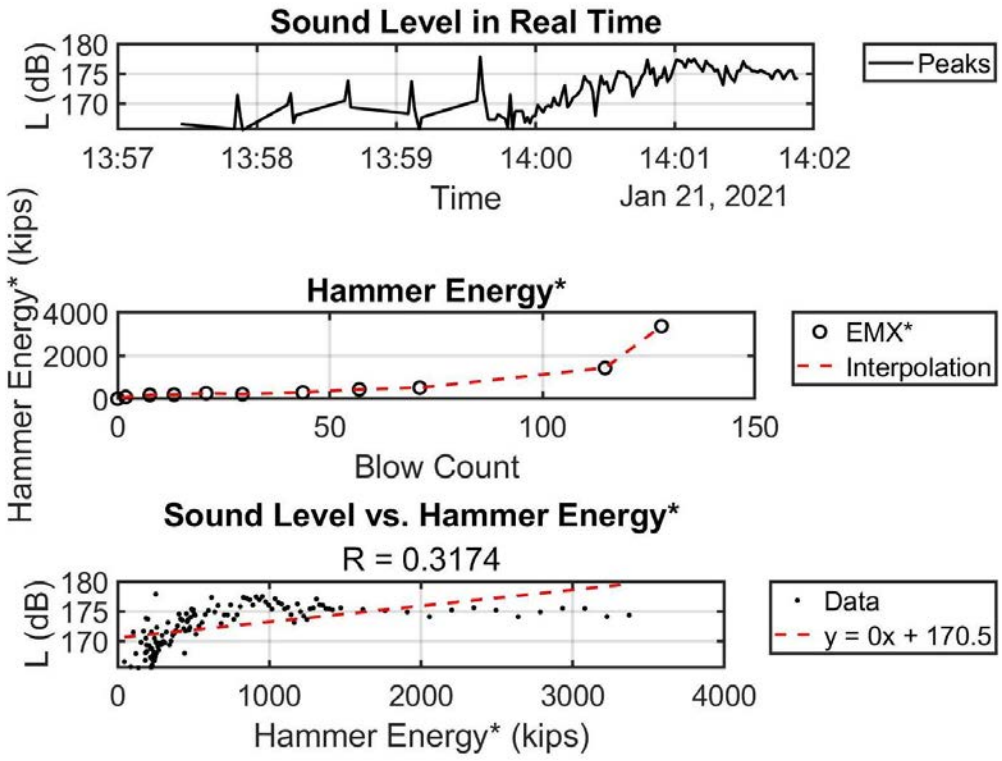

Figure 3-85. Sound Level vs. Hammer Energy normalized by Blow Count

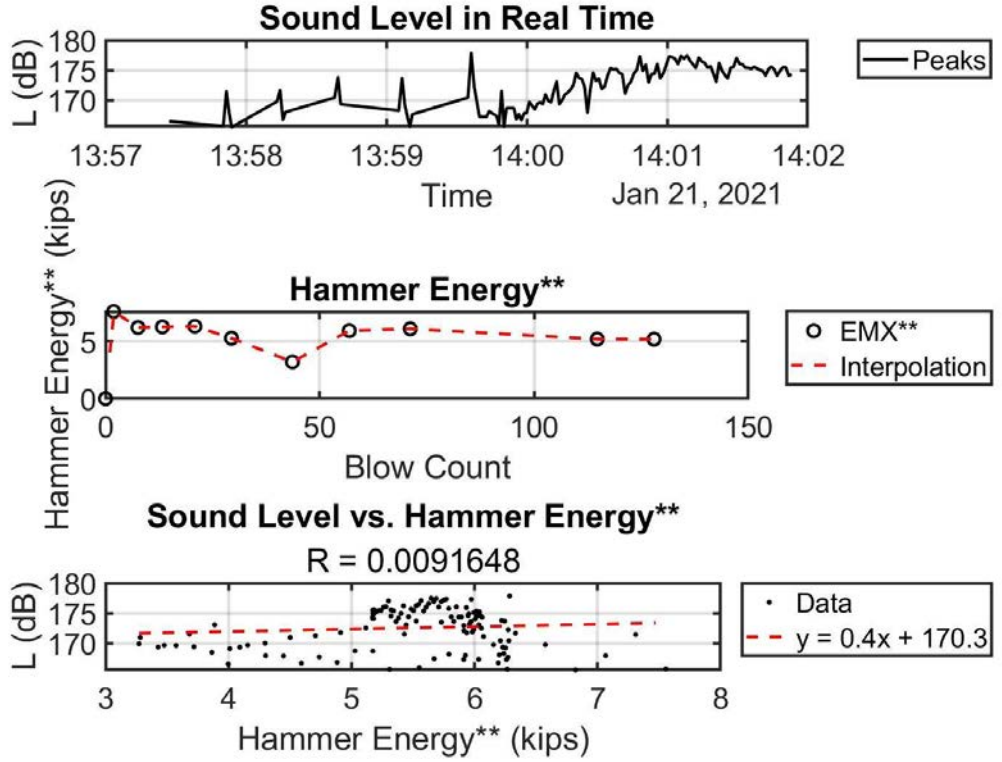

Figure 3-86. Sound Level vs. Hammer Energy normalized by Hammer Stroke Height

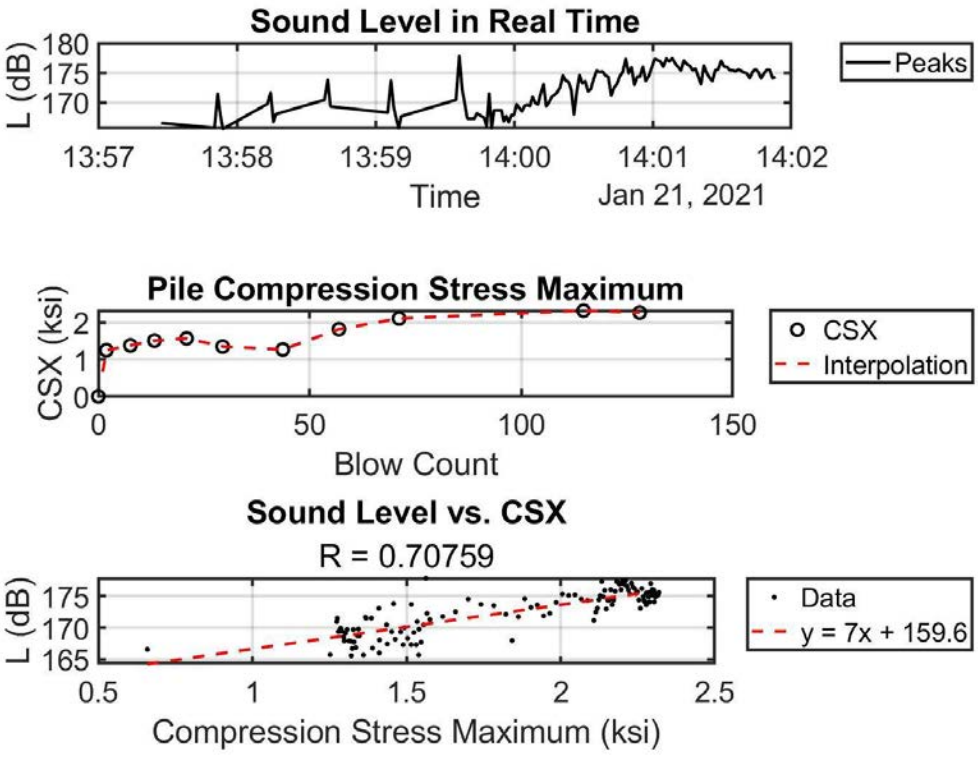

Figure 3-87. Sound Level vs. Maximum Pile Compression Stress

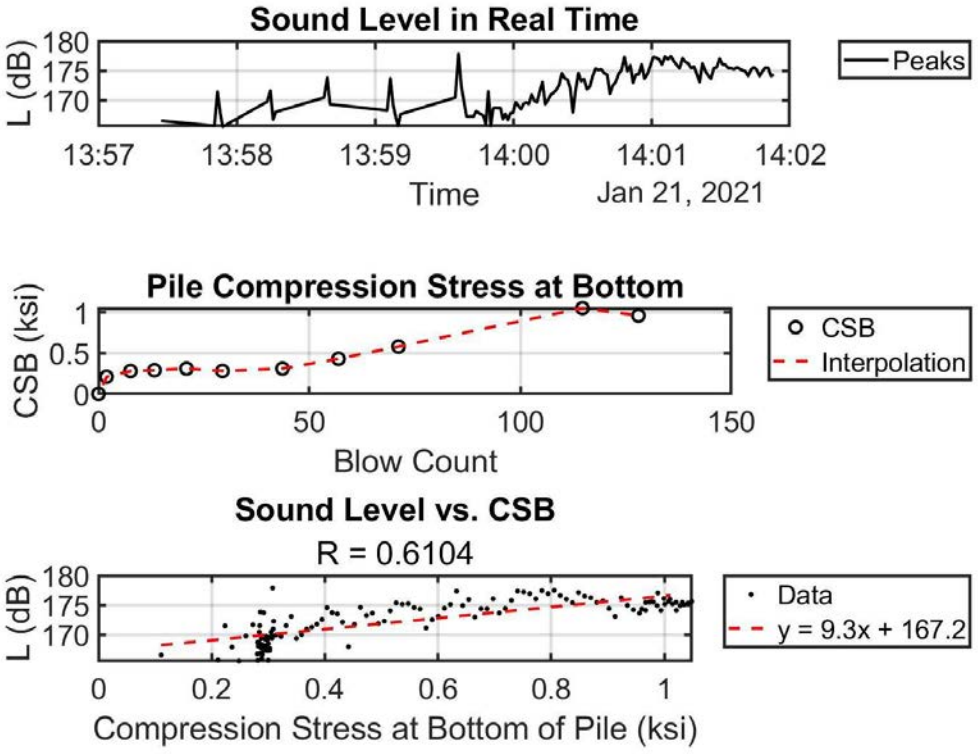

Figure 3-88. Sound Level vs. Pile Compression Stress at Bottom

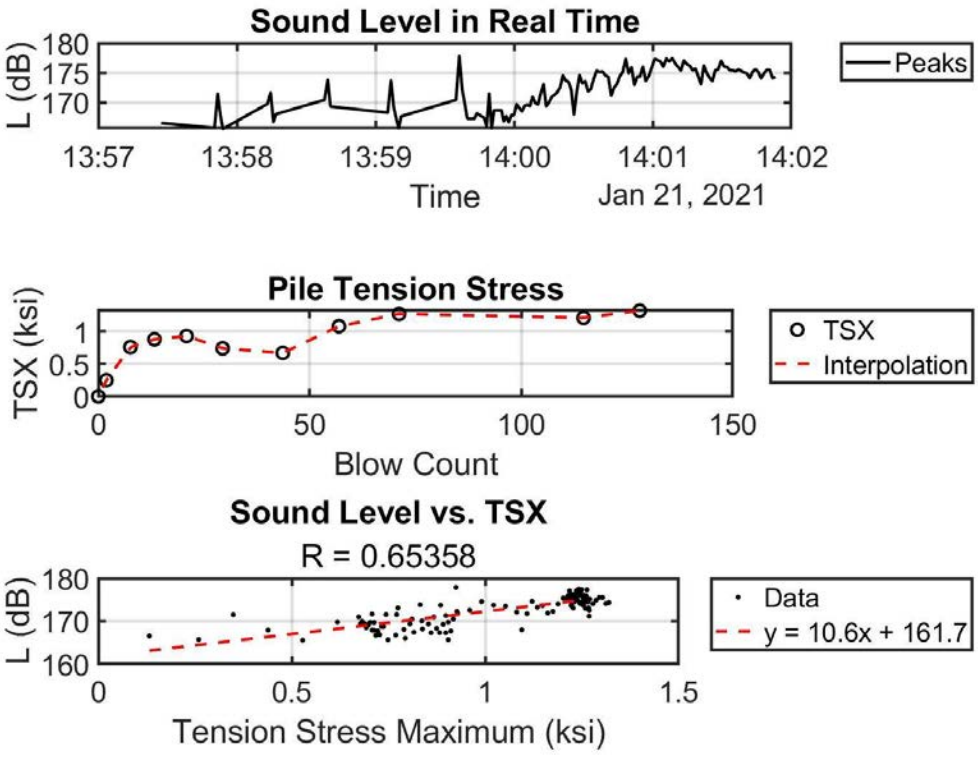

Figure 3-89. Sound Level vs. Pile Tension Stress

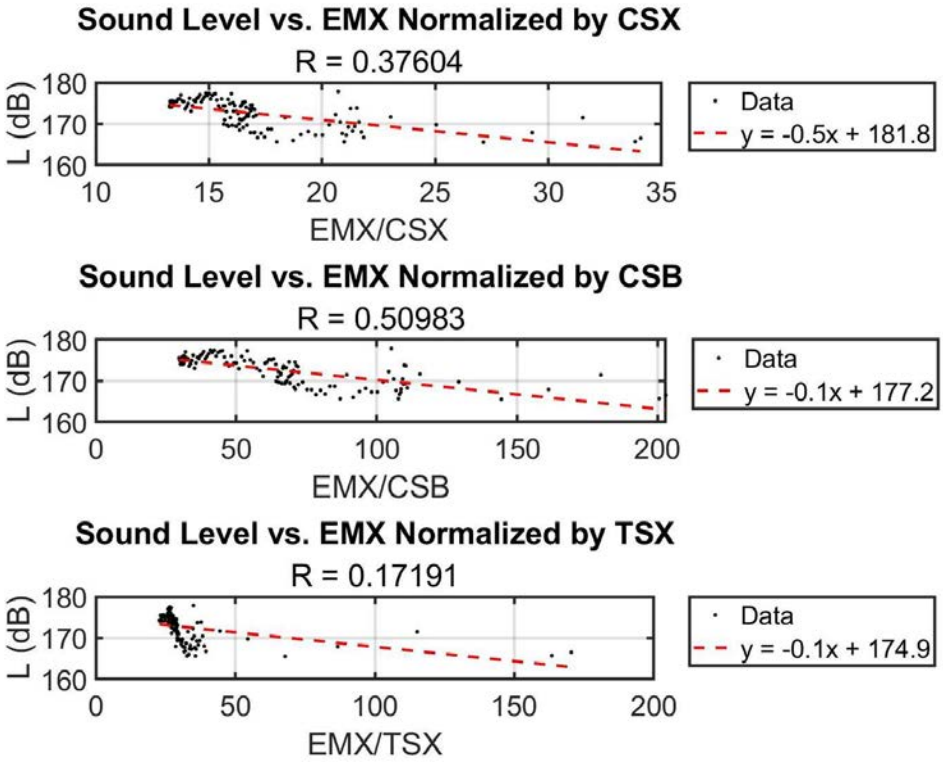

Figure 3-90. Sound Level vs. Hammer Energy normalized by Pile Stresses

3.3.11 SR-23 over Black Creek, FL – Pile 12

- Date: 01/21/2021
- Pile: Intermediate Pier 4 Pile 12
- Dimensions: 24” x 90’ PSC Production Pile

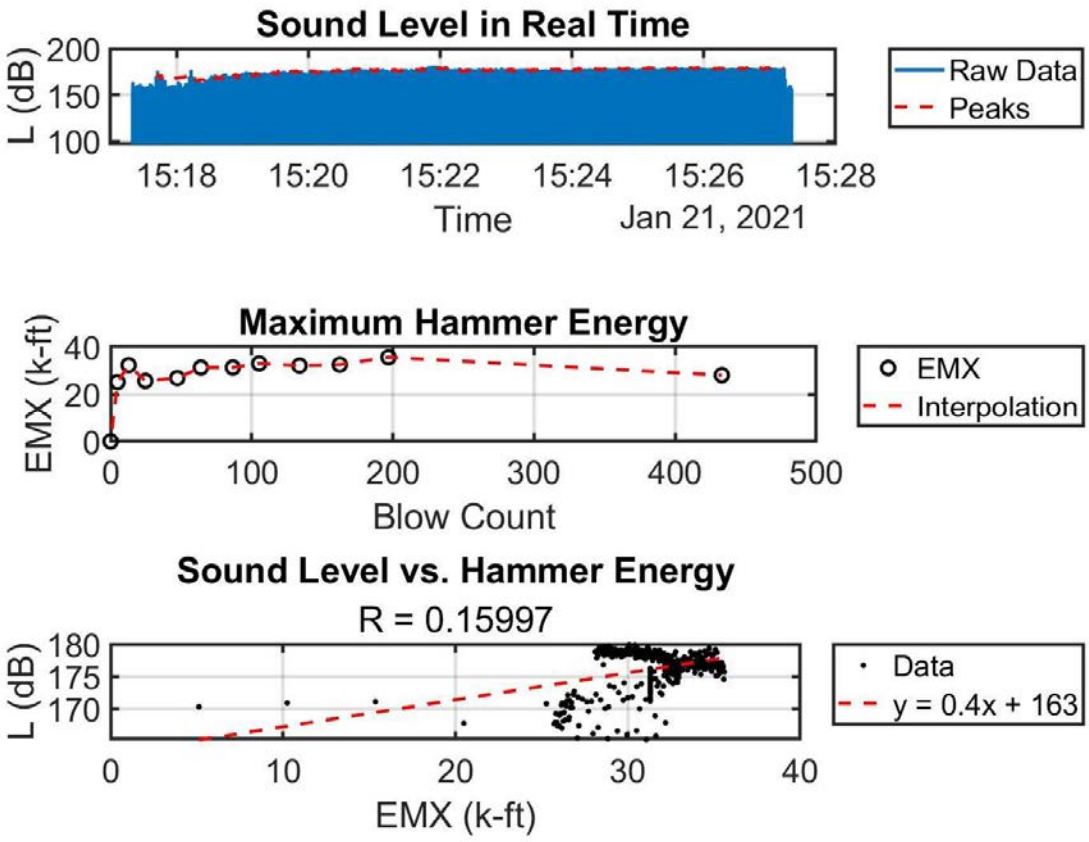

Figure 3-91. Sound Level vs. Hammer Energy (EMX)

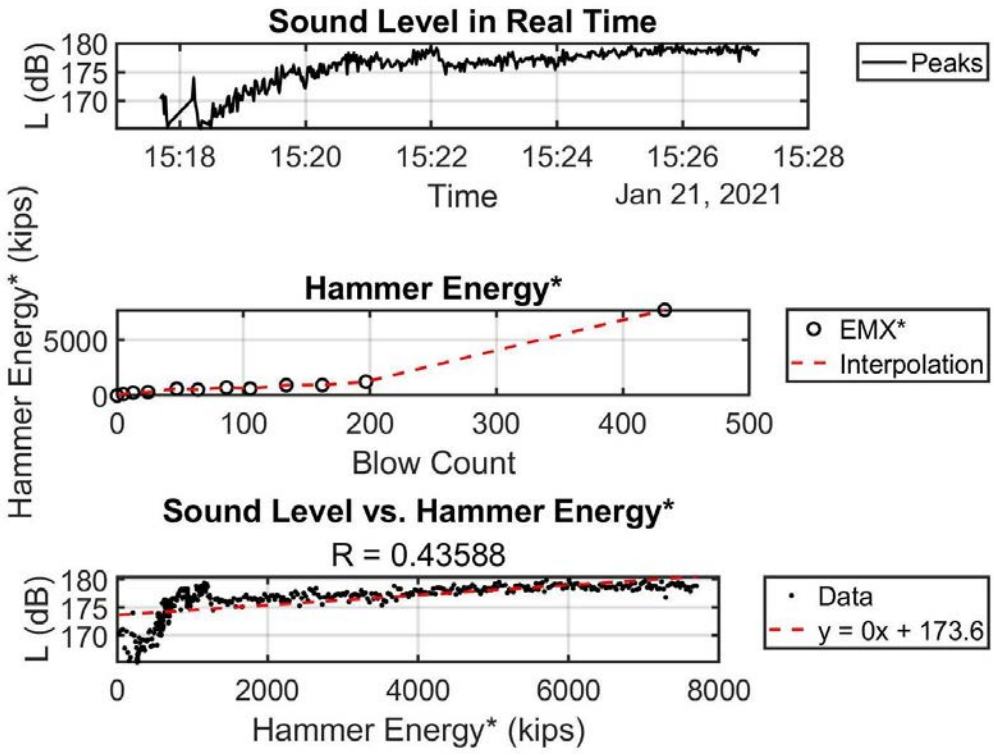

Figure 3-93. Sound Level vs. Hammer Energy normalized by Blow Count

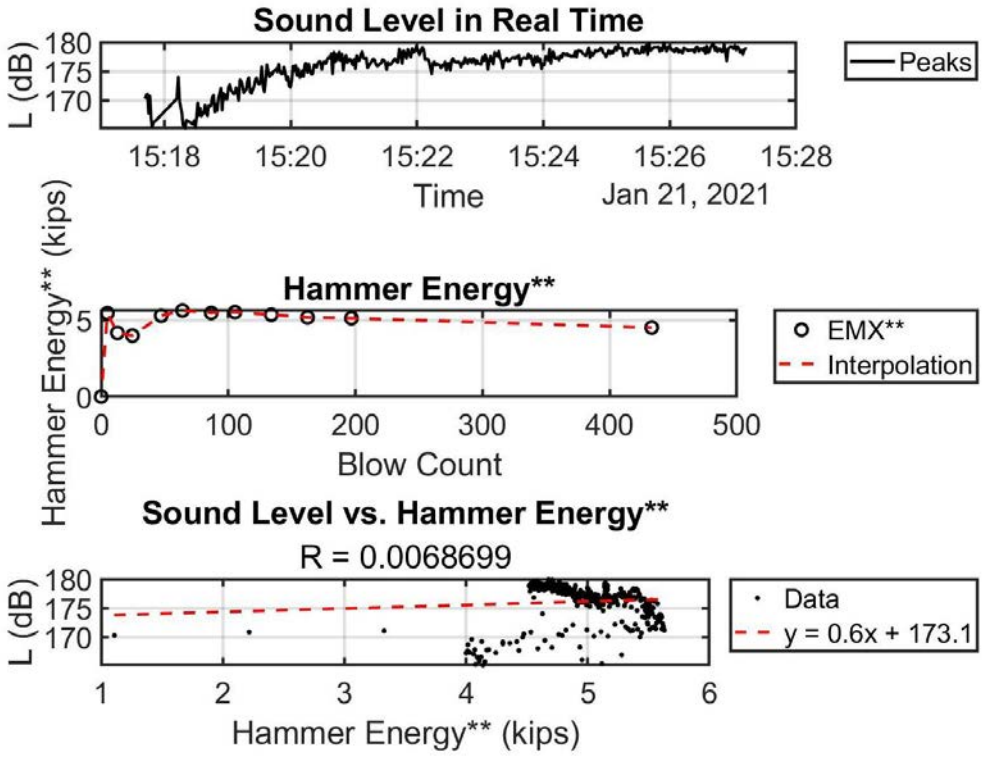

Figure 3-94. Sound Level vs. Hammer Energy normalized by Hammer Stroke Height

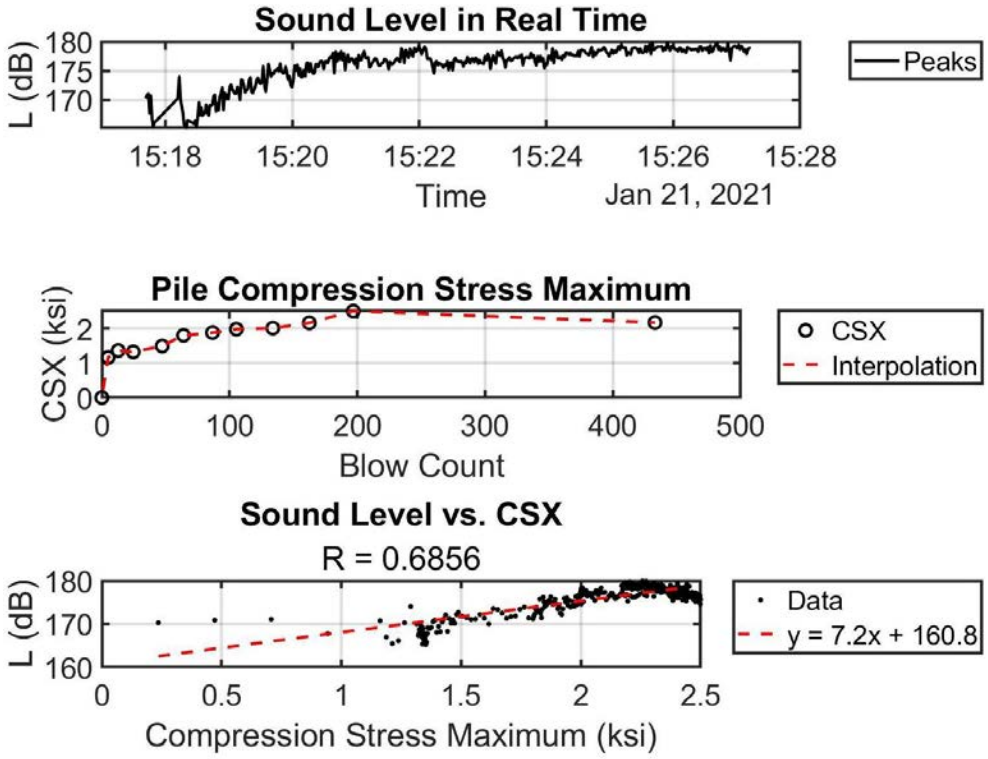

Figure 3-95. Sound Level vs. Maximum Pile Compression Stress

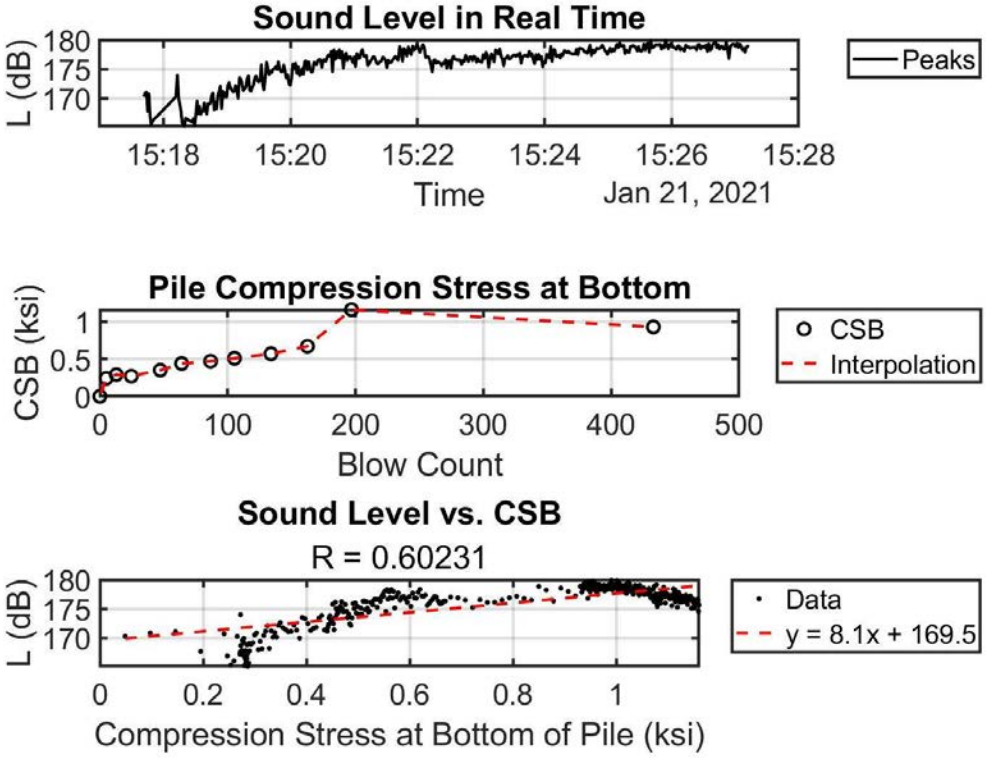

Figure 3-96. Sound Level vs. Pile Compression Stress at Bottom

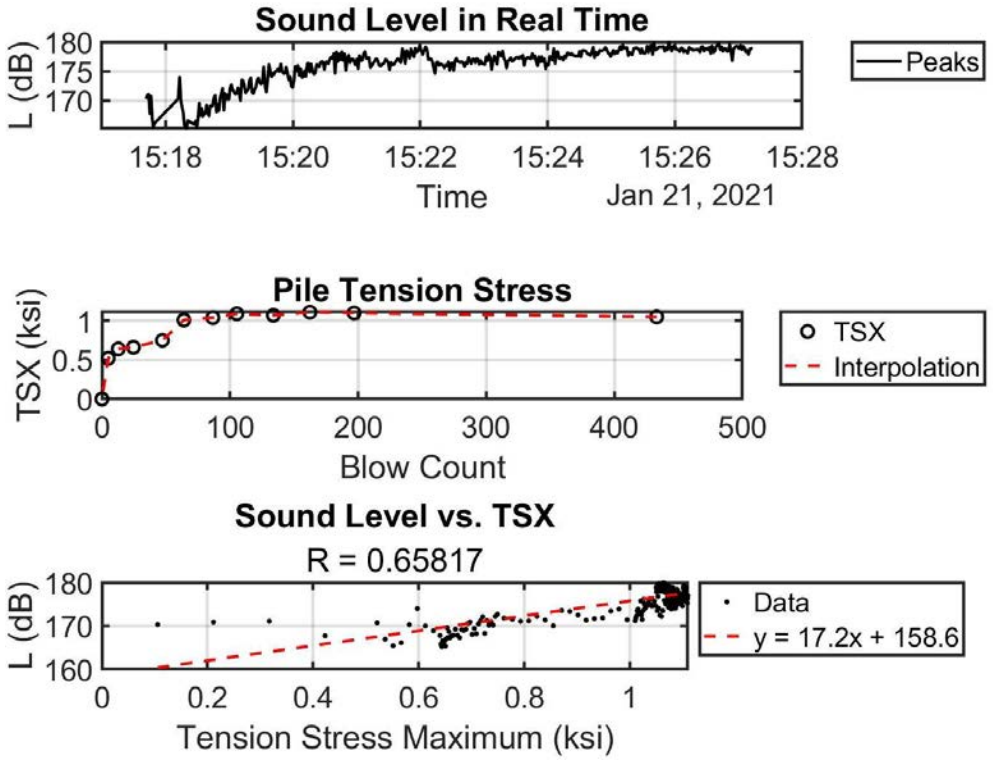

Figure 3-97. Sound Level vs. Pile Tension Stress

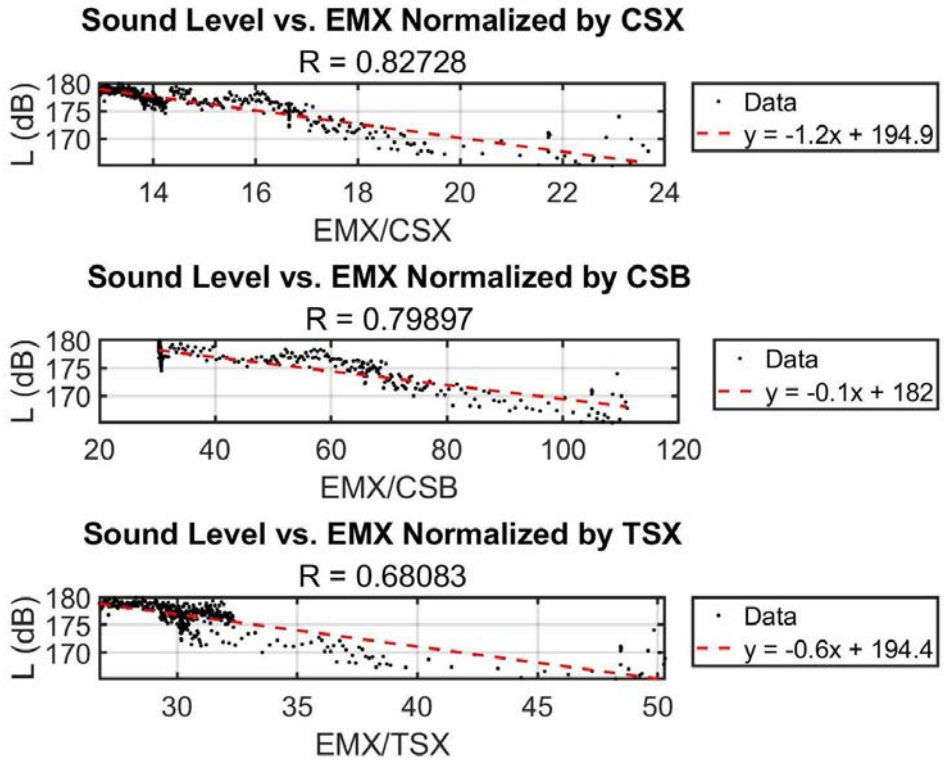

Figure 3-98. Sound Level vs. Hammer Energy normalized by Pile Stresses

3.4 SR-23 over Black Creek, FL – Combined Pile Drives Performed on 1/21/2021

Analysis of results from Section 3.1 through Section 3.3 appeared to indicate that CSX, CSB, and TSX consistently produced the strongest correlations between PDA and sound level data. Since data were collected at slightly different distances from different sites on different days, directly comparing all the drives to one another did not appear to be appropriate. However, at SR-23, multiple drives occurred at the same approximate distances for multiple drives on each day. As such, on each day, results from CSX, CSB, and TSX were combined and combined correlations were developed (Figs. 3-99 through 3-XX below).

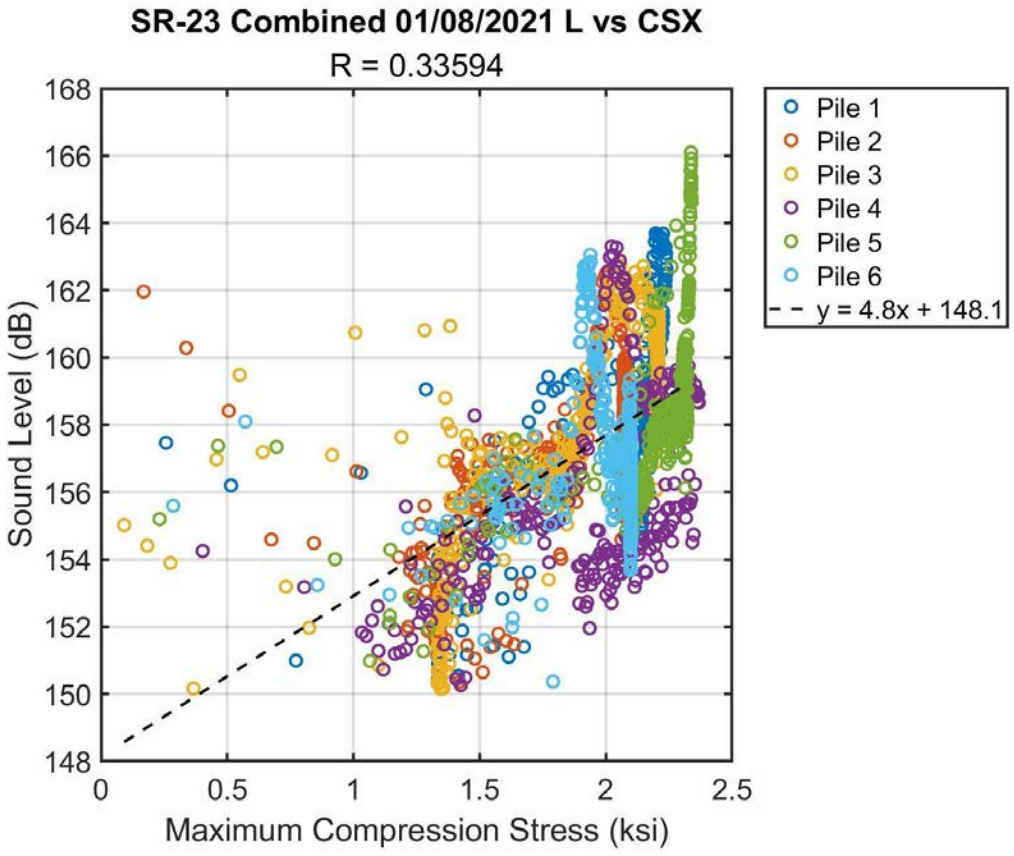

Figure 3-99. Sound Level (L) vs. Maximum Compression Stress (CSX) for pile drives performed on 1/08/2021 at SR-23

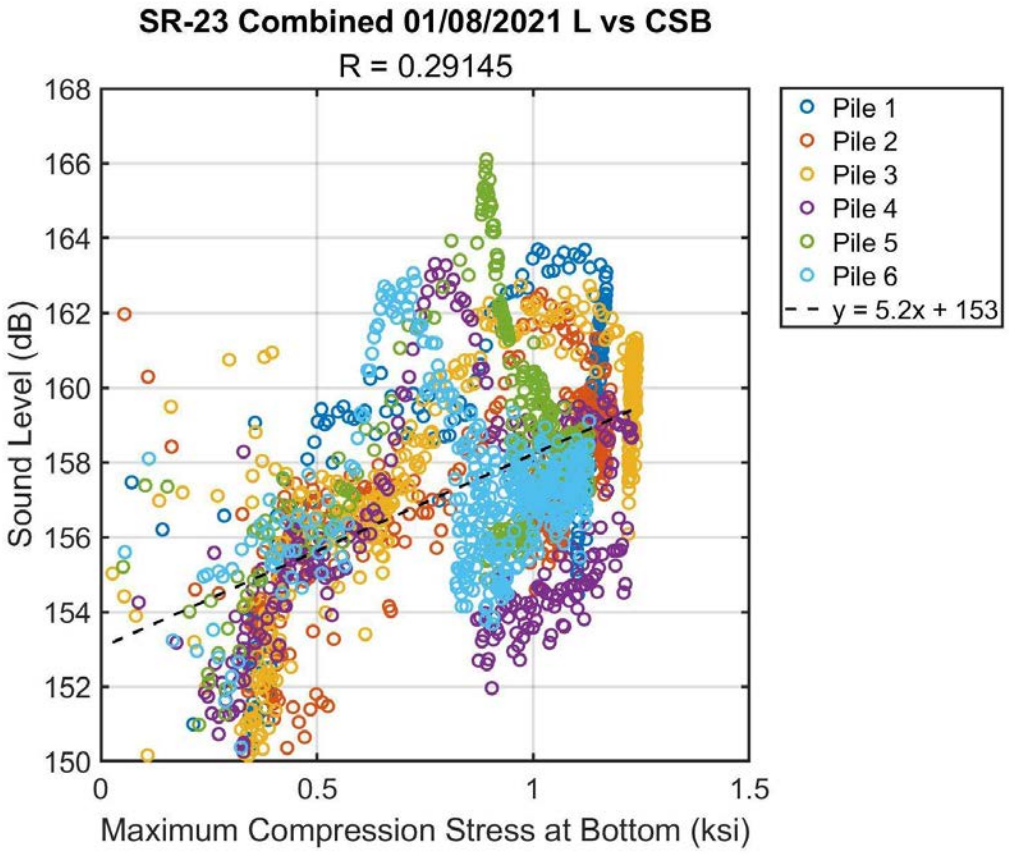

Figure 3-100. Sound Level (L) vs. Maximum Compression Stress at Bottom (CSB) for pile drives performed on 1/08/2021 at SR-23

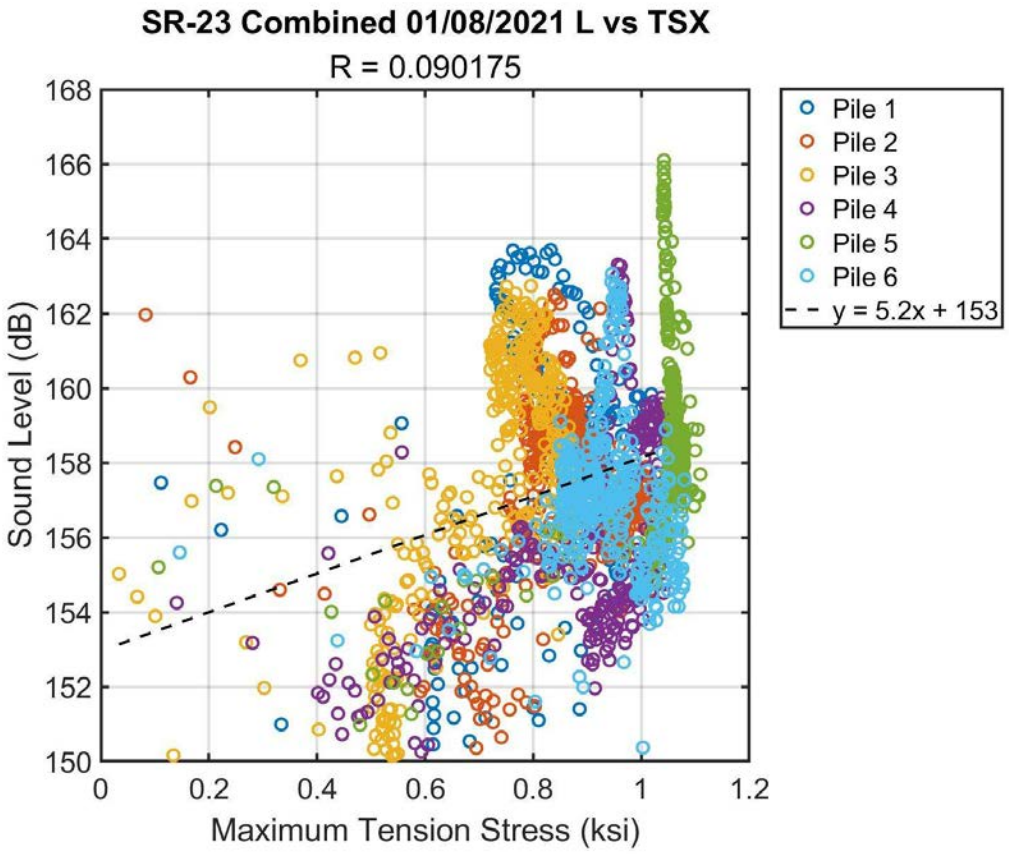

Figure 3-101. Sound Level (L) vs. Maximum Tension Stress (TSX) for pile drives performed on 1/08/2021 at SR-23

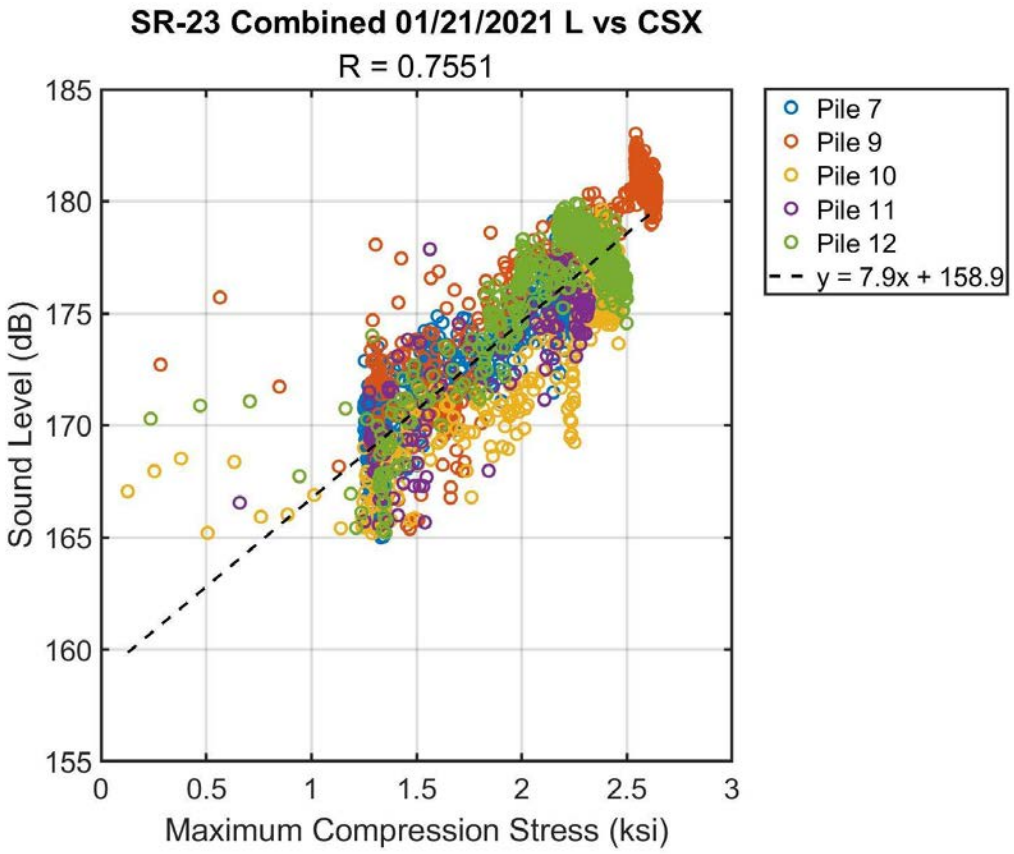

Figure 3-102. Sound Level (L) vs. Maximum Compression Stress (CSX) for pile drives performed on 1/21/2021 at SR-23

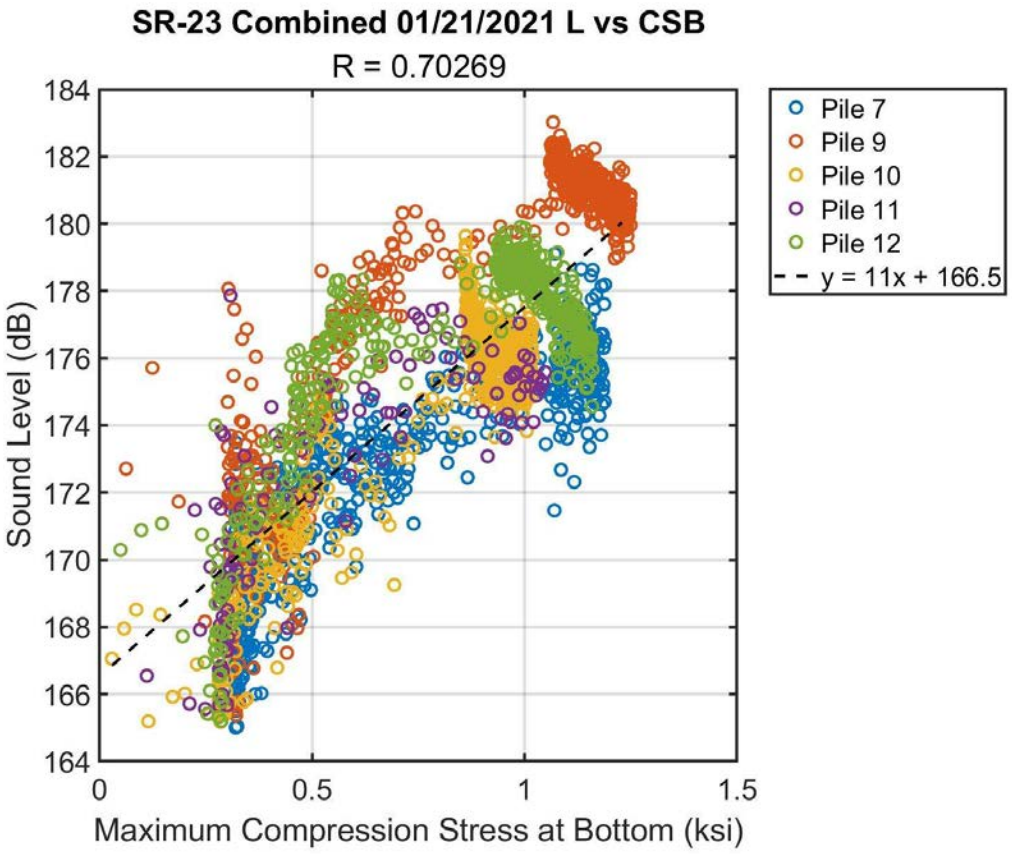

Figure 3-103. Sound Level (L) vs. Compression Stress at Bottom (CSB) for pile drives performed on 1/21/2021 at SR-23.

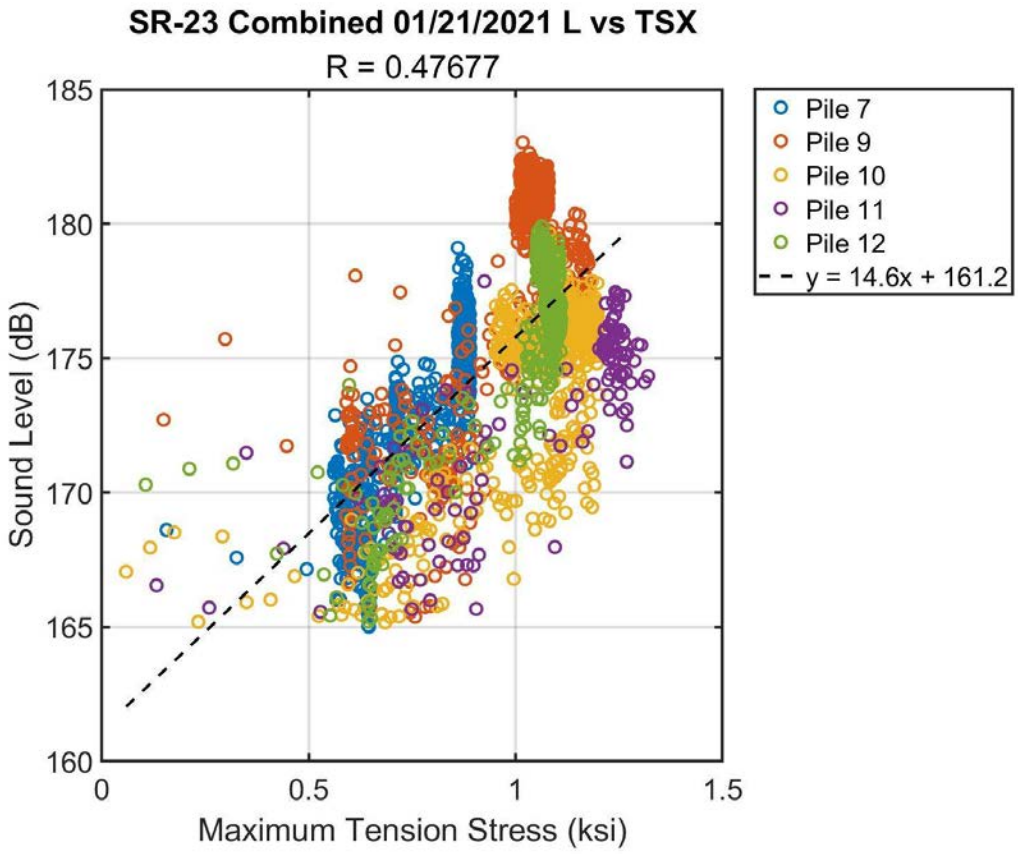

Figure 3-104. Sound Level (L) vs. Maximum Tension Stress (TSX) for pile drives performed on 1/21/2021 at SR-23.

Since Sound Level and CSX have the best correlation once combined, the remainder of this study focused on analyzing this apparent correlation. In an effort to compare data from all days, a new technique was used to estimate the sound-level data directly at the pile's locus and to develop combined plots from all drives on all days. This new method relies upon a model developed by (Bosco, 2021) which the TL coefficient and $L(R)$ are estimated based upon the manner in which the sound was initially generated. The Bosco (2021) model implies an amplitude-dependency on sound level such that louder sounds tend to attenuate more quickly than quieter sounds. This model is based upon similar data collected at 10 sites during over 50 drive events from concrete

piles, driven steel piles, and vibrated steel piles, and data appear to be consistent across the state. To utilize this model, L_r, the sound at any location, *R* is given by:

$$L_r = a_1 A + a_2 - A \log_{10}(R) \quad (3\text{-}1)$$

where $a_1 = 2.50$, $a_2 = 147$, and *A* is given by:

$$A = \frac{L_m - a_2}{a_1 - \log_{10}(R_1)} \quad (3\text{-}2)$$

in which L_m is some sound-level measured at a range R_1. Note that this model was developed for RMS data and not necessarily data from each individual hammer strike, so there may be some question about its applicability. But, in the context of this problem, this is was the best known method available.

The range, R used for this calculation was the average distance measured between the Buoy GPS and the Pile Drive coorinates for each site. These values are summarized below in Table 3-1.

Table 3-1: Range, R used to shift Sound Level, L back to source for combined correlation using (Bosco, 2021) model

Site	Ribault	CR218	CR218	SR23	SR23
Date	05/07/2019	12/04/2020	01/15/2021	01/08/2021	01/21/2021
R (m)	29.9326	33.1589	41.6811	62.848	29.1219

This technique was first performed on SR-23 for Piles 1-6 conducted on 1/08/2021 shown in Figure 3-105 and again for Piles 7, 9-12 conducted on 1/21/2021 shown in Figure 3-106. By using R_1 equal to 1m the calculated Sound Level L_m is estimated as the source sound level. Thus, both sets of data represented the same driving site now at the source of sound. All drives from SR-23 for multiple days were

combined shown in Figure 3-107. This technique was also perfomed at all other sites to as shown in Figure 3-108.

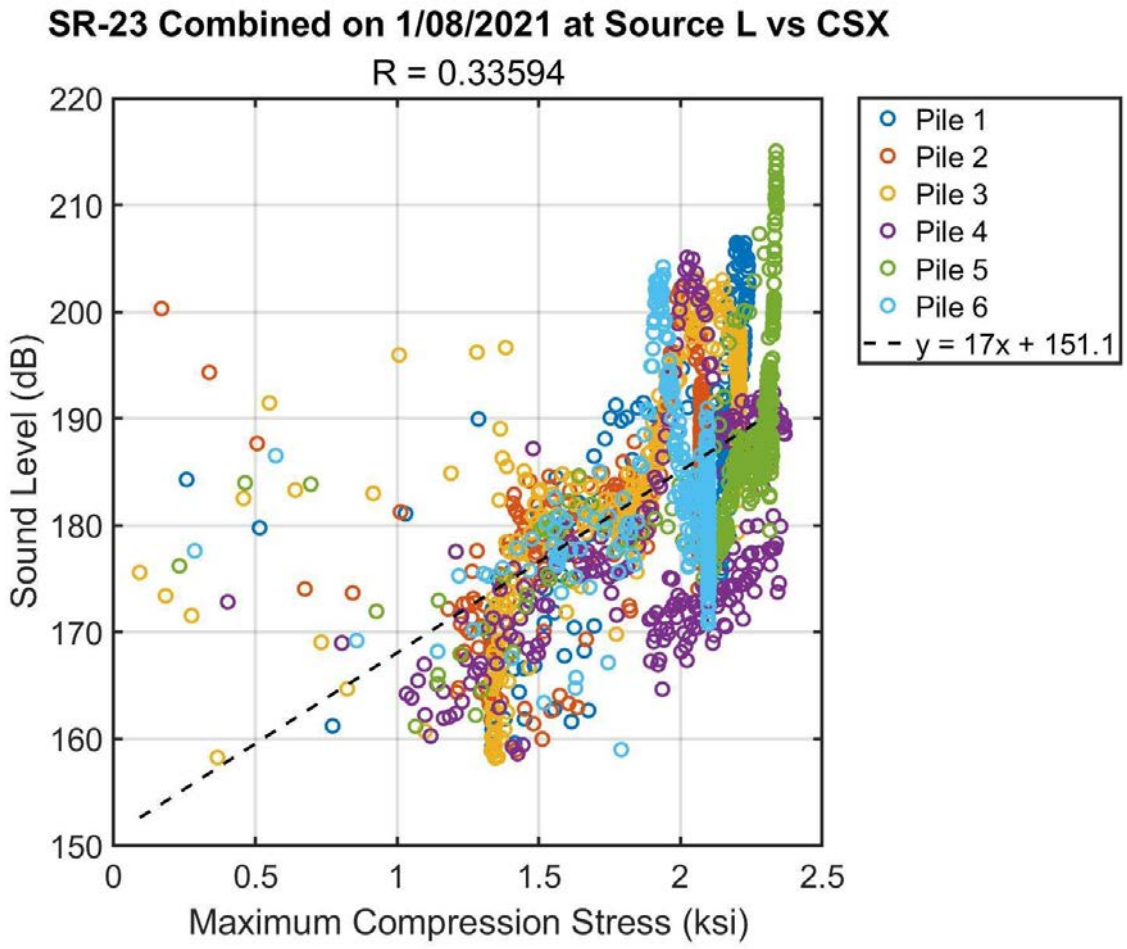

Figure 3-105. L vs. CSX for pile drives performed on 1/08/2021 at SR-23 shifted back to sound source.

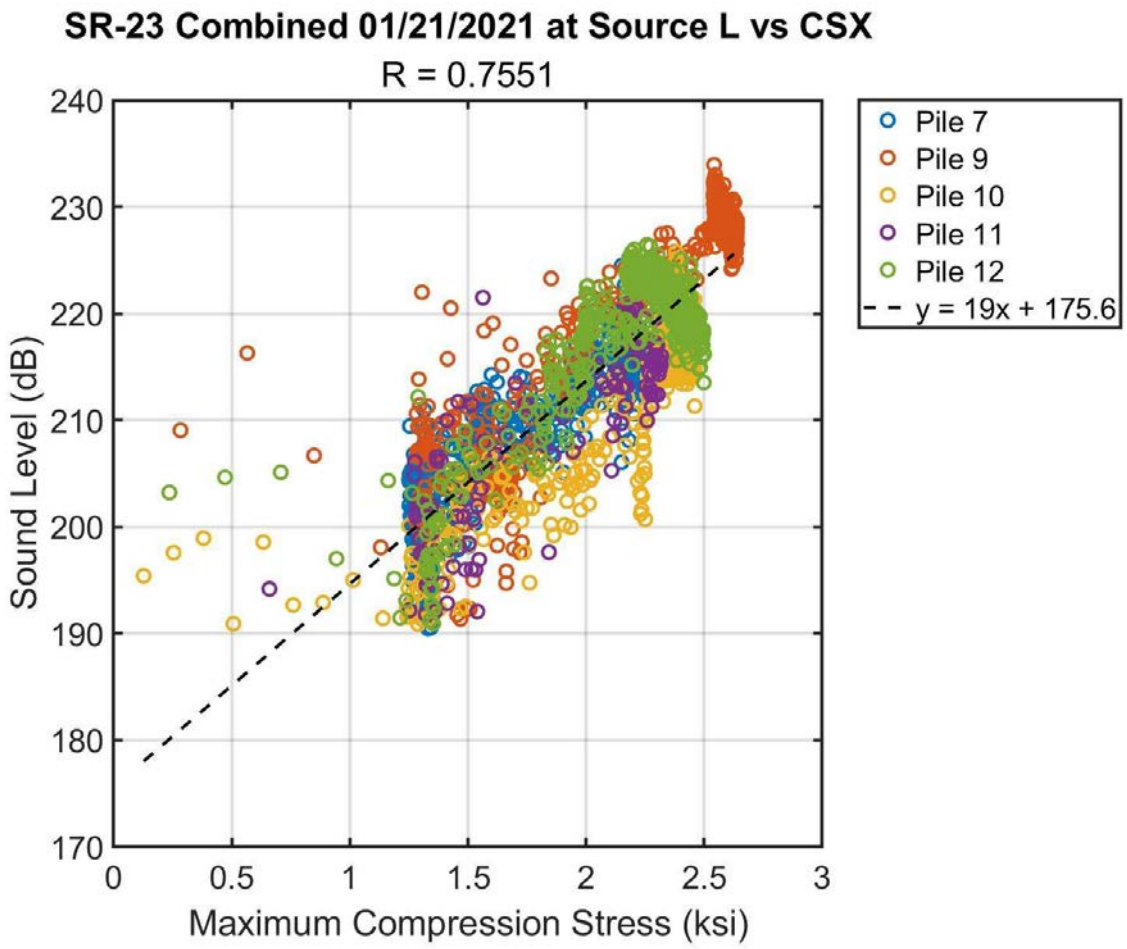

Figure 3-106. L vs. CSX for pile drives performed on 1/21/2021 at SR-23 shifted back to sound source.

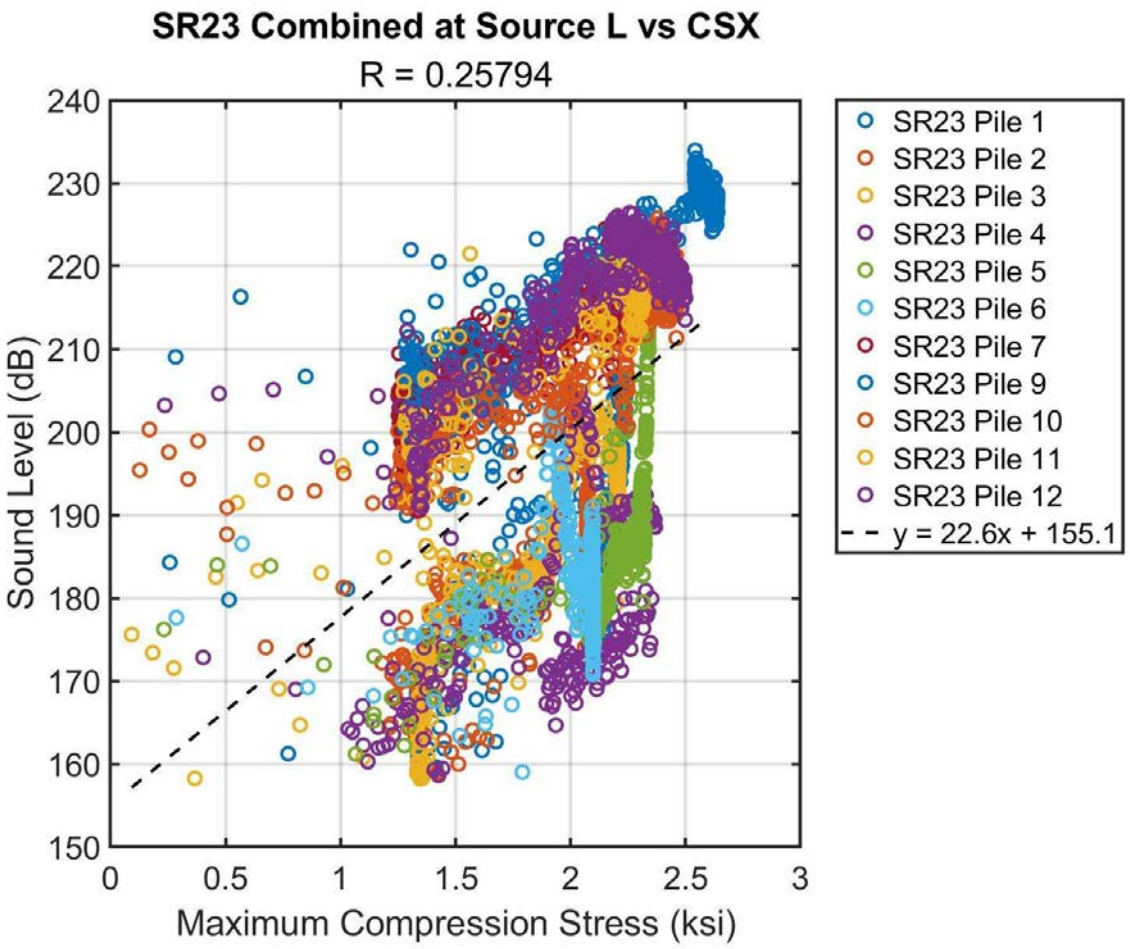

Figure 3-107. L vs. CSX for all pile drives performed at SR-23 shifted back to sound source.

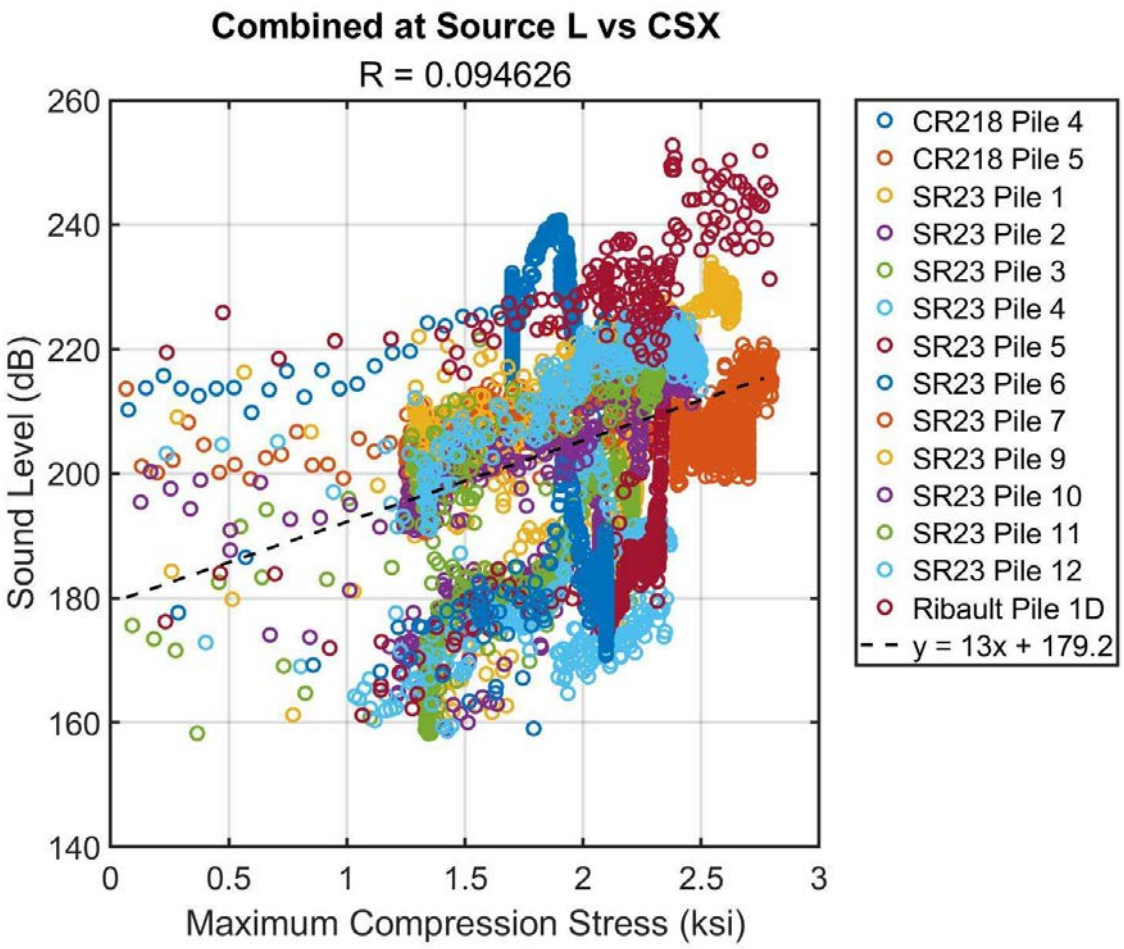

Figure 3-108. L vs. CSX for all pile drives shifted back to sound source.

Upon review of Figure 3-107 and Figure 3-108, it was noticed that there appears to be two distinct trendlines with similar slopes but different intercepts depending on the days on which sound data were collected. Note that the range associated with each data collection day at SR-23 was slightly different on the first day and the second day. It is possible that there could be some errors with the Bosco (2021) model that caused the source data shift to be somewhat inaccurate. To compensate, a manual shift of +27 dB was added to all sound data from SR-23's second data. Results are shown in Fig. 3-109:

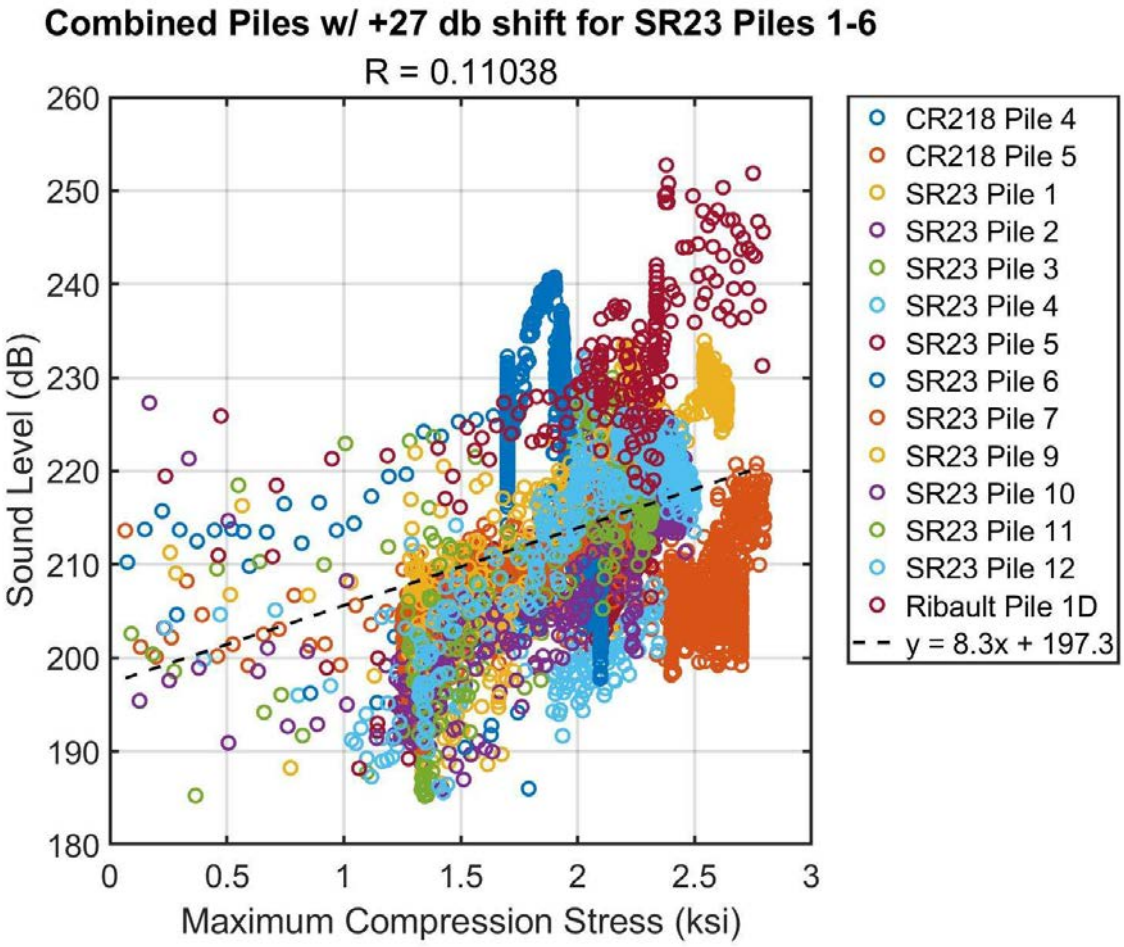

Figure 3-109. L vs. CSX for all pile drives shifted back to sound source including manual shift for SR-23 1/08/2021.

Finally, a Cook's Distance analysis was conducted to attempt to remove any possible outliers that existed in the final combined data. Values that exceeded three times the mean of the data were removed. A final correlation between sound level and compression stress for all piles is shown in Figure 3-110.

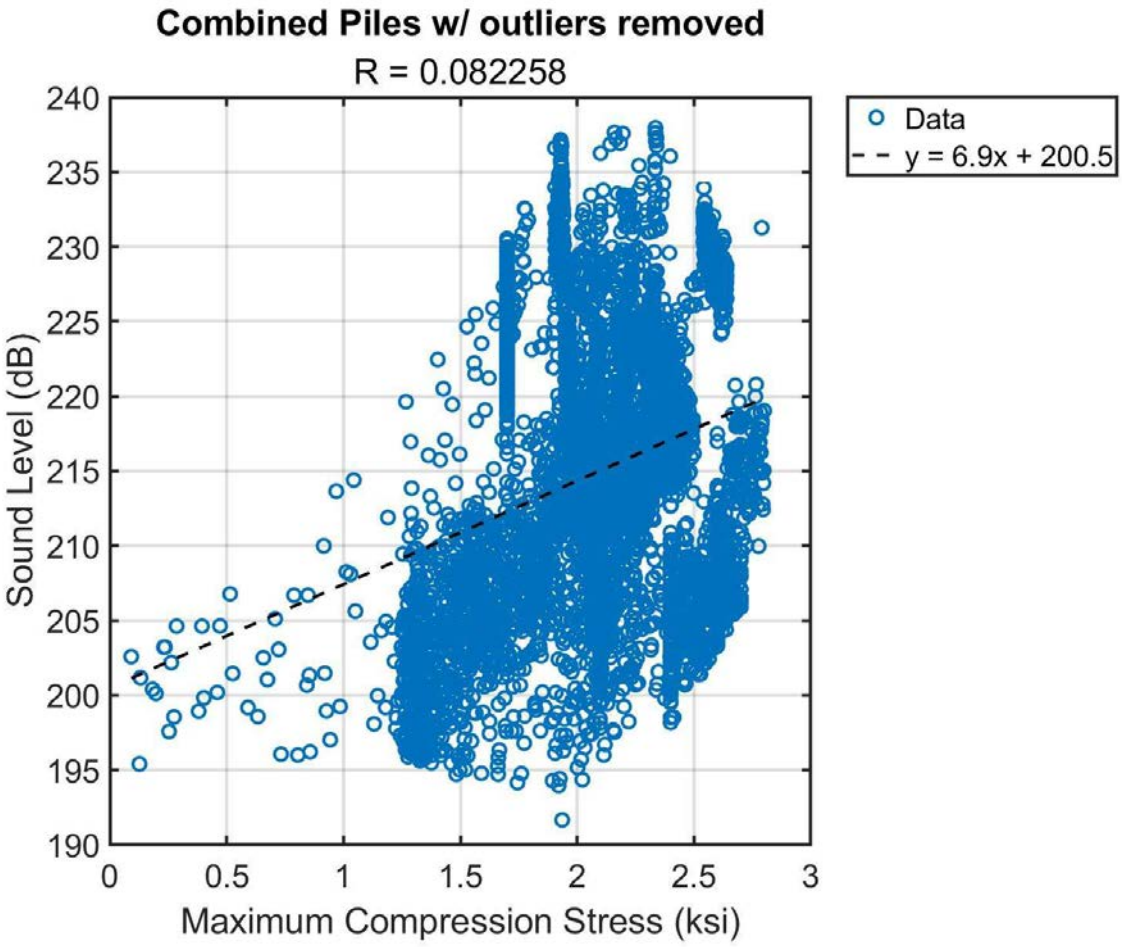

Figure 3-110. L vs. CSX for all pile drives shifted back to sound source including manual shift for SR-23 1/08/2021 and removal of outliers.

CHAPTER 4
DISCUSSION

This chapter provides a discussion on the results computed in Chapter 3 for all testing sites: Ribault River, FL; SR-23 Black Creek, FL; and CR-218 South Fork Black Creek, FL. Additional drive specific details outlined in the driving logs are summarized.

4.1 Howell Dr. over Ribault River, FL

4.1.1 Howell Dr. over Ribault River, FL – Pile 1

Driving logs indicated that the contractor utilized a vibratory hammer to break apart hard layers in preparation to drive the pile. This accounts for the first 58 lines of the PDA system blow count. Additionally, the hammer was dry fired to seat the pile prior to driving, which was also registered in the PDA. This may be the reason for the sound level maxima observed from 13:14 to 13:17 to be lower than the remaining raw maxima. During the drive there were two additional stoppages for measurement marking and equipment setting changes at approximately 13:17, continuing at 13:20, then again just after 13:20, continuing at 13:24 until drive stop. Of the 178 PDA system blow count, 176 blows were analyzed, and 175 sound peaks were identified in post-processing.

The correlation coefficients of Howell Dr. over Ribault River, FL – Pile 1 are summarized in Table 4-1. The strongest correlation exists between the sound level as a function of compression stress at the bottom of the pile. A slightly improved correlation was noticed between sound level and hammer energy (EMX when the hammer energy was normalized by the blow count (EMX*). By comparison, poor correlations were existed between sound level and tension stress.

Table 4-1: Summary of R-values for Howell Dr. over Ribault River, FL – Pile 1

L vs	EMX	EMX*	EMX**	CSX	CSB	TSX	EMX/CSX	EMX/CSB	EMX/TSX
Correlation Coefficient (R)	0.451	0.471	0.200	0.417	0.531	0.109	0.056	0.347	0.083

4.2 CR218 over South Fork Black Creek, FL

4.2.1 CR218 over South Fork Black Creek, FL – Pile 4

Driving logs indicated that this drive was continuous without intermittent stops. The drive stopped after high pile rebound and high-tension stress was computed by the PDA system. Of the 1059 PDA system blow count, 1058 blows were analyzed, and 1050 sound peaks were identified in post-processing.

The correlation coefficients of CR218 over South Fork Black Creek, FL – Pile 4 are summarized in Table 4-2. The strongest correlation exists between the sound level as a function of EMX normalized by CSX. A similar correlation was calculated by sound level as a function of EMX*. By comparison, the remaining comparisons exhibited poor correlations.

Table 4-2: Summary of R-values for CR218 over South Fork Black Creek, FL – Pile 4

L vs	EMX	EMX*	EMX**	CSX	CSB	TSX	EMX/CSX	EMX/CSB	EMX/TSX
Correlation Coefficient (R)	0.144	0.467	0.033	0.015	0.003	0.148	0.490	0.024	0.038

4.2.2 CR218 over South Fork Black Creek, FL – Pile 5

The drive was stopped at approximately 15:46 due to weather and resumed at 16:40 until end of drive. Of the 1029 PDA system blow count, 1029 blows were analyzed, and 1050 sound peaks were identified in post-processing.

The correlation coefficients of CR218 over South Fork Black Creek, FL – Pile 5 are summarized in Table 4-3. The strongest correlation exists between the sound level as a function of EMX normalized by blow count. A similar correlation was calculated by sound level as a function of EMX*. No other significant correlations were determined.

Table 4-3: Summary of R-values for CR218 over South Fork Black Creek, FL – Pile 5

L vs	EMX	EMX*	EMX**	CSX	CSB	TSX	EMX/CSX	EMX/CSB	EMX/TSX
Correlation Coefficient (R)	0.057	0.333	0.053	0.093	0.069	0.054	0.004	5.7e--4	0.033

4.3 SR-23 over Black Creek, FL

4.3.1 SR-23 over Black Creek, FL – Pile 1

Driving logs indicated the drive was stopped at 240 blows as only 6” of depth were achieved in the final 125 blows. This high blow count, high rebound, and high-tension stresses resulted in the pile not being accepted. Of the 240 PDA system blow count, 240 blows were analyzed, and 230 sound peaks were identified in post-processing.

The correlation coefficients of SR-23 over Black Creek, FL – Pile 1 are summarized in Table 4-4. The strongest correlation exists between the sound level as a function of EMX normalized by CSX. A similar correlation was calculated for sound level as a function of EMX normalized by CSB and also sound level as a function of CSB. No other significant correlations were observed.

Table 4-4: Summary of R-values for SR-23 over Black Creek, FL – Pile 1

L vs	EMX	EMX*	EMX**	CSX	CSB	TSX	EMX/CSX	EMX/CSB	EMX/TSX
Correlation Coefficient (R)	0.019	0.004	0.220	0.527	0.473	0.066	0.566	0.542	0.101

4.3.2 SR-23 over Black Creek, FL – Pile 2

Driving logs indicate the drive was stopped at 414 blows as only 11” of depth were achieved in the final 240 blows. This high blow count, high rebound, and high-tension stresses resulted in the pile not being accepted. An equipment fuel setting change occurred from F2 to F1 at 140 blows. Of the 414 PDA system blow count, 414 blows were analyzed, and 410 sound peaks were identified in post-processing.

The correlation coefficients of SR-23 over Black Creek, FL – Pile 2 are summarized in Table 4-5. The strongest correlation was observed between the sound level as a function of TSX. Weaker correlations exist for sound level as a function of EMX/CSX and similarly EMX/CSB. Sound level as function of EMX/TSX showed no significant correlation.

Table 4-5: Summary of R-values for SR-23 over Black Creek, FL – Pile 2

L vs	EMX	EMX*	EMX**	CSX	CSB	TSX	EMX/CSX	EMX/CSB	EMX/TSX
Correlation Coefficient (R)	0.087	0.024	0.231	0.320	0.443	0.788	0.402	0.470	0.002

4.3.3 SR-23 over Black Creek, FL – Pile 3

Driving logs indicated the drive was stopped at 392 blows as only 6” of depth were achieved in the final 120 blows. This high blow count, high rebound, and high-tension stresses resulted in the pile not being accepted. An equipment fuel setting change occurred from F2 to F3 at 55 blows, then again from F3 to F4 after an additional 30 blows. Of the 392 PDA system blow count, 392 blows were analyzed, and 372 sound peaks were identified in post-processing.

The correlation coefficients of SR-23 over Black Creek, FL – Pile 3 are summarized in Table 4-6. The strongest correlation exists between the sound level as a function of EMX/CSB and similarly EMX/CSX. By observation, weaker correlations exist between sound level as a function of CSX and also CSB.

Table 4-6: Summary of R-values for SR-23 over Black Creek, FL – Pile 3

L vs	EMX	EMX*	EMX**	CSX	CSB	TSX	EMX/CSX	EMX/CSB	EMX/TSX
Correlation Coefficient (R)	0.017	0.179	0.140	0.560	0.613	0.297	0.694	0.719	0.432

4.3.4 SR-23 over Black Creek, FL – Pile 4

Driving logs indicated the drive was stopped at 269 blows as only 2.5” of depth were achieved in the final 100 blows. This high blow count, high rebound, and high-tension stresses resulted in the pile not being accepted. An equipment fuel setting change occurred from F2 to F1 at start. Of the 269 PDA system blow count, 269 blows were analyzed, and 254 sound peaks were identified in post-processing.

The correlation coefficients of SR-23 over Black Creek, FL – Pile 4 are summarized in Table 4-7. The strongest correlation exists between the sound level as a function of TSX. No other significant correlations were found. By observation, poor correlation was shown between between sound level and EMX**.

Table 4-7: Summary of R-values for SR-23 over Black Creek, FL – Pile 4

L vs	EMX	EMX*	EMX**	CSX	CSB	TSX	EMX/CSX	EMX/CSB	EMX/TSX
Correlation Coefficient (R)	0.291	0.092	0.015	0.286	0.142	0.305	0.124	0.154	0.115

4.3.5 SR-23 over Black Creek, FL – Pile 5

Driving logs indicate the drive was stopped at 363 blows as only 3” of depth were achieved in the final 120 blows. This high blow count, high rebound, and high-tension stresses resulted in the pile not being accepted. Of the 363 PDA system blow count, 363 blows were analyzed, and 354 sound peaks were identified in post-processing.

The correlation coefficients of SR-23 over Black Creek, FL – Pile 5 are summarized in Table 4-8. The strongest correlation exists between the sound level as a function of CSX. No other significant correlations were found.

Table 4-8: Summary of R-values for SR-23 over Black Creek, FL – Pile 5

L vs	EMX	EMX*	EMX**	CSX	CSB	TSX	EMX/CSX	EMX/CSB	EMX/TSX
Correlation Coefficient (R)	0.252	0.193	0.018	0.311	0.088	0.155	0.081	0.095	0.013

4.3.6 SR-23 over Black Creek, FL – Pile 6

Driving logs indicated the drive was stopped at 407 blows as only 11” of depth were achieved in the final 240 blows. This high blow count, high rebound, and high-tension stresses resulted in the pile not being accepted. An equipment fuel setting change occurred from F3 to F2 at 130 blows, then again from F2 to F1 after an additional 10 blows. Of the 407 PDA system blow count, 407 blows were analyzed, and 396 sound peaks were identified in post-processing.

The correlation coefficients of SR-23 over Black Creek, FL – Pile 6 are summarized in Table 4-9. No significant correlations were found.

Table 4-9: Summary of R-values for SR-23 over Black Creek, FL – Pile 6

L vs	EMX	EMX*	EMX**	CSX	CSB	TSX	EMX/CSX	EMX/CSB	EMX/TSX
Correlation Coefficient (R)	0.006	0.103	0.007	0.016	0.014	1.2e-4	0.065	0.079	0.027

4.3.7 SR-23 over Black Creek, FL – Pile 7

Diving logs indicate the drive was stopped at 587 blows as only 6" of depth were achieved in the final 120 blows. Tension limits were reached resulting in the pile not being accepted. Of the 587 PDA system blow count, 587 blows were analyzed, and 566 sound peaks were identified in post-processing.

The correlation coefficients of SR-23 over Black Creek, FL – Pile 7 are summarized in Table 4-10. The strongest correlation exists between sound level as a function of CSX. Similar correlations exist between sound level as a function of CSB and EMX/CSB as well as EMX/CSX. A weaker correlation was found between sound level and EMX**.

Table 4-10: Summary of R-values for SR-23 over Black Creek, FL – Pile 7

L vs	EMX	EMX*	EMX**	CSX	CSB	TSX	EMX/CSX	EMX/CSB	EMX/TSX
Correlation Coefficient (R)	0.098	0.199	0.430	0.763	0.754	0.688	0.663	0.743	0.124

4.3.8 SR-23 over Black Creek, FL – Pile 9

Driving logs indicate the drive was stopped at 564 blows as only 4.25" of depth were achieved in the final 120 blows. Tension limits were reached resulting in the pile not being accepted. Of the 564 PDA system blow count, 564 blows were analyzed, and 562 sound peaks were identified in post-processing.

The correlation coefficients of SR-23 over Black Creek, FL – Pile 9 are summarized in Table 4-11. The strongest correlation exists between sound level as a function of EMX/CSX. Strong correlations exist between sound level and all forms of pile stress and effective hammer energy.

Table 4-11: Summary of R-values for SR-23 over Black Creek, FL – Pile 9

L vs	EMX	EMX*	EMX**	CSX	CSB	TSX	EMX/CSX	EMX/CSB	EMX/TSX
Correlation Coefficient (R)	0.180	0.465	0.464	0.840	0.810	0.605	0.858	0.847	0.649

4.3.9 SR-23 over Black Creek, FL – Pile 10

Driving logs indicate the drive was stopped at 616 blows as only 12” of depth were achieved in the final 240 blows. Though high blow counts were calculated, tension stresses were at allowable limits resulting in the pile being accepted. Of the 617 PDA system blow count, 616 blows were analyzed, and 604 sound peaks were identified in post-processing.

The correlation coefficients of SR-23 over Black Creek, FL – Pile 10 are summarized in Table 4-12. The strongest correlation exists between sound level as a function of EMX/CSB. Strong correlations exist between sound level and both forms of pile compression stress. By observation, poor correlation was shown between between sound level and EMX**.

Table 4-12: Summary of R-values for SR-23 over Black Creek, FL – Pile 10

L vs	EMX	EMX*	EMX**	CSX	CSB	TSX	EMX/CSX	EMX/CSB	EMX/TSX
Correlation Coefficient (R)	0.447	0.591	5.95e-4	0.809	0.818	0.533	0.782	0.818	0.424

4.3.10 SR-23 over Black Creek, FL – Pile 11

Driving logs indicate the drive was stopped at 135 blows as only 1.5” of depth were achieved in the final 14 blows. High tension stresses exceeded allowable limits resulting in the pile being not accepted. Of the 135 PDA system blow count, 135 blows were analyzed, and 128 sound peaks were identified in post-processing.

The correlation coefficients of SR-23 over Black Creek, FL – Pile 11 are summarized in Table 4-13. The strongest correlation exists between sound level as a function of CSX. By obseration, poor correlation was shown between between sound level and EMX**.

Table 4-13: Summary of R-values for SR-23 over Black Creek, FL – Pile 11

L vs	EMX	EMX*	EMX**	CSX	CSB	TSX	EMX/CSX	EMX/CSB	EMX/TSX
Correlation Coefficient (R)	0.190	0.317	0.009	0.708	0.610	0.654	0.376	0.510	0.172

4.3.11 SR-23 over Black Creek, FL – Pile 12

Driving logs indicate the drive was stopped at 440 blows as only 10.5” of depth were achieved in the final 240 blows. High tension stresses reached limits resulting in the pile being not accepted. Of the 440 PDA system blow count, 440 blows were analyzed, and 433 sound peaks were identified in post-processing.

The correlation coefficients of SR-23 over Black Creek, FL – Pile 12 are summarized in Table 4-14. The strongest correlation exists between sound level as a function of EMX/CSX with similar correlation between sound level and EMX/CSB. Strong correlations exist between sound level and all forms of pile stresses. By observation, poor correlation was shown between between sound level and EMX**.

Table 4-14: Summary of R-values for SR-23 over Black Creek, FL – Pile 12

L vs	EMX	EMX*	EMX**	CSX	CSB	TSX	EMX/CSX	EMX/CSB	EMX/TSX
Correlation Coefficient (R)	0.160	0.436	0.007	0.686	0.602	0.658	0.827	0.799	0.681

4.4 SR-23 over Black Creek, FL – Combined Pile Drives

Upon discovery of the consistent correlation coefficients for SR-23 piles 7, 9, 10, 11, and 12 which were performed on the same date, 1/21/2021, further analysis was conducted on the sound level vs pile stress relationships specific to this site for both days. The resulting data is summarized in Table 4-15.

Table 4-15: Summary of R-values for SR-23 over Black Creek, FL

Combined Drives Performed on 1/08/2021			
L vs	CSX	CSB	TSX
Correlation Coefficient (R)	0.336	0.291	0.090

Combined Drives Performed on 1/21/2021			
L vs	CSX	CSB	TSX
Correlation Coefficient (R)	0.755	0.703	0.477

This analysis indicates, specific to the data from 1/21/2021, that maximum pile compressive stress measured by the PDA system has strong correlation to the sound level measured in the field with an R-value of 0.755. The data in this combined correlation are a makeup of 5 of the 13 drives analyzed in this study.

It was determined that the remaining dataset were limited providing possible reasoning for differing correlation results. At Howell Dr. over Ribault River, FL, there was only one data set recorded and analyzed for one pile drive. Further there were only 176 hammer blows analyzed by the PDA system. For this reason, the data set is very limited

in confirming any correlations for this study. At CR218 over South Fork, Black Creek, FL, there were two data sets recorded and analyzed for a total of two piles. The correlations were not strong and favored a stronger correlation between sound level and EMX instead of pile stress.

This study included 11 pile drives for site SR 23 over Black Creek, FL. Of these drives the data collected on 1/8/2021 does not have consistent results as the data collected on 1/21/2021. As stated previously, the data analyzed from 1/8/2021 was that from the second closest to the pile due to high sound levels at the closest buoy which prevented the finding of peak sound levels. This may be the reason for differing results.

4.5 Piles Shifted back to Source – Combined Pile Drives

Use of the Bosco (2021) model allowed for data from all sites to be combined and anaylzed by using the known range from the source as disussed in the previous chapter. The resulting data are summarized in Table 4-16.

Table 4-16: Summary of R-values for Piles shifted back to source

SR-23 Combined Drives at Source	
L vs CSX	
Correlation Coefficient (R)	0.258

All Combined Drives at Source	
L vs CSX	
Correlation Coefficient (R)	0.095

All Combined Drives at Source w/ additional shift	
L vs CSX	
Correlation Coefficient (R)	0.110

All Combined Drives at Source w/ additional shift and removal of outliers	
L vs CSX	
Correlation Coefficient (R)	0.082

Though the correlation between sound level and maximum compression stressed was strong for SR-23 from the 1/21/2021 data, the inclusion of the SR-23 data from 1/8/2021 did not have such conclusive results with a combined correlation coefficient of 0.258. This correlation was further put in question when all piles were combined after shifting the sound levels to the course with a correlation coefficient of 0.095 and after removing outliers, the correlation coefficient was 0.082. For similar reasons discussed in section 4.3, combining the pile drives after shifting the sound levels may not have addressed the differences in sites. Furthermore, given the limitations of the PDA system data the values for hammer energy and pile stresses are do not span a broad range of values in comparison to sound level which may have led to inconclusive results.

CHAPTER 5
CONCLUSIONS

5.1 Research Conclusions

As shown in the analysis in Chapter 4, the results from SR-23 over Black Creek for pile drives performed on 1/21/2021 for piles 7, 9, 10, 11, and 12 showed strong correlations between sound level and hammer energy as well as between sound level and pile stresses. The correlation that was most consistently strong was that of sound level and maximum pile compression stress (L vs. CSX). This correlation further evaluated in Chapter 4 shows that for this specific site and date, the collective drives had a correlation of 0.7551 for L vs. CSB. The remaining piles analyzed provided inconsistencies in these correlations. Further inconsistencies were found when attemting to shift data to the same source sound distance for direct comparison. This study is limited to the raw sound data and driving logs collected. Though these different sites are similar intercoastal sites and project specifications, no data were collected on the water or geotechnical characteristics which may explain inconsistencies between sites and dates.

A correlation of sound and data analysis by the PDA system would provide a significant advantage in determining anthropogenic noise sound levels generated from pile driving. A correlation between sound level and the compression stress at the bottom of the pile would reflect the hammer energy applied to the pile which is than transmitted through the pile to the sublayer. As this medium imposes resistance to the pile bottom, the pile undergoes compression stress. The resultant energy not used kinetically, is than scattered mechanically as sound through the water. The greater the compression stress at the bottom of the pile, the greater the sound level at the source of the drive.

5.2 Recommendations for Future Research

This study confirmed that a correlation between sound level and hammer energy as well as sound energy and pile stress is possible. The strongest relationship appears to between sound level and compression stress at the bottom of the pile. The first area of improvement for this study would be to gather more data for further analysis. With such a limited data set, it is difficult to establish confidence in a correlation. However, the preliminary data appear to indicate that developing such a correlation may be possible in the long-term with additional data.

LIST OF REFERENCES

Berube, J. P. (2019). *An Analysis of Hydroacoustic Transmission Loss Associated with Marine Pile Driving.* Retrieved from UNF Graduate Theses and Dissertations: https://digitalcommons.unf.edu/etd/918

Bosco, M. (2021). Analysis of Shallow Water Underwater Noise from Marine Pile Driving using Computational Fluid Dynamics and Empirical Data Fitting. *M.S. Thesis, University of North Florida, Jacksonville, FL*.

Buehler, D., Oestman, R., Reyff, J., Pommerench, K., & Mitchell, B. (2015). *Technical Guidance for Assessment and Mitigation of the Hydroacoustic Effects of Pile Driving on Fish.* Sacramento, CA: California Department of Transportation Division of Environmental Analysis.

Crowley, R., Bosco, M., Sypula, D., Schaaf, A., Rivera, B., Kopp, B. T., . . . Gelsleichter, J. G. (2022). Analysis of Anthropogenic Noise due to Pile Driving Using Computational Fluid Dynamics. *Geo-Congress.* Charlotte, NC.

Dahl, P. H., & Dall'Osto, D. R. (2017). On the underwater sound field from impact pile driving: Arrival structure, precursor arrivals, and energy streamlines. *Acoustical Society of America*, 1141-1155.

Dahl, P. H., & Dall'Ostro, D. R. (2017). On the underwater sound field from impact pile driving: Arrival structure, precursor arrivals, and energy streamlines. *The Journal of the Acoustical Society of America*, 142.

Dahl, P. H., & Reinhall, P. G. (2013). Beam forming of the underwater sound field from impact pile driving. *Acoustical Society of America*, EL1-EL6.

Dahl, P. H., Dall'Osto, D. R., & Farrell, D. M. (2015). The underwater sound field from vibratory pile driving. *Acoustical Society of America*, 3544-3554.

Galindo-Romero, M., Lippert, T., & Gavrilov, A. (2015). Empirical prediction of peak pressure levels in anthropogenic impulsive noise. Part I: Airgun arrays signals. *The Journal of the Acoustical Society of America*, 138.

Guan, S., Brookens, T., & Vignola, J. (2021). Use of Underwater Acoustics in Marine Conservation and Policy: Previous Advances, Current Status, and Future Needs. *Journal of Marine Science and Engineering*, 173.

Hawkins, A. D., Johnson, C., & Popper, A. N. (2020). How to set sound exposure criteria for fishes. *The Journal of the Acoustical Society of America*, 147, 1762.

Lippert, T., & Estorff, O. (2014). The significance of parameter uncertainties for the prediction of offshore pile driving noise. *Acoustical Society of America*, 2463-2471.

Lippert, T., Ainslie, M. A., & Estorff, O. (2018). Pile driving acoustics made simple: Damped cylindrical spreading model. *Acoustical Society of America*, 143.

Lippert, T., Galindo-Romero, M., Gavrilov, A. N., & Estorff, O. (2015). Empirical estimation of peak pressure level from sound exposure level. Part II: Offshore impact pile driving noise. *Acoustical Society of America*, EL287-EL292.

Martin, B. S., & Barclay, D. R. (2019). Determining the dependence of marine pile driving sound levels on strike energy, pile penetration, and propagation effects using a linear mixed model based on damped cylindrical spreading. *The Journal of the Acoustical Society of America*, 109-121.

Martin, S. B., Lucke, K., & Barclay, D. R. (2020). Techniques for distinguishing between impulsive and non-impulsive sound in the context of regulating sound exposure for marine mammals. *The Journal of the Acoustical Society of America*, 147, 2159.

Popper, A. N., & Hawkins, A. D. (2019). An overview of fish bioacoustics and the impacts of anthropogenic sounds on fishes. *Journal of Fish Biology*, 692-713.

Reinhall, P. G., & Dahl, P. H. (2011). Underwater Mach wave radiation from impact pile driving: Theory and observation. *The Journal of the Acoustical Society of America*, 130.

University of Rhode Island and Inner Space Center. (n.d.). *Discovery of Sound in the Sea*. Retrieved from Science of Sound: https://dosits.org/science/advanced-topics/cylindrical-vs-spherical-spreading/

Zampoli, M., Nijhof, M. J., de Jong, C. A., Ainslie, M. A., Jansen, E. H., & Quesson, B. A. (2013). Validation of fintie element computations for the quantitative prediction of underwater noise from impact pile driving. *Acoustical Society of America*, 72-81.

BIOGRAPHICAL SKETCH

Lieutenant Rivera is a native of Rochester, NY. He graduated from Clarkson University in 2013 with a Bachelor of Science in Civil Engineering and commissioned through Officer Candidate School.

His first assignment was to Naval Mobile Construction Battalion THREE where he served as ALFA Company Platoon Commander. In June 2015, he deployed to PACOM as the Officer-in-Charge (OIC) of Detail Fuji until selected for the Junior Officer OIC Program for the Underwater Construction Teams. In June 2016, he graduated from Naval Diving and Salvage Training Center and reported to Underwater Construction Team ONE. He served as OIC of Construction Dive Detachment ALFA and Assistant Operations Officer, leading the detachment in various missions across EUCOM, AFRICOM, and NORTHCOM.

Lieutenant Rivera assumed duties as a Construction Manager, Public Works Department Oceana in June 2018. While a member of NAVFAC MIDLANT, he managed $6M in construction contracts supporting the East Coast Master Jet Base and geographically distant NOSC Facilities. In 2019 he was selected for the U.S. Navy Ocean Facilities Program and attended the University of North Florida.

Lieutenant Rivera is a Seabee Combat Warfare Officer, Joint Diving Officer, and Professional Engineer in the State of Nevada. His personal decorations include Navy and Marine Corps Commendation Medal (2nd Award), Navy and Marine Corps Achievement Medal, and various personal, service, and unit awards.